

Neuronal Adaptations during Amygdala-Dependent Learning and Memory

Behdokht Hosseini

Financial support for the printing of this thesis was kindly provided by
The Erasmus University Medical Centre

ISBN: 978-94-6299-439-3

Printed by: Ridderprint BV, Ridderkerk

Copyright © Behdokht Hosseini, 2016

All rights reserved. No parts of this book may be reproduced, stored in a retrieval system, or transmitted in any form or by any means, without the prior permission of the author.

Neuronal Adaptations during Amygdala-Dependent Learning and Memory

Neuronal Aanpassingen tijdens Amygdala-Afhankelijk Leren en Geheugen

Thesis

to obtain the degree of Doctor from the Erasmus University Rotterdam

by command of the rector magnificus

Prof.dr. H.A.P. Pols

and in accordance with the decision of the Doctorate Board

The public defense shall be held on

Wednesday 30 November 2016 at 11:30 hours

by

Behdokht Hosseini

born in Firoozkooh-Tehran, Iran

Doctoral Committee:

Promoter: Prof.dr. S.A. Kushner

Other members: Prof.dr. Y. Elgersma
Dr. H. Krugers
Dr. T. Ruigrok

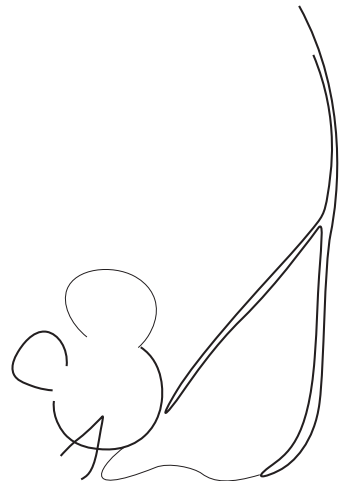
Copromoter: Dr. P. Rao-Ruiz

To Behrooz

Table of Contents

Chapter 1	9	
<i>General Introduction</i>		
Chapter 2	33	
<i>Arc expression identifies the lateral amygdala fear memory trace</i>		
Chapter 3	73	
<i>Novel fear learning-dependent activity of Arc in the ventrolateral subregion of lateral amygdala</i>		
Chapter 4	99	
<i>Modulation of cerebellar-dependent associative learning by the amygdala</i>		
Chapter 5	121	
<i>General Discussion</i>		
Appendices	141	
<i>Summary</i>		<i>143</i>
<i>Samenvatting</i>		<i>145</i>
<i>PhD Portfolio</i>		<i>147</i>
<i>List of Publications</i>		<i>149</i>
<i>Curriculum Vitae</i>		<i>151</i>
<i>Acknowledgment</i>		<i>153</i>

Chapter 1
General Introduction



1. Classical conditioning a model of associative learning

A reductionist definition of learning is the set of biological processes that govern the durable encoding of new skills and information about the outside world¹. Learning can be acquired through both associative and non-associative models. Associative learning occurs when a given stimulus comes to predict the occurrence of another independent stimulus, following their previous temporally-ordered presentation². Non-associative learning results from a change in the response to a given stimulus after repeated exposure³.

Associative conditioning, also known as classical conditioning, was first introduced by Ivan Pavlov (investigations between 1890-1930). While studying digestion and the nervous system by measuring the amount of salivation in response to food quantities, Pavlov noticed that there were some things that a dog did not need to learn. For example, dogs did not appear to require learning to salivate when they saw food. This reflex appeared to be ‘hard wired’ in the dog. However, he discovered that any object or event which the dogs learned to associate with food (e.g., a bell in his experiments), would trigger the same response. This is because at one point, the dogs had not yet made that association, but there came a point when they started. Therefore, their behavior had changed as a result of learning. In behaviorist terms, the bell was originally a neutral or conditioned stimulus, which had become associated with an unconditioned stimulus (US), in this case food. Pavlov found that for this association to be made, the conditioned stimulus (CS), in this case bell, and unconditioned stimulus (food) had to be presented closely together in time. He called this the law of temporal contiguity. If the time between the conditioned stimulus (bell) and unconditioned stimulus (food) was too great, then learning did not occur⁴.

Associative conditioning paradigms typically employ emotionally valent US stimuli, such as appetitive (e.g., food, water or addictive drugs) or aversive (e.g., foot-shock, loud noise or corneal air puff) stimuli, and neutrally valent CS stimuli (e.g., benign odor, innocuous light or mild tone). Once a neutrally valent CS comes to be associated with an US through temporally contiguous CS-US pairings, it is considered a CS which now evokes a conditioned response (CR) during non-reinforced presentations (i.e., CS presentations in the absence of the US)⁵.

The chapters of this thesis focus on two types of aversive associative conditioning:

- i. Auditory fear conditioning: a well-established and robust model to study fear learning, wherein an animal learns that a tone (CS) predicts the subsequent onset of a foot-shock (US). The lateral nucleus of the amygdala is a major site of plasticity responsible for the encoding of the CS-US association⁶.
- ii. Eye-blink conditioning: one of the most widely used models to study motor learning, during which animals learn that a light or tone (CS) predict the subsequent onset of an aversive corneal air puff (US). The cerebellum is a critical brain region required for the acquisition of eye blink conditioning⁷. However, new evidence presented in Chapter 4 suggests that proper functioning of the central nucleus of the amygdala is also necessary for acquisition of eye-blink conditioning.

1.1 Fear conditioning as a model for associative learning

In the widely used fear conditioning paradigm, a neutral CS is paired with an aversive stimulus like a foot-shock (US). The animals learn to associate the two, and successive exposure to the CS alone elicits CRs, typically characterized by a variety of fear-related behaviors, including immobility or freezing, analgesic response, increased heart rate and increased blood pressure³. The learning curve is typically very rapid, with CS-US associations acquired often in just a few, or even in just a single trial^{6,8,9}. In 1927, Robert Rescorla and Allen Wagner introduced a mathematical model (Rescorla-Wagner model) to explain several phenomena of classical conditioning, including acquisition of the CR to a neutral CS. Their model suggests that a CS predicts the US once the association of CS and US has occurred. It argues that there is a limit to the strength of conditioning when the CS and US are associated, in which the nature of the US defines this limitation¹⁰. This indicates that the intensity, painfulness, and element of surprise of the US determine both the rate of acquisition and maximal strength of the CS-US association.

The most commonly used and well-established model of aversive conditioning is the fear-conditioning paradigm, which is generally thought to result in the acquisition of at least two different quantifiable, albeit frequently co-varying, CS-US associations:

i. Auditory/cued fear conditioning occurs when an auditory CS is presented contingent with a foot-shock (US). When the CS-US presentation is co-terminating, the rate of learning is maximized, and is known as delay conditioning. When an interval separates the end of the CS and the start of the US, this is known as trace conditioning. In order to improve the specificity and strength of the tone-shock association, animals are often pre-exposed to the context without a US¹¹. This allows animals the opportunity to process information about the context, and encode a contextual representation, independent of the auditory CS or the shock US. Conditioning to an auditory CS is typically assessed in a novel context to avoid the confounding CR of the background contextual CS-US association that is often acquired during auditory fear conditioning¹². The long-term encoding of auditory fear conditioning has been well demonstrated to be dependent upon the integrity of the lateral amygdala^{3,14}.

ii. Contextual fear conditioning occurs when a context functions as a CS to predict the occurrence of an aversive US (e.g., foot-shock). Re-exposure to the same context generally evokes avoidance responses, including freezing¹⁵. Moreover, re-exposure to similar, but not identical contexts, will also evoke avoidance responses, with the extent of similarity and the specific nature of the differences being determinant in the level of fear evoked and can be used an index of CS generalization¹⁶. Although several brain areas have been shown to participate in the encoding of contextual fear conditioning memories, the hippocampus and amygdala have been the most widely studied. Notably, however, the function of the hippocampus and amygdala during contextual conditioning appears to be distinct: while the amygdala functions as the critical site for encoding of the CS-US association (analogous to that of auditory fear conditioning), the hippocampus functions to encode the representation of the contextual CS independent of emotional valence^{13,17}.

1.2 Eye-blink conditioning as a model for associative learning

During the 1980s, Michael D. Mauk and Richard F. Thompson performed a series of detailed Pavlovian eye-blink conditioning experiments, the results of which led to the Thompson-Mauk model that proposed a neural mechanism by which

CS-US associations were flexibly encoded and responsible for the emergence of the eye-blink CR¹⁸. This model defines the brainstem and cerebellum as the key sites for the neural circuits that are necessary and sufficient for the expression of conditioned eye-blink responses. Moreover, this model addresses directly the involvement of the CR pathway within these structures while providing indirect evidence that the US pathway may also be involved.

Eye-blink conditioning is in essence another form of fear/defensive conditioning, which has been studied in cats, rabbits, ferrets and rodents¹⁹⁻²⁴. There are two fundamentally different types of eye-blink conditioning; delay and trace eye-blink conditioning. In delay eye-blink conditioning, the CS and US overlap and co-terminate, such that the eye-blink and/or nictitating membrane response is a result of pairing between an aversive US (e.g., corneal air puff or electrical stimulation) with a previously neutral CS (e.g., tone or light). Initially, the CS does not evoke reliable or robust eye-blink responses. However, following repeatedly paired CS-US presentations (typically a few hundred pairings), animals gradually develop a precisely timed eyelid closure response (CR)^{25,26,27}. In trace eye-blink conditioning, there is a short baseline interval that separates the CS and the US²⁷. Unlike delay eye-blink conditioning, which appears to have non-declarative memory properties, trace eye-blink conditioning shares several features with declarative memory, most notably the fact that learning depends on the hippocampus^{28,29}.

2. Role of the Amygdala's distinct nuclei in fear and eye-blink conditioning

Numerous studies have tried to detect and distinguish brain region(s) that govern the formation of fear and eye-blink conditioning. Here, I will describe the overall view and understanding of how different amygdala nuclei have roles in the neural circuitry of these two different types of associative learning paradigms.

2.1 Lateral and central nuclei of amygdala required in fear conditioning

Since fear learning is rapid, robust and generally long-lasting, fear conditioning has become the most widely used paradigm for investigating the neural circuitry underlying the formation of emotionally-valent memories. In the late 1930s,

researchers observed that damage to the temporal lobe resulted in vital changes of several behaviors including fear reactivity³⁰. In particular, it became evident that damage to the amygdala accounted for changes in emotional processing³¹. The amygdala is an almond-shaped structure deep within the medial temporal lobe, which consists of approximately 13 different regions/nuclei³². Amongst these, the interconnected lateral (LA), basal (B) (the LA and B together forms the basolateral complex), central (CeA), and accessory basal (AB) nuclei are most critical to fear learning^{6,32}.

Studies to determine the role of the CeA in the neural circuit of fear conditioning were initiated in 1972 by Blanchard³³. Lesion studies or pharmacological manipulations exclusive to or including the CeA resulted in a disruption of the acquisition and expression of autonomic and behavioral conditioned fear responses³⁴⁻³⁹. This is due to the fact that the CeA projects to brainstem regions that regulate the expression of fear responses⁴⁰, indicating that this region is a major output nucleus of the amygdala. Considerable evidence suggested that the CeA receives direct projections from the LA^{41,42,43}, which led to more investigations, initiated by LeDoux in 1990, to study the role of the LA in fear conditioning processing. LeDoux demonstrated that electrolytic lesions of the LA interfered with fear expression/freezing responses to an auditory CS¹⁴. This finding shifted the emphasis from the central to the lateral nucleus in the search for sites of plasticity. Later, more detailed studies indicated that the LA projects to the CeA, also, indirectly through the B and BA nuclei of the amygdala^{44,45} as lesions of these two nuclei have no effect on fear conditioning responses to an auditory CS^{46,47,48}. Anterograde and retrograde tracing, as well as single-neuron recordings experiments revealed that during fear conditioning, auditory (CS) and aversive (US) information are conveyed from auditory thalamus/cortex and somatosensory thalamus/cortex into the LA respectively, which is the site of termination of both the CS and US inputs pathways^{49,50,51} as well as the primary site of their anatomical convergence⁵². Moreover, only in the dorsal subregion of the LA does the convergence of the CS and US occur⁵², indicating that dorsal LA is particularly crucial in the neural pathways underlying the CS-US association.

The LA connects with the CeA through the B, AB and intercalated cell masses (ICM) of the amygdala¹². In turn, the CeA connects with the hypothalamic and brainstem

areas, where defensive behavior and autonomic and endocrine responses are expressed and controlled^{6,53,54,55} (Figure 1). It has also been shown that the prelimbic cortex is involved in fear expression⁵⁶.

Several studies with disruption approaches were performed to understand the influence or direct effects of these regions on fear conditioning acquisition and/or expression. For example, lesions or temporary inactivation of the LA during conditioning interfered with the acquisition of conditioned fear responses^{14,47,57,58}. Moreover, it was reported that the CeA lesions caused deficits of aversive conditioning^{38,34,47}. In addition, local infusions of drugs affecting the CeA during acquisition prevented the formation of long-term memory⁵⁹. Damage to the lateral hypothalamus affected blood pressure but not freezing responses, and damage to the periaqueductal gray matter in the brainstem interfered with freezing but not blood pressure responses⁴⁰.

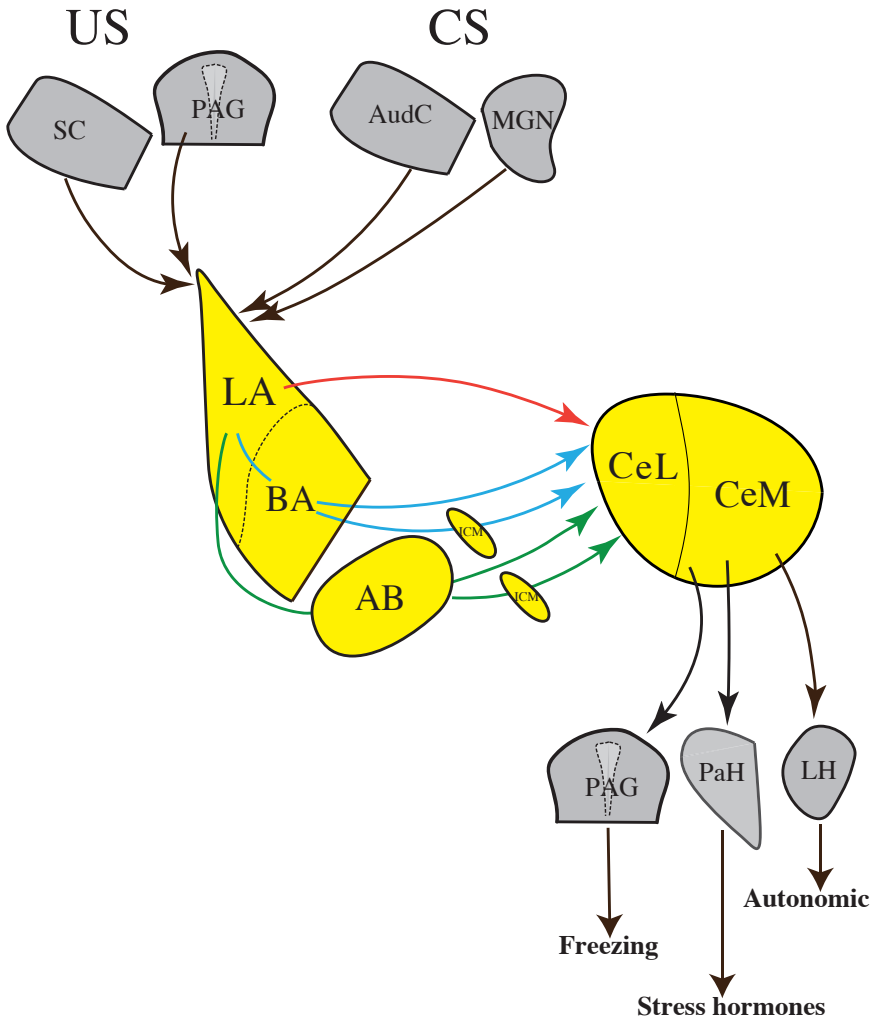


Fig1: Fear conditioning circuit. Auditory inputs via cortical and thalamic (MGN) auditory pathways converge with the cortical and thalamic somatosensory inputs in the LA, leading to synaptic plasticity in the LA. LA connects with CeL directly and indirectly through B, AB, and ICM. CeM connects with hypothalamus and brainstem regions (PAG) that control the expression of fear responses, such as freezing and autonomic and hormonal responses. LA: lateral amygdala, BA: basal amygdala, AB: accessory basal, ICM: intercalated cell masses, CeL: lateral division of central nucleus of amygdala (CeA), CeM: medial division of the CeA, PAG: periaqueductal gray, LH: lateral hypothalamus, PaH: paraventricular nucleus of the hypothalamus, AudC: auditory cortex, SC: somatosensory cortex, MGN: medial geniculate nucleus.

2.2 Amygdala involvement in cerebellar dependent eye-blink conditioning

Eye-blink conditioning has proven to be another widely employed paradigm for studying the neural structures and mechanisms underlying cerebellar learning and memory. Historically, the cerebellum was thought to be critical to this form of learning with the first evidence coming in 1984, when Thompson and colleagues showed that lesions to the cerebellum prevented eye-blink conditioning. Single-unit recordings suggested that conditioned responding to the CS, in the form of eyelid closure, was generated by activation of the deep cerebellar interpositus nucleus^{60,7}. Since then, extensive studies have defined the rather complex neural circuits of eye-blink conditioning. The auditory CS engages mossy fibers derive from the pontine nuclei⁶¹, while the aversive US activates climbing fibers originate in the inferior olivary nucleus⁶². Anatomical and physiological studies reveal that mossy fibers and climbing fibers terminate in the cerebellar nuclei and cerebellar cortex (onto Purkinje cells) respectively^{63,64,65}, indicating that these two regions are the sites of CS-US convergence. Centers in the brainstem are the targets of cerebellar output, where spinal descending pathways originate and account for motor control^{66,67}.

It has long been argued that while the cerebellum is the key structure involved in the acquisition of learned eye-blink responses, other brain regions including the amygdala are also engaged. In 1992, it was reported for the first time that lesions to the amygdala in rabbits significantly reduced the rate of eye-blink conditioning⁶⁸. Furthermore, electrical stimulation of the central nucleus of amygdala in rabbits increased the amplitude of the eye-blink UR induced by a corneal air puff (US)⁶⁹. In addition, the amygdala has been shown to have a modulatory effect on eye-blink conditioning in rats, increasing the effectiveness of the CS⁷⁰. Until 1980, eye-blink conditioning studies were done mostly in cats, rabbits, ferrets, and to a lesser extent in rats. The advent of transgenic mice during the 1980s and 1990s, along with more advanced techniques to measure eyelid movements, opened new doors to investigating the neuronal mechanisms underlying eye-blink conditioning in mice. For example, electromyography (EMG), a method widely used for measuring eye-blink responses in rabbits, was too indirect and sensitive to be used in mice^{71,72}. Therefore, in 2003, Koekkoek and colleagues developed the Magnetic Distance Measurement Technique (MDMT) to overcome this problem. This new method uses magnetically-sensitive

chips, which allows direct and precise detection of the actual eyelid movements with high spatio-temporal resolution in mice⁷³. Using this technique, two different peaks were detected between the startle reflex and the UR: a short-latency response (SLR) and a CR^{74,71}. The SLR was previously introduced by Tonegawa⁷⁵, and confirmed by other studies as well⁷². MDMT allowed for the precise measurement of the timing, duration and peak-amplitude of eyelid responses (Figure 2). Unlike CRs that require repeated CS-US pairings to be induced, the SLR forms at an early stage after only a few CS-US pairings. Given the fact that the acquisition of cerebellar responses and learning is a gradual process and since the SLR is a learned eyelid response acquired rapidly relative to the CR, it raises the question of whether the cerebellum similarly mediates the SLR as previously observed for the CR. In particular, Boele and colleagues proposed in 2010 that the amygdala may be responsible for mediating the SLR in a manner akin to fear conditioning, given the rapid acquisition typical for amygdala-dependent learning⁷⁶.

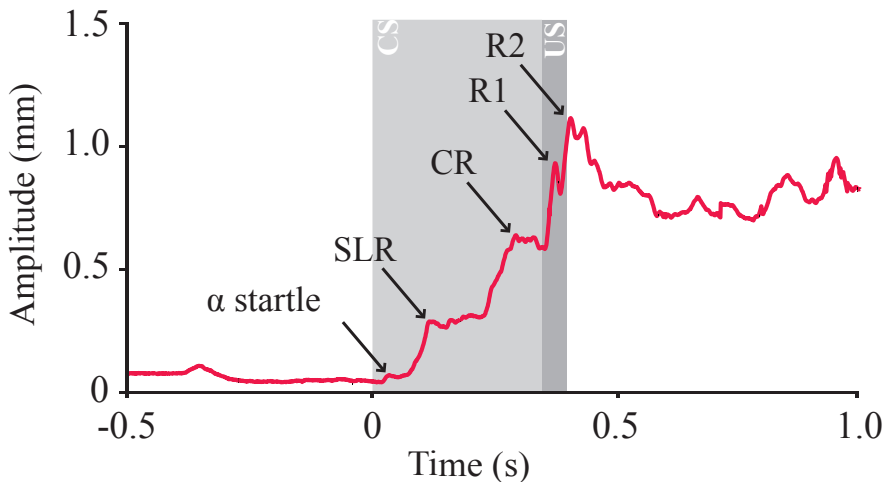


Fig2: Raw data traces from mice during eye-blink conditioning and acoustic startle reflexes. Several peaks can be detected, a small startle response, a short-latency response (SLR), a conditioned response (CR), and two or more unconditioned response peaks (UR1 and UR2). At amplitude 0mm, the eyelid is maximally opened, while at 1mm the eyelid is fully closed. The figure is adopted from H.J. Boele (2010)

2.3 Amygdala- Cerebellum- Dynamic- Conditioning model (ACDC model)

Boele and De Zeeuw introduced a model in 2010, which suggested that the amygdala is involved in the SLR. The Amygdala-Cerebellum Dynamic Conditioning (ACDC) model predicts that while the cerebellum is mainly involved in regulating the well-timed eyelid closure CR, the amygdala contributes to the early associative SLR⁷⁶. This model specifies that during eye-blink conditioning, the tone (CS) and corneal air puff (US) converge on both the amygdala and the cerebellum. These two brain areas collectively control facial nucleus activity, which leads to eyelid closure. They hypothesize that during the early learning phase, after just a few CS-US pairings, the rapidly acquired plasticity of the lateral amygdala leads to conditioned fear CS-US associations, including rapid facial responses such as eyelid closure (SLR). Only following a more extensive number of CS-US pairings does cerebellar-dependent learning (CR) become evident. Direct projections from the amygdala to the pontine nuclei might also contribute to the afferent CS input into the cerebellum⁷⁶.

3. Neural mechanisms of fear memory

To understand the cellular mechanisms that mediate fear memory formation, it is essential to explore the changes in neural activity that occur during fear conditioning, which are facilitated by enhanced transmission at synapses that process the CS, allowing the CS to induce defensive responses^{18,32,77,78}. Structural synaptic changes have long been considered as the neural mechanism underlying the encoding and maintenance of persistent memories. In 1894, Cajal was the first to propose the strengthening of synaptic connections between existing neurons as a possible mechanism of memory formation⁷⁹. In 1949, Hebb proposed a theoretical model that created the modern paradigm for memory research. Hebb's model explains associative learning as a process that involves synaptic modifications and plasticity. When activity in a presynaptic neuron coincides with activity in a postsynaptic neuron, synaptic input may be strengthened⁸⁰. In 1973, Bliss and colleagues investigated this more extensively and presented an experimental model of synaptic plasticity, an activity-dependent long-lasting enhancement of synaptic transmission, termed long term potentiation (LTP), in which brief stimulation with a high-frequency train of action potentials resulted in a prolonged synaptic strength in hippocampal synapses⁸¹.

Later, the cellular model of experience-dependent plasticity LTP was discovered and studied extensively in the hippocampus^{82,83}, which is the foundation of memory formation in the mammalian brain. In a Hebbian model of fear conditioning, neurons of the LA that receive direct auditory and aversive sensory input from the thalamus and cortex, undergo post-synaptically mediated long-term synaptic plasticity mediated by the coincidence between strong depolarization elicited by the US and glutamate binding of post-synaptic receptors from presynaptic inputs carrying CS information inputs^{32,84,85,86}. Electrophysiological recordings both *in vivo* and *ex vivo* indicate that the LA neurons become more responsive to the CS after CS-US pairings^{78,87-90}. Therefore, when a weak input that is normally insufficient to induce LTP is paired with a strong input, the weak input will become potentiated. It has been suggested that LTP induction in pathways that transmit CS input to the LA increases auditory-evoked field potentials, in which LTP-like associative processes occur during auditory fear conditioning^{91,87}.

4. Neuronal identity of fear memory trace

The concept of a memory trace was introduced by Hebb, who proposed that learning resulted from the strengthening of synaptic connections between neurons⁸⁰. He was also the first to suggest that competition between neurons is often needed for refining neural circuitry during development. Extensive approaches have been designed to detect changes in neural substrates from molecular to circuit levels induced by external (associative) sensory inputs, and to define the neural ensemble during encoding, storing and recovering a particular memory. Electrophysiological recordings of single units show that memories are sparsely encoded in neuronal networks⁹²⁻⁹⁶.

Moreover, imaging techniques as well as transgenic methods have been developed to capture learning-induced changes. One of these powerful and widely used tools is based on the induction of immediate early genes (IEGs)⁹⁷⁻¹⁰¹. IEGs are a family of genes that are transcribed transiently and rapidly in response to biological events. Their induction does not require the expression of other genes^{101,102}. Such genes have transcriptional machinery poised just downstream of the start site, resulting in the fastest possible transcriptional activation¹⁰³.

To identify neurons that are active during encoding and investigate them at time points after initial consolidation, multiple studies have been designed based on the activity of various IEGs, including *activity-regulated cytoskeleton-associated protein (Arc)*, finkel-biskis-jinkins murine osteogenic sarcoma virus (FBJ MSV) or *c-Fos*, and *Zif268*^{104–109}. Given the fact that endogenous IEGs are transiently expressed and in order to tackle this temporal limitation, transgenic mice have been engineered in which the IEG promoter region is used to drive the transcription of a genetically-encoded reporter^{110,111,112}.

4.1 Neuronal trace selection

Although an ~70% of the neurons in the LA receive auditory inputs during fear conditioning, only ~25% exhibit learning-induced synaptic plasticity^{78,77}. Viral overexpression of CREB in a small, random subset (~15%) of neurons in the LA resulted in their preferential recruitment into a subsequently encoded fear memory trace¹¹³. Moreover, selective ablation of these neurons after fear conditioning resulted in a loss of expression of that particular fear memory¹¹⁴. Since overexpression of CREB did not change the total number of neurons recruited to a memory trace, the authors concluded that competitive neuronal processes determine cellular participation in the memory trace. In line with this, another study showed that the inactivation of a subset of LA neurons expressing fluorescently-tagged CREB during training resulted in disruption of fear memory¹¹⁵. Whole-cell recordings of these transduced neurons revealed that neurons with higher CREB showed higher neuronal excitability at the time of learning. This study led to a model whereby CREB functions to regulate the allocation of fear memory to specific cells in the LA. In other studies, *Arc* RNA expression was used to screen recently active neurons. Neurons with higher CREB activity at the time of training had a higher probability to be active during retrieval compared to their neighbors with lower CREB activity. This indicated the regulatory effect of CREB on neuronal activation during retrieval¹¹⁶. These studies suggest that the recruitment of neurons into a fear memory trace has a selective nature, and there seems to be a competition amongst the neurons based on their state of activity, arguing that the increased level of the CREB transcription has a defining role during fear memory neuronal selection. Overall, these selection approaches revealed how a particular driving element can bias a learning-induced alteration and

allocation exclusive to a subset of neurons. However, excessive expression of CREB results in significant alterations of intrinsic cell physiology, thereby precluding the assessment of endogenous physiological alterations during encoding.

5. Scope and outline of this thesis

Aversive associative learning is a process that requires experience-dependent synaptic modifications among a small subset of neurons. The mechanism by which specific cells undergo plastic changes is a critical question in the field of learning and memory. Moreover, defining the distribution pattern of the cells within the regions that are activated due to a memory formation can shed light on the differential involvement of neuronal subsets within that memory trace. Therefore, reliable methods are necessary to capture, visualize, and monitor learning-induced changes in specific neuronal ensembles responsible for encoding a given memory.

In chapter 2, we used the *Arc::dVenus* transgenic mouse as a reporter of *Arc* transcription to detect cells that are recruited into the LA fear memory trace. We showed that intrinsic neuronal excitability governs the selective recruitment of LA neurons into the fear memory trace. We also demonstrated that the potentiation of glutamatergic synaptic transmission from the thalamic input pathway to the LA was learning-specific, and highly localized in the *Arc* expressing neurons.

In chapter 3, we distinguished *Arc* expression in a specific subpopulation in the ventrolateral part of the LA. We found that this subset of neurons is induced only due to new learning, when there is a prominent difference between expectation and experience.

In chapter 4, we used the eye-blink conditioning paradigm to study the role of the central nucleus of the amygdala (CeA) in aversive learning. We applied an optogenetic approach using the somatostatin (SST)-Cre mouse to investigate the origin of the short-latency eyelid response. We examined the distinct role of somatostatin cells in the lateral division of the CeA in generating conditioned eyelid responses. In addition, we also suggested a regulating function of the CeA for acquisition of cerebellum-dependent eye-blink conditioning.

Finally, in chapter 5, I will discuss the main outcomes of each of the above studies, giving an overview of the major conclusions of my research, and suggest future studies that might tackle some additional open questions, which are still unanswered in the field.

References

1. Kandel, E. R., Dudai, Y. & Mayford, M. R. The molecular and systems biology of memory. *Cell* **157**, 163–86 (2014).
2. Levitan, I. B. & Kaczmarek, L. K. *The neuron : cell and molecular biology*. (Oxford University Press, 1991).
3. Groves, P. M. & Thompson, R. F. Habituation: a dual-process theory. *Psychological review* **77**, 419–50 (1970).
4. Pavlov, I. P. *Conditioned reflexes*. (1927).
5. Grosso, A., Cambiaghi, M., Concina, G., Sacco, T. & Sacchetti, B. Auditory cortex involvement in emotional learning and memory. *Neuroscience* **299**, 45–55 (2015).
6. LeDoux, J. E. Emotion circuits in the brain. *Annual review of neuroscience* **23**, 155–84 (2000).
7. McCormick, D. A. & Thompson, R. F. Cerebellum: essential involvement in the classically conditioned eyelid response. *Science (New York, N.Y.)* **223**, 296–9 (1984).
8. BROWN, J. S., KALISH, H. I. & FARBER, I. E. Conditioned fear as revealed by magnitude of startle response to an auditory stimulus. *Journal of experimental psychology* **41**, 317–28 (1951).
9. Bolles, R. C. & Fanselow, M. S. A perceptual–defensive–recuperative model of fear and pain.
10. Rescorla, R. A. & Wagner, A. R. “A theory of Pavlovian conditioning: Variations in the effectiveness of reinforcement,.” **Vol. 2**, (1972).
11. Huff, N. C., Wright-Hardesty, K. J., Higgins, E. A., Matus-Amat, P. & Rudy, J. W. Context pre-exposure obscures amygdala modulation of contextual-fear conditioning. *Learning & memory (Cold Spring Harbor, N.Y.)* **12**, 456–60
12. Johansen, J. P., Cain, C. K., Ostroff, L. E. & LeDoux, J. E. Molecular mechanisms of fear learning and memory. *Cell* **147**, 509–24 (2011).
13. Phillips, R. G. & LeDoux, J. E. Differential contribution of amygdala and hippocampus to cued and contextual fear conditioning. *Behavioral neuroscience* **106**, 274–85 (1992).
14. LeDoux, J. E., Cicchetti, P., Xagoraris, A. & Romanski, L. M. The lateral amygdaloid nucleus: sensory interface of the amygdala in fear conditioning. *The Journal of neuroscience : the official journal of the Society for Neuroscience* **10**, 1062–9 (1990).
15. Maren, S., Phan, K. L. & Liberzon, I. The contextual brain: implications for fear conditioning, extinction and psychopathology. *Nature reviews. Neuroscience* **14**, 417–28 (2013).
16. Frankland, P. W., Cestari, V., Filipkowski, R. K., McDonald, R. J. & Silva, A. J. The dorsal hippocampus is essential for context discrimination but not for contextual conditioning. *Behavioral neuroscience* **112**, 863–74 (1998).

17. Tallot, L., Doyère, V. & Sullivan, R. M. Developmental emergence of fear/threat learning: neurobiology, associations and timing. *Genes, Brain and Behavior* **15**, 144–154 (2016).
18. Mauk, M. D. & Thompson, R. F. Retention of classically conditioned eyelid responses following acute decerebration. *Brain research* **403**, 89–95 (1987).
19. Mauk, M. D., Steinmetz, J. E. & Thompson, R. F. Classical conditioning using stimulation of the inferior olive as the unconditioned stimulus. *Proceedings of the National Academy of Sciences of the United States of America* **83**, 5349–53 (1986).
20. McCormick, D. A. *et al.* The engram found? Role of the cerebellum in classical conditioning of nictitating membrane and eyelid responses. *Bulletin of the Psychonomic Society* **18**, 103–105 (2013).
21. McCormick, D. A., Lavond, D. G. & Thompson, R. F. Concomitant classical conditioning of the rabbit nictitating membrane and eyelid responses: correlations and implications. *Physiology & behavior* **28**, 769–75 (1982).
22. Yeo, C. H. & Hardiman, M. J. Cerebellar cortex and eyeblink conditioning: a reexamination. *Experimental brain research* **88**, 623–38 (1992).
23. Hesslow, G. & Ivarsson, M. Suppression of cerebellar Purkinje cells during conditioned responses in ferrets. *Neuroreport* **5**, 649–52 (1994).
24. Rasmussen, A., Jirenhed, D.-A. & Hesslow, G. Simple and complex spike firing patterns in Purkinje cells during classical conditioning. *Cerebellum (London, England)* **7**, 563–6 (2008).
25. Gormezano, I. Investigations of defense and reward conditioning in the rabbit. *Current research and theory* 151–181 (1972).
26. J, G. I. & K. E. Classical conditioning: Some methodological conceptual issues. *In Handbook of learning and cognitive processes, ed. W. K. Estes* **2**, 143–179 (1975).
27. Kehoe, E. J., Ludvig, E. A. & Sutton, R. S. Magnitude and timing of conditioned responses in delay and trace classical conditioning of the nictitating membrane response of the rabbit (*Oryctolagus cuniculus*). *Behavioral neuroscience* **123**, 1095–101 (2009).
28. Clark, R. E. & Squire, L. R. Classical conditioning and brain systems: the role of awareness. *Science (New York, N.Y.)* **280**, 77–81 (1998).
29. McGlinchey-Berroth, R., Carrillo, M. C., Gabrieli, J. D., Brawn, C. M. & Disterhoft, J. F. Impaired trace eyeblink conditioning in bilateral, medial-temporal lobe amnesia. *Behavioral neuroscience* **111**, 873–82 (1997).
30. Kluver H, B. P. “Psychic blindness” and other symptoms following bilateral temporal lobectomy in Rhesus monkeys. *Am J Physiol* 352– 353 (1937).
31. LaBar, K. S. & Phelps, E. A. Arousal-Mediated Memory Consolidation: Role of the Medial Temporal Lobe in Humans. *Psychological Science* **9**, 490–493 (1998).

32. Sah, P., Faber, E. S. L., Lopez De Armentia, M. & Power, J. The amygdaloid complex: anatomy and physiology. *Physiological reviews* **83**, 803–34 (2003).
33. Blanchard, D. C. & Blanchard, R. J. Innate and conditioned reactions to threat in rats with amygdaloid lesions. *Journal of comparative and physiological psychology* **81**, 281–90 (1972).
34. Kapp, B. S., Frysinger, R. C., Gallagher, M. & Haselton, J. R. Amygdala central nucleus lesions: effect on heart rate conditioning in the rabbit. *Physiology & behavior* **23**, 1109–17 (1979).
35. Gallagher, M., B. S. Kapp, J. P. Pascoe, and R. P. R. A neuropharmacology of the amygdala systems which contribute to learning and memory. In *The Amygdaloid Complex, Elsevier, Amsterdam*. Y. Ben-Ari, ed 343–354 (1981).
36. Gentile, C. G., Jarrell, T. W., Teich, A., McCabe, P. M. & Schneiderman, N. The role of amygdaloid central nucleus in the retention of differential pavlovian conditioning of bradycardia in rabbits. *Behavioural brain research* **20**, 263–73 (1986).
37. Hitchcock, J. M., and M. D. Amygdala lesions block fearenhanced startle using either visual or auditory conditioned stimuli. *Sot. Neurosci Abstr* 752 (1986).
38. Iwata, J., LeDoux, J. E., Meeley, M. P., Arneric, S. & Reis, D. J. Intrinsic neurons in the amygdaloid field projected to by the medial geniculate body mediate emotional responses conditioned to acoustic stimuli. *Brain research* **383**, 195–214 (1986).
39. Krettek, J. E. & Price, J. L. A description of the amygdaloid complex in the rat and cat with observations on intra-amygdaloid axonal connections. *The Journal of comparative neurology* **178**, 255–80 (1978).
40. LeDoux, J. E., Iwata, J., Cicchetti, P. & Reis, D. J. Different projections of the central amygdaloid nucleus mediate autonomic and behavioral correlates of conditioned fear. *The Journal of neuroscience : the official journal of the Society for Neuroscience* **8**, 2517–29 (1988).
41. Roberts, G. W., Woodhams, P. L., Polak, J. M. & Crow, T. J. Distribution of neuropeptides in the limbic system of the rat: the amygdaloid complex. *Neuroscience* **7**, 99–131 (1982).
42. Amaral, D. G. & Amaral, D. G. in *Comprehensive Physiology* (John Wiley & Sons, Inc., 2011). doi:10.1002/cphy.cp010507
43. Nitecka, L. & Frotscher, M. Organization and synaptic interconnections of GABAergic and cholinergic elements in the rat amygdaloid nuclei: single- and double-immunolabeling studies. *The Journal of comparative neurology* **279**, 470–88 (1989).
44. Pitkänen, A., Savander, V. & LeDoux, J. E. Organization of intra-amygdaloid circuitries in the rat: an emerging framework for understanding functions of the amygdala. *Trends in neurosciences* **20**, 517–23 (1997).

45. Paré, D. & Smith, Y. Intrinsic circuitry of the amygdaloid complex: common principles of organization in rats and cats. *Trends in neurosciences* **21**, 240–1 (1998).
46. Nader, K. Damage to the Lateral and Central, but Not Other, Amygdaloid Nuclei Prevents the Acquisition of Auditory Fear Conditioning. *Learning & Memory* **8**, 156–163 (2001).
47. Amorapanth, P., LeDoux, J. E. & Nader, K. Different lateral amygdala outputs mediate reactions and actions elicited by a fear-arousing stimulus. *Nature neuroscience* **3**, 74–9 (2000).
48. Majidishad, P., Pelli, D. G. & LeDoux, J. E. Disruption of fear conditioning to contextual stimuli but not to a tone by lesions of the accessory basal nucleus of the amygdala. *Soc. Neurosci. Abstr* 1116 (1996).
49. Shi, C. & Davis, M. Pain Pathways Involved in Fear Conditioning Measured with Fear-Potentiated Startle: Lesion Studies. *J. Neurosci.* **19**, 420–430 (1999).
50. LeDoux, J. E., Farb, C. & Ruggiero, D. A. Topographic organization of neurons in the acoustic thalamus that project to the amygdala. *The Journal of neuroscience : the official journal of the Society for Neuroscience* **10**, 1043–54 (1990).
51. Romanski, L. M. & LeDoux, J. E. Information cascade from primary auditory cortex to the amygdala: corticocortical and corticoamygdaloid projections of temporal cortex in the rat. *Cerebral cortex (New York, N.Y. : 1991)* **3**, 515–32
52. Romanski, L. M., Clugnet, M. C., Bordi, F. & LeDoux, J. E. Somatosensory and auditory convergence in the lateral nucleus of the amygdala. *Behavioral neuroscience* **107**, 444–50 (1993).
53. Fanselow, M. S. & Poulos, A. M. The neuroscience of mammalian associative learning. *Annual review of psychology* **56**, 207–34 (2005).
54. Davis, M. & Whalen, P. J. The amygdala: vigilance and emotion. *Molecular psychiatry* **6**, 13–34 (2001).
55. Kim, J. J. & Jung, M. W. Neural circuits and mechanisms involved in Pavlovian fear conditioning: a critical review. *Neuroscience and biobehavioral reviews* **30**, 188–202 (2006).
56. Sotres-Bayon, F. & Quirk, G. J. Prefrontal control of fear: more than just extinction. *Current opinion in neurobiology* **20**, 231–5 (2010).
57. Maren, S. Neurobiology of Pavlovian fear conditioning. *Annual review of neuroscience* **24**, 897–931 (2001).
58. Ledoux, J. E. & Muller, J. Emotional memory and psychopathology. *Philosophical transactions of the Royal Society of London. Series B, Biological sciences* **352**, 1719–26 (1997).
59. Bahar, A., Samuel, A., Hazvi, S. & Dudai, Y. The amygdalar circuit that

- acquires taste aversion memory differs from the circuit that extinguishes it. *European Journal of Neuroscience* **17**, 1527–1530 (2003).
60. McCormick, D. A. & Thompson, R. F. Neuronal responses of the rabbit cerebellum during acquisition and performance of a classically conditioned nictitating membrane-eyelid response. *The Journal of neuroscience : the official journal of the Society for Neuroscience* **4**, 2811–22 (1984).
 61. Aitkin, L. M. & Boyd, J. Acoustic input to the lateral pontine nuclei. *Hearing research* **1**, 67–77 (1978).
 62. Sears, L. L. & Steinmetz, J. E. Dorsal accessory inferior olive activity diminishes during acquisition of the rabbit classically conditioned eyelid response. *Brain research* **545**, 114–22 (1991).
 63. Eccles, J. C., Ito, M. & Szentágothai, J. *The Cerebellum as a Neuronal Machine*. (Springer Berlin Heidelberg, 1967). doi:10.1007/978-3-662-13147-3
 64. Llinas, R. *Handbook of Physiology II. The Nervous System* (ed. Brokks, V. B.). (1981).
 65. Voogd, J. & Glickstein, M. The anatomy of the cerebellum. *Trends in neurosciences* **21**, 370–5 (1998).
 66. Middleton, F. A. & Strick, P. L. Cerebellar output channels. *International review of neurobiology* **41**, 61–82 (1997).
 67. Ito, M. *The Cerebellum and Neural Control*. (1984).
 68. Weisz, D. J., Harden, D. G. & Xiang, Z. Effects of amygdala lesions on reflex facilitation and conditioned response acquisition during nictitating membrane response conditioning in rabbit. *Behavioral neuroscience* **106**, 262–73 (1992).
 69. Whalen, P. J. & Kapp, B. S. Contributions of the amygdaloid central nucleus to the modulation of the nictitating membrane reflex in the rabbit. *Behavioral neuroscience* **105**, 141–53 (1991).
 70. Ng, K. H. & Freeman, J. H. Amygdala inactivation impairs eyeblink conditioning in developing rats. *Developmental psychobiology* **56**, 999–1007 (2014).
 71. Koekkoek, S. K. E. *et al.* Deletion of FMR1 in Purkinje cells enhances parallel fiber LTD, enlarges spines, and attenuates cerebellar eyelid conditioning in Fragile X syndrome. *Neuron* **47**, 339–52 (2005).
 72. Vogel, R. W., Ewers, M., Ross, C., Gould, T. J. & Woodruff-Pak, D. S. Age-related impairment in the 250-millisecond delay eyeblink classical conditioning procedure in C57BL/6 mice. *Learning & memory (Cold Spring Harbor, N.Y.)* **9**, 321–36
 73. Koekkoek, S. K. E., Den Ouden, W. L., Perry, G., Highstein, S. M. & De Zeeuw, C. I. Monitoring kinetic and frequency-domain properties of eyelid responses in mice with magnetic distance measurement technique. *Journal of neurophysiology* **88**, 2124–33 (2002).

74. Koekkoek, S. K. E. *et al.* Cerebellar LTD and learning-dependent timing of conditioned eyelid responses. *Science (New York, N.Y.)* **301**, 1736–9 (2003).
75. Aiba, A. *et al.* Deficient cerebellar long-term depression and impaired motor learning in mGluR1 mutant mice. *Cell* **79**, 377–88 (1994).
76. Boele, H.-J., Koekkoek, S. K. E. & De Zeeuw, C. I. Cerebellar and extra-cerebellar involvement in mouse eyeblink conditioning: the ACDC model. *Frontiers in cellular neuroscience* **3**, 19 (2010).
77. Rumpel, S., LeDoux, J., Zador, A. & Malinow, R. Postsynaptic receptor trafficking underlying a form of associative learning. *Science (New York, N.Y.)* **308**, 83–8 (2005).
78. Repa, J. C. *et al.* Two different lateral amygdala cell populations contribute to the initiation and storage of memory. *Nature neuroscience* **4**, 724–31 (2001).
79. Cajal, S. R. Y. The Croonian Lecture: La Fine Structure des Centres Nerveux. *Proceedings of the Royal Society of London* **55**, 444–468 (1894).
80. Hebb, D. . *The Organization of Behavior*. (John Wiley and Sons, 1949).
81. Bliss, T. V & Lomo, T. Long-lasting potentiation of synaptic transmission in the dentate area of the anaesthetized rabbit following stimulation of the perforant path. *The Journal of physiology* **232**, 331–56 (1973).
82. Mulkey, R. M. & Malenka, R. C. Mechanisms underlying induction of homosynaptic long-term depression in area CA1 of the hippocampus. *Neuron* **9**, 967–75 (1992).
83. Kandel, E. R. & Spencer, W. A. Cellular neurophysiological approaches in the study of learning. *Physiological reviews* **48**, 65–134 (1968).
84. Blair, H. T., Schafe, G. E., Bauer, E. P., Rodrigues, S. M. & LeDoux, J. E. Synaptic plasticity in the lateral amygdala: a cellular hypothesis of fear conditioning. *Learning & memory (Cold Spring Harbor, N.Y.)* **8**, 229–42
85. Paré, D. Mechanisms of Pavlovian fear conditioning: has the engram been located? *Trends in neurosciences* **25**, 436–7; discussion 437–8 (2002).
86. Sah, P., Westbrook, R. F. & Lüthi, A. Fear conditioning and long-term potentiation in the amygdala: what really is the connection? *Annals of the New York Academy of Sciences* **1129**, 88–95 (2008).
87. Rogan, M. T., Stäubli, U. V & LeDoux, J. E. Fear conditioning induces associative long-term potentiation in the amygdala. *Nature* **390**, 604–7 (1997).
88. Paré, D. & Collins, D. R. Neuronal correlates of fear in the lateral amygdala: multiple extracellular recordings in conscious cats. *The Journal of neuroscience : the official journal of the Society for Neuroscience* **20**, 2701–10 (2000).
89. Maren, S. Auditory fear conditioning increases CS-elicited spike firing in lateral amygdala neurons even after extensive overtraining. *The European journal of neuroscience* **12**, 4047–54 (2000).
90. McKernan, M. G. & Shinnick-Gallagher, P. Fear conditioning induces a

- lasting potentiation of synaptic currents in vitro. *Nature* **390**, 607–11 (1997).
91. Rogan, M. T. & LeDoux, J. E. LTP is accompanied by commensurate enhancement of auditory-evoked responses in a fear conditioning circuit. *Neuron* **15**, 127–36 (1995).
 92. O’Keefe, J. Place units in the hippocampus of the freely moving rat. *Experimental neurology* **51**, 78–109 (1976).
 93. Sutherland, G. R. & McNaughton, B. Memory trace reactivation in hippocampal and neocortical neuronal ensembles. *Current opinion in neurobiology* **10**, 180–6 (2000).
 94. Thompson, R. F. In Search of Memory Traces. (2004). at <<http://www.annualreviews.org/doi/abs/10.1146/annurev.psych.56.091103.070239>>
 95. Sigurdsson, T., Doyère, V., Cain, C. K. & LeDoux, J. E. Long-term potentiation in the amygdala: A cellular mechanism of fear learning and memory. *Neuropharmacology* **52**, 215–227 (2007).
 96. Oh, M. M., Kuo, A. G., Wu, W. W., Sametsky, E. A. & Disterhoft, J. F. Water-maze learning enhances excitability of CA1 pyramidal neurons. *Journal of neurophysiology* **90**, 2171–9 (2003).
 97. Guzowski, J. F. Insights into immediate-early gene function in hippocampal memory consolidation using antisense oligonucleotide and fluorescent imaging approaches. *Hippocampus* **12**, 86–104 (2002).
 98. Horn, G. Pathways of the past: the imprint of memory. *Nature reviews. Neuroscience* **5**, 108–20 (2004).
 99. Horn, G. *Memory, imprinting, and the brain : an inquiry into mechanisms*. (Clarendon Press, 1985).
 100. Radulovic, J., Kammermeier, J. & Spiess, J. Relationship between fos production and classical fear conditioning: effects of novelty, latent inhibition, and unconditioned stimulus preexposure. *The Journal of neuroscience : the official journal of the Society for Neuroscience* **18**, 7452–61 (1998).
 101. Guzowski, J. F., McNaughton, B. L., Barnes, C. A. & Worley, P. F. Environment-specific expression of the immediate-early gene Arc in hippocampal neuronal ensembles. *Nature neuroscience* **2**, 1120–4 (1999).
 102. Sakaguchi, M. *et al.* Catching the engram: strategies to examine the memory trace. *Molecular Brain* **5**, 32 (2012).
 103. Saha, R. N. *et al.* Rapid activity-induced transcription of Arc and other IEGs relies on poised RNA polymerase II. *Nature neuroscience* **14**, 848–56 (2011).
 104. Greenberg, M. E. & Ziff, E. B. Stimulation of 3T3 cells induces transcription of the c-fos proto-oncogene. *Nature* **311**, 433–8
 105. Curran, T. & Morgan, J. I. Superinduction of c-fos by nerve growth factor in the presence of peripherally active benzodiazepines. *Science (New York, N.Y.)* **229**, 1265–8 (1985).
 106. Morgan, J. I. & Curran, T. Stimulus-transcription coupling in neurons: role of

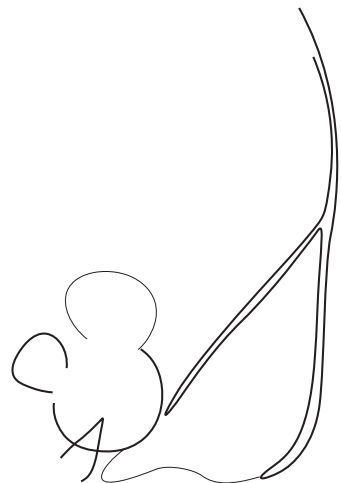
- cellular immediate-early genes. *Trends in neurosciences* **12**, 459–62 (1989).
107. Link, W. *et al.* Somatodendritic expression of an immediate early gene is regulated by synaptic activity. *Proceedings of the National Academy of Sciences of the United States of America* **92**, 5734–8 (1995).
108. Lyford, G. L. *et al.* Arc, a growth factor and activity-regulated gene, encodes a novel cytoskeleton-associated protein that is enriched in neuronal dendrites. *Neuron* **14**, 433–45 (1995).
109. Hall, J., Thomas, K. L. & Everitt, B. J. Cellular imaging of zif268 expression in the hippocampus and amygdala during contextual and cued fear memory retrieval: selective activation of hippocampal CA1 neurons during the recall of contextual memories. *The Journal of neuroscience : the official journal of the Society for Neuroscience* **21**, 2186–93 (2001).
110. Reijmers, L. G., Perkins, B. L., Matsuo, N. & Mayford, M. Localization of a stable neural correlate of associative memory. *Science (New York, N.Y.)* **317**, 1230–3 (2007).
111. Denny, C. A. *et al.* Hippocampal memory traces are differentially modulated by experience, time, and adult neurogenesis. *Neuron* **83**, 189–201 (2014).
112. Guenther, C. J., Miyamichi, K., Yang, H. H., Heller, H. C. & Luo, L. Permanent genetic access to transiently active neurons via TRAP: targeted recombination in active populations. *Neuron* **78**, 773–84 (2013).
113. Han, J.-H. *et al.* Neuronal competition and selection during memory formation. *Science (New York, N.Y.)* **316**, 457–60 (2007).
114. Han, J.-H. *et al.* Selective erasure of a fear memory. *Science (New York, N.Y.)* **323**, 1492–6 (2009).
115. Zhou, Y. *et al.* CREB regulates excitability and the allocation of memory to subsets of neurons in the amygdala. *Nat Neurosci* **12**, 1438–43 (2009).
116. Josselyn, S. A. Continuing the search for the engram: examining the mechanism of fear memories. *Journal of psychiatry & neuroscience : JPN* **35**, 221–8 (2010).

Chapter 2

Arc expression identifies the lateral amygdala fear memory trace

Gouty-Colomer LA, Hosseini B, Marcelo IM, Schreiber J, Slump DE,
Yamaguchi S, Houweling AR, Jaarsma D, Elgersma Y, Kushner SA

Molecular Psychiatry **21**, 364–375 (2016)



*Arc expression identifies the lateral amygdala
fear memory trace*

Gouty-Colomer LA^{1,6,7*}, Hosseini B^{1*}, Marcelo IM^{1,2}, Schreiber J³, Slump DE¹, Yamaguchi S^{4,5}, Houweling AR³, Jaarsma D³, Elgersma Y³, Kushner SA¹

**equal Contribution*

¹ Department of Psychiatry, Erasmus University Medical Center, Dr. Molewaterplein 50, 3015 GE Rotterdam, The Netherlands

² Champalimaud Neuroscience Programme, Champalimaud Centre for the Unknown, Av. Brasília s/n, 1400-038 Lisbon, Portugal

³ Department of Neuroscience, Erasmus Medical Centre, Dr. Molewaterplein 50, 3015 GE Rotterdam, The Netherlands

⁴ Division of Morphological Neuroscience, Gifu University Graduate School of Medicine, 1-1 Yanagido, Gifu 501-1194, Japan

⁵ PRESTO, Japan Science and Technology Agency (JST), 4-1-8 Honcho Kawaguchi, Saitama 332-0012, Japan

⁶ Present address: Aix Marseille Université UMR 901, Marseille, France

⁷ Present address: Institut national de la Recherche Médicale et de la Santé Inserm, INMED UMR 901, Marseille, France

Molecular Psychiatry **21**, 364–375 (2016)

Running title: Defining the lateral amygdala fear memory trace.

ABSTRACT

Memories are encoded within sparsely distributed neuronal ensembles. However, the defining cellular properties of neurons within a memory trace remain incompletely understood. Using a fluorescence-based *Arc* reporter, we were able to visually identify the distinct subset of lateral amygdala (LA) neurons activated during auditory fear conditioning. We found that *Arc* expressing neurons have enhanced intrinsic excitability and are preferentially recruited into newly encoded memory traces. Furthermore, synaptic potentiation of thalamic inputs to the LA during fear conditioning is learning-specific, postsynaptically-mediated, and highly localized to *Arc* expressing neurons. Taken together, our findings validate the immediate-early gene *Arc* as a molecular marker for the LA neuronal ensemble recruited during fear learning. Moreover, these results establish a model of fear memory formation in which intrinsic excitability determines neuronal selection, while learning-related encoding is governed by synaptic plasticity.

INTRODUCTION

Fear conditioning is a robust form of associative learning in which a previously neutral conditioned stimulus (CS) comes to predict an aversive unconditioned event, eliciting defensive behaviours and fearful emotions¹. The neurobiological circuitry underlying auditory fear learning has been extensively investigated, for which the lateral amygdala (LA) has overwhelming evidence as a critical site of plasticity^{2,3}. In particular, long-term N-methyl-D-aspartate receptor (NMDAR)-dependent synaptic potentiation of glutamatergic inputs onto LA principal neurons remains the leading candidate mechanism for fear memory encoding⁴. Accordingly, both genetic and pharmacological blockade of synaptic plasticity in the LA prevent the formation of long-term fear memories⁵⁻⁹, while potentiation of glutamatergic synaptic transmission onto LA pyramidal neurons is induced by fear conditioning^{5,6,10-12}.

Intriguingly, only a limited subset of neurons appears to be recruited during fear memory encoding. In particular, recent studies have implicated the cAMP response element-binding protein (CREB) as a critical factor guiding LA neuron recruitment into a fear memory network. Targeted restoration of CREB expression selectively

into the LA of CREB-deficient mice is sufficient to fully restore auditory fear conditioning¹³. Furthermore, optogenetic activation of neurons with elevated CREB levels at the time of training is sufficient to induce fear memory retrieval¹⁴. Moreover, studies using virus-mediated mosaic overexpression of CREB in wild-type mice have shown that recruitment of LA neuron during fear learning is not merely a cell autonomous process¹³, but rather is dependent upon relative neuronal excitability at the time of learning^{15,16}. Importantly however, the hypothesis that the recruitment of LA neurons into fear memory networks is determined by their relative excitability has never been evaluated under endogenous physiological conditions.

Recent computational modeling has proposed that the encoding of fear memories in the LA is constrained to a limited subset of neurons by the local microcircuitry through a combination of intrinsic excitability and synaptic plasticity¹⁷. Consistent with this model, *in vivo* extracellular single-unit recordings have demonstrated that only a minority of LA neurons undergo significant changes in tone-evoked firing during auditory fear conditioning^{18,19}. Furthermore, *ex vivo* whole-cell patch-clamp recordings also found that learning-induced plasticity was restricted to a limited subset of LA neurons⁵. Recent studies have provided strong experimental support that immediate-early genes (IEGs), including the proto-oncogene *c-Fos* and the activity-regulated cytoskeleton-associated protein (*Arc*), represent time-limited molecular tags of these sparsely encoded neurons in both sensory representations^{20–22} and memory networks^{13,23–27}. Inhibition or ablation of IEG-tagged neurons disrupts the recall and maintenance of fear conditioning memories, respectively^{15,28}. Conversely, artificial activation of this sparse IEG-tagged population is sufficient to induce fear memory recall²⁹ or falsely modify contextual memories^{30,31}. Importantly however, no previous studies have performed targeted electrophysiological recordings from a defined memory trace, a crucial step towards achieving a comprehensive understanding of how the brain encodes learned associations.

Therefore, in order to investigate the neurophysiological properties of individual LA neurons recruited during fear conditioning, we utilized a fluorescence-based reporter of *Arc* as a time-limited molecular tag of these sparsely encoded neurons. We found that neurons with elevated baseline intrinsic excitability were preferentially recruited into the fear memory network. Furthermore, synaptic potentiation of thalamic inputs

to the LA during fear conditioning was learning-specific and highly localized to *Arc* expressing neurons. Taken together, our findings establish a model of fear memory formation in which intrinsic excitability determines neuronal selection, while learning-related encoding is governed by synaptic plasticity.

MATERIALS AND METHODS

Animals

Arc::dVenus mice were backcrossed more than 10 generations into C57BL/6J³². Mice were maintained on a 12h light/dark cycle with food and water available *ad libitum*. All experiments were performed during the light phase, using adult mice (postnatal weeks 8-11). Mice were individually housed for 5 days prior to the start of experiments. Randomization was assigned based on the outcome of the littermate genotyping, and experimenter blinding was performed whenever possible. All experiments were approved by the Dutch Ethical Committee and in accordance with the Institutional Animal Care and Use Committee (IACUC) guidelines.

Auditory fear conditioning

Fear conditioning was performed using a Med Associates Standard Fear Conditioning chamber (30.5 cm x 24.1 cm x 21.0 cm) with a stainless steel electrifiable grid floor, and enclosed within a larger sound-attenuating box. Video images were recorded using a progressive scan CCD video camera with a visible light filter suitable for near-infrared imaging. Mice in the naïve group received no handling or exposure to the training context. Naïve mice remained in their standard housing conditions until immediately prior to behavioral testing for CS-evoked freezing, perfusion for confocal imaging, or sacrifice for electrophysiology. In contrast, mice in the unpaired and paired training groups were habituated to the conditioning chamber, 24 h prior the training session. Habituation sessions consisted of a 30 min exposure to the training context without any tone or shock presentations. On the day of conditioning, mice receiving paired training were placed in the conditioning chamber for 180 s, followed by a series of 3 co-terminating presentations of a tone CS (30 s, 5 KHz, 85dB) and scrambled footshock US (2 s, 0.75 mA). The intertrial interval between tone-shock presentations was 210 s. The experiments shown in Supplementary Figure 2

comparing the strength of conditioning and *Arc*-dVenus activation following 1, 3, or 9 CS-US pairings used independent groups of mice. Training was implemented using the same parameters (180 s placement-to-shock interval, 210 s interstimulus interval) and CS/US stimuli as the paired condition. Mice in the unpaired group received the identical CS and US stimuli but in an explicitly unpaired sequence. The unpaired protocol consisted of 3 US presentations (10 s interstimulus interval) in which the first shock was delivered immediately upon placement in the chamber, and followed by 3 CS presentations initiated 400 s after the last US presentation (90 s interstimulus interval). Previous studies using similar explicitly unpaired controls have demonstrated that subjects acquire minimal or no associative fear of the CS^{1,33}. Tone-evoked freezing was tested 24 h after conditioning in a novel context (120 s baseline, 180 s tone). Freezing was defined as the cessation of all movement except for respiration and scored using an automated algorithm³⁴.

Immunofluorescence

After deep anesthesia induced by intra-peritoneal injection of pentobarbital (50mg/kg), mice were transcardially perfused with saline, followed by 4% paraformaldehyde (PFA). Brains were dissected and post-fixed in 4% PFA for 2h at 4°C. After post-fixation, the brains were transferred into 10% sucrose phosphate buffer (PB 0.1M, pH 7.3) and stored overnight at 4°C. Embedding was performed in a 10% gelatin + 10% sucrose block, with fixation in 10% PFA + 30% sucrose solution for 2h at room temperature and immersed in 30% sucrose at 4°C. 40 µm coronal sections were collected serially (rostral to caudal) using a freezing microtome (Leica, SM 2000R) and stored in 0.1M PB. Free-floating sections were incubated in sodium citrate (10 mM) at 80°C for 1h and rinsed with tris-buffered saline (TBS, pH 7.6). Sections were pre-incubated with a blocking TBS buffer containing 0.5% Triton X-100 and 10% normal horse serum (NHS, Invitrogen) for 1h at room temperature. Sections were incubated in a mixture of primary antibodies, in TBS buffer containing 0.4% Triton X-100 and 2% NHS for 72 h at 4°C.

The following primary antibodies were used: mouse anti-NeuN (1:2000, Millipore MAB377), goat anti-choline acetyltransferase (ChAT) (1:200, Millipore AB144P), rabbit anti-Tbr1 (1:2000, Millipore AB10554), mouse anti-Arc

(C-7, 1:200, Santa Cruz sc-17839), rabbit anti-c-Fos (ab-5, 1:10000, Millipore PC38), mouse anti-GAD67 (1:1000, Millipore MAB5406). Sections were washed with TBS, and incubated with corresponding Alexa-conjugated secondary antibodies (1:200, Invitrogen) and cyanine dyes (1:200, Sanbio) in TBS buffer containing 0.4% Triton X-100, 2% NHS for 2h at room temperature. For some experiments, nuclear staining was performed using DAPI (1:10000, Invitrogen). Sections were washed with PB 0.1M and mounted on slides, cover slipped with Vectashield H1000 fluorescent mounting medium (Vector Labs), and sealed.

Fluorescent in situ hybridization (FISH)

FISH was performed using mice perfused at 5 min post-training, in order to optimally visualize nuclear foci of *dVenus* and *Arc* transcription²³. Coronal brain sections (40 μ m) were collected in RNase-free 0.1 M PB as described in the immunofluorescence section. The cDNA templates encoding the following mRNAs were used for single-stranded RNA probe synthesis: *Arc/Arg3.1* (3.5 kb, full length probe, GeneID: 11838; Image Clone number: 349057; generously provided by J. Holstege and M. Hosseini); *Venus fluorescent protein* (720 kb probe from pISH-Venus Addgene plasmid 15865, kindly deposited by P. Mombaerts). The riboprobes were obtained by linearizing the recombinant plasmids with the appropriate restriction enzymes (Fermentas, New England BioLabs) and RNA polymerases. Transcription was performed in the presence of digoxigenin (DIG) or fluorescein labeled 11-UTP (Roche), for *Venus* or *Arc* riboprobes respectively, using a commercial RNA labeling kit (Roche). Riboprobes were purified by standard LiCl precipitation protocol. Integrity and yield of riboprobes was confirmed by gel electrophoresis and Nanodrop® spectrophotometry (Thermo Scientific). All solutions used until the completion of hybridization were treated with Diethylpyrocarbonat (DEPC) to ensure optimal RNase-free working conditions.

The protocol used for fluorescent in situ hybridization was adapted from Hossaini *et al.* (2010)³⁵. Free-floating sections were first washed in 0.1 M PB, treated for 5 minutes with 0.2% glycine in PBS, rinsed in PBS, and fixed for 10 minutes in 4% PFA. After another rinse in PBS, sections were treated (10 min) in PBS containing 0.1 M triethanolamine (Merck) pH 8.0 and 0.0025% acetic anhydride

(Sigma-Aldrich). Sections were then washed in 4x standard saline citrate (SSC, pH 4.5) and prehybridized for 1 hour at 65°C in hybridization solution consisting of 5x SSC (pH 4.5), 50% formamide (Sigma-Aldrich), 2% Blocking Reagent (Roche), 0.05% 3-[(3-cholamidopropyl)dimethylammonio]-1-propanesulfonate (CHAPS, Sigma-Aldrich), 1 µg/ml yeast tRNA (tRNA brewer's yeast, Sigma), 50 µg/ml Heparin (Sigma-Aldrich) and 5 mM Ethylenediaminetetraacetic acid (EDTA, pH 8.0, Sigma-Aldrich). Sections were hybridized for 18-24 hours at 65°C in hybridization solution containing 1.2 µg/ml of each anti-sense riboprobe, *Arc/Arg3.1* and *Venus*. After hybridization, sections were washed in 2x SSC (pH 4.5), followed by three washes of 15 minutes at 65°C in 2x SSC (pH 4.5) and 50% formamide, and a final wash in PBS. The sections were then pre-incubated for 90 minutes at room temperature in blocking buffer, consisting of 0.5% Triton X-100 and 10% NHS in TBS. For detection of the DIG and fluorescein tags in riboprobes, sections were incubated in 0.4% Triton X-100 and 2% NHS in TBS (pH 7.6), with primary sheep polyclonal anti-digoxigenin (1:500, Thermo Scientific) and mouse monoclonal anti-fluorescein (1:500, Roche) antibodies, for 72 hours at 4°C. Subsequently, sections were washed with TBS and detection of anti-DIG and anti-fluorescein primary antibodies was carried out using anti-sheep Cy3 from donkey (1:200, Jackson Laboratories) and anti-mouse Alexa647 from donkey (1:200, Jackson Laboratories) respectively, in 0.4% Triton X-100 and 2% NHS in TBS (pH 7.6) at room temperature, for 2 hours. Sections were then washed in 0.1M PB and stained using DAPI (1:10000, Invitrogen) as a nuclear marker. Sections were then mounted on slides, cover slipped with Vectashield H1000 fluorescent mounting medium (Vector Labs), and sealed.

Confocal imaging

Stained LA images were acquired using a Zeiss LSM 700 confocal microscope (Carl Zeiss) equipped with Zeiss Plan-Apochromat 10x/0.45, 20x/0.8, and 40x/1.3 (oil immersion) objectives. Native dVenus, Cy3, Alexa647, and DAPI were imaged using the excitation wavelengths of 488, 555, 639, and 405 nm, respectively. Native dVenus fluorescence intensity was quantified using ImageJ (NIH, 1.42q) with the Multi Measure plug-in. The mean fluorescence intensity of each *Arc*-dVenus⁺ neuron was determined by drawing a region of interest (ROI) around the cell soma.

Stereology

Coronal brain sections were collected serially through the entire extent of the LA of each mouse, with a section thickness of 40 μm and interval distance of 160 μm (Supplementary Figure 1). Sections were immunofluorescently labeled with anti-NeuN and anti-ChAT, to identify mature neurons and to define the border between the lateral and basolateral nuclei of the amygdala³⁶, respectively. Furthermore, in order to optimally standardize the stereological analysis and in light of recent findings demonstrating hemispheric lateralization of *Arc* expression within the insular cortex following taste learning³⁷, all stereological and fluorescence intensity data was collected exclusively from the left hemisphere.

Stereological estimation of the total population (NeuN^+) and *Arc*-dVenus⁺ subset of neurons was performed using the Optical Fractionator probe within Stereo Investigator (version 10, MBF Bioscience, USA). Stacks of confocal images (156 x 156 x 1 μm) across the thickness of the sections (with a separation level of 1 μm) of *Arc*-dVenus⁺ and NeuN^+ neurons were systematically collected. A counting frame size of 100 μm x 100 μm was used to mark *Arc*-dVenus⁺ neurons throughout the entire grid, using an exhaustive sampling configuration. NeuN^+ cells were counted using 35 μm x 35 μm counting frames, which were selected in a systematic random procedure by the analysis software. The grid size of both exhaustive and random sampling configurations was set to 100 μm x 100 μm .

The section thickness was assessed empirically at every sampling site to precisely calculate any potential thickness variation across the sections as a result of post-processing of the tissue. Guard zones (2 μm) were used at the top and bottom of each section with a dissector height of 15 μm . Accuracy in the estimation of the total number of quantified cells per subject was estimated using the coefficient of error (*CE*) equations^{38–40}. *CE* values were <0.1 in all mice analyzed.

Brain slice electrophysiology

Mice were anesthetized using isoflurane, decapitated and the brain dissected in ice-cold modified artificial cerebrospinal fluid (ACSF) containing the following (in mM): 110 NaCl, 2.5 KCl, 2 CaCl₂, 2 MgCl₂, 1 NaH₂PO₄, 25 NaHCO₃, 10 glucose,

0.2 ascorbate, 0.2 thiourea. Acute coronal slices (300 μm) containing the LA were cut using a vibratome (Microm 650V, Thermo scientific) and transferred to a storage chamber in ACSF, saturated with 95% O_2 /5% CO_2 and maintained at 32-34°C. After at least 1 hour of recovery time, slices were transferred to the recording chamber where they were continuously perfused with oxygenated ACSF at a perfusion rate of 1.5-2 ml/min.

Whole-cell patch-clamp recordings of LA neurons were performed at 32-34°C under infrared differential interference contrast visual guidance using an upright microscope (Nikon Eclipse E600FN). *Arc*-dVenus⁺ fluorescence cells were detected via illumination of a mercury lamp using a YFP filter (Semrock). Borosilicate glass pipettes (4-7 M Ω) were connected to an Axon Multiclamp 700B amplifier (Molecular Devices) and data were acquired at 20 KHz, filtered at 3 KHz, stored and analyzed using the pClamp software (pClamp 10, Molecular Devices). Pipettes were filled with the following medium (in mM): 130 KMeSO₃, 11 KCl, 10 HEPES, 5 NaCl, 0.1 EGTA, 1 MgCl₂, 2 Mg-ATP, 0.3 Na-GTP, 5 phosphocreatine, 50U/ml creatin phosphokinase, the pH was adjusted to 7.2, and osmolarity to 290 mOsm. Slices were continuously superfused with ACSF, saturated with 95% O_2 /5% CO_2 and maintained at 32-34°C. Liquid junction potential was left uncorrected. Except for measurements of intrinsic properties, the GABAA receptor blocker picrotoxin (PTX 100 μM) was added to the ACSF. Large, pyramidal-like somata were visualized targeted for recordings, and readily distinguished from fast-spiking neurons, characteristic of LA interneurons⁴¹⁻⁴³. No fast-spiking neurons were found in the *Arc*-dVenus⁺ population, consistent with *Arc* expression in the LA being limited to glutamatergic principal neurons⁴⁴.

Passive membrane properties were analyzed using a 10 mV hyperpolarizing voltage step in voltage-clamp mode. Resting membrane potential was measured immediately after establishing the whole-cell configuration. Single APs were evoked by a 10 ms current injection whose amplitude was minimally sufficient to reach the threshold from a potential of -75 mV. The threshold was defined as the inflection point at the foot of the regenerative upstroke. AP amplitude and after-hyperpolarizing potential were measured from the threshold to the peak and to the maximal hyperpolarizing value, respectively. AP duration was measured at half of the maximal amplitude.

For evoked postsynaptic currents, thalamic fibers of the ventral part of the striatum were stimulated using a bipolar Platinum-Iridium electrode (FHC). Postsynaptic responses were recorded from *Arc*-dVenus⁻ and *Arc*-dVenus⁺ neighboring cells, thereby reducing interslice variability. Input-output curves were constructed by varying the stimulus intensity from 0 to 200 μ A (in 25 μ A increments) at 0.1 Hz. EPSC amplitude was normalized by the cell capacitance. Paired-pulse ratio was analyzed as the ratio of the second to the first EPSC resulting from two consecutive stimulations, in which the interstimulus interval ranged from 25–100 ms (in 15 ms increments) and from 100–300 ms (in 25 ms increments). For AMPA/NMDA recordings, the intracellular solution was modified by substituting KMeSO₃ and KCl with CsMeSO₃ and CsCl, respectively. The AMPA component was measured as the peak current recorded at -70 mV. The NMDA component was recorded at +40 mV (measured 100 ms after stimulus onset), and entirely blocked in presence of 1-Amino-phosphovaleric acid (APV, 50 μ M).

Statistical analysis

Significance of observations was established by unpaired Student's t test or ANOVA followed by Tukey's post hoc test. Cumulative probability distributions of fluorescence intensity were compared using the Kolmogorov-Smirnov test. Data are expressed as mean \pm SEM. Significance threshold was set at $P < 0.05$ for all statistical comparisons.

RESULTS

Arc-dVenus expression accurately reflects endogenous *Arc* transcription

In order to visualize LA neurons recruited during fear learning, we utilized a recently engineered mouse line expressing destabilized Venus fluorescent protein (dVenus) under the control of a transgenic *Arc* promoter (*Arc::dVenus* mice), thereby leaving the endogenous *Arc* genes unmodified³². Hence, these mice function as a fluorescence-based reporter of *Arc* transcription without interfering with the function of endogenous *Arc* itself. Using compartmental analysis of temporal gene transcription by fluorescence *in situ* hybridization²³, we confirmed the high co-localization of *Arc*-dVenus and endogenous *Arc* nuclear RNA in the LA after auditory fear

conditioning, thereby demonstrating the validity of *Arc::dVenus* reporter mice for visualizing LA cells with recent endogenous *Arc* activation (Fig. 1b).

In order to examine the specificity of *Arc*-dVenus activation during fear learning, we used three independent groups: naïve (homecage) controls, explicitly unpaired presentations of tone and shock, or paired tone-shock conditioning (Fig. 1a). Mice were sacrificed 5 hours after fear conditioning, consistent with previous reports demonstrating that maximal experience-driven *Arc*-dVenus expression occurs within 4-6 h^{32,45}. *Arc*-dVenus fluorescence was robustly increased in the LA of mice receiving paired training (Fig. 1c-e). In contrast, naïve mice and those receiving unpaired training showed relatively weaker fluorescence, confirming the specificity of *Arc*-dVenus activation in the LA to fear learning.

Previous studies have demonstrated that endogenous *Arc* expression is localized to principal neurons within the forebrain⁴⁴. Therefore, in order to confirm the cell-type specificity of the *Arc::dVenus* reporter in the LA, we performed immunohistochemical labeling with antibodies against Tbr1 or GAD67, markers for glutamatergic projection neurons or GABAergic interneurons, respectively⁴⁶. Indeed, we found that *Arc*-dVenus⁺ neurons in the LA were always NeuN⁺ (Fig. 1c-e) and Tbr1⁺ (Fig. 1f). Conversely, we never observed an *Arc*-dVenus⁺ neuron that was GAD67⁺ (Fig. 1g), thereby confirming that *Arc*-dVenus expression is exclusively limited to glutamatergic neurons in the LA, consistent with the cell-type specificity of endogenous *Arc*.

Fear learning robustly and selectively induces Arc-dVenus expression

Using confocal stereology, we quantified the percentage and fluorescence intensity of *Arc*-dVenus⁺ neurons in the LA following fear conditioning (Fig. 2; Supplementary Figure 1). In naïve mice, only weak levels of *Arc*-dVenus fluorescence were detectable in LA neurons, consistent with the low baseline expression of endogenous *Arc*⁴⁷. Unpaired conditioning did not influence the percentage of *Arc*-dVenus⁺ neurons. In contrast, the percentage of *Arc*-dVenus⁺ neurons observed in mice receiving paired conditioning was significantly increased compared to naïve ($P<0.01$) and unpaired ($P<0.05$) groups (Fig. 2b). Moreover, paired training induced a strong right-shift of the cumulative probability distribution of *Arc*-dVenus fluorescence, compared

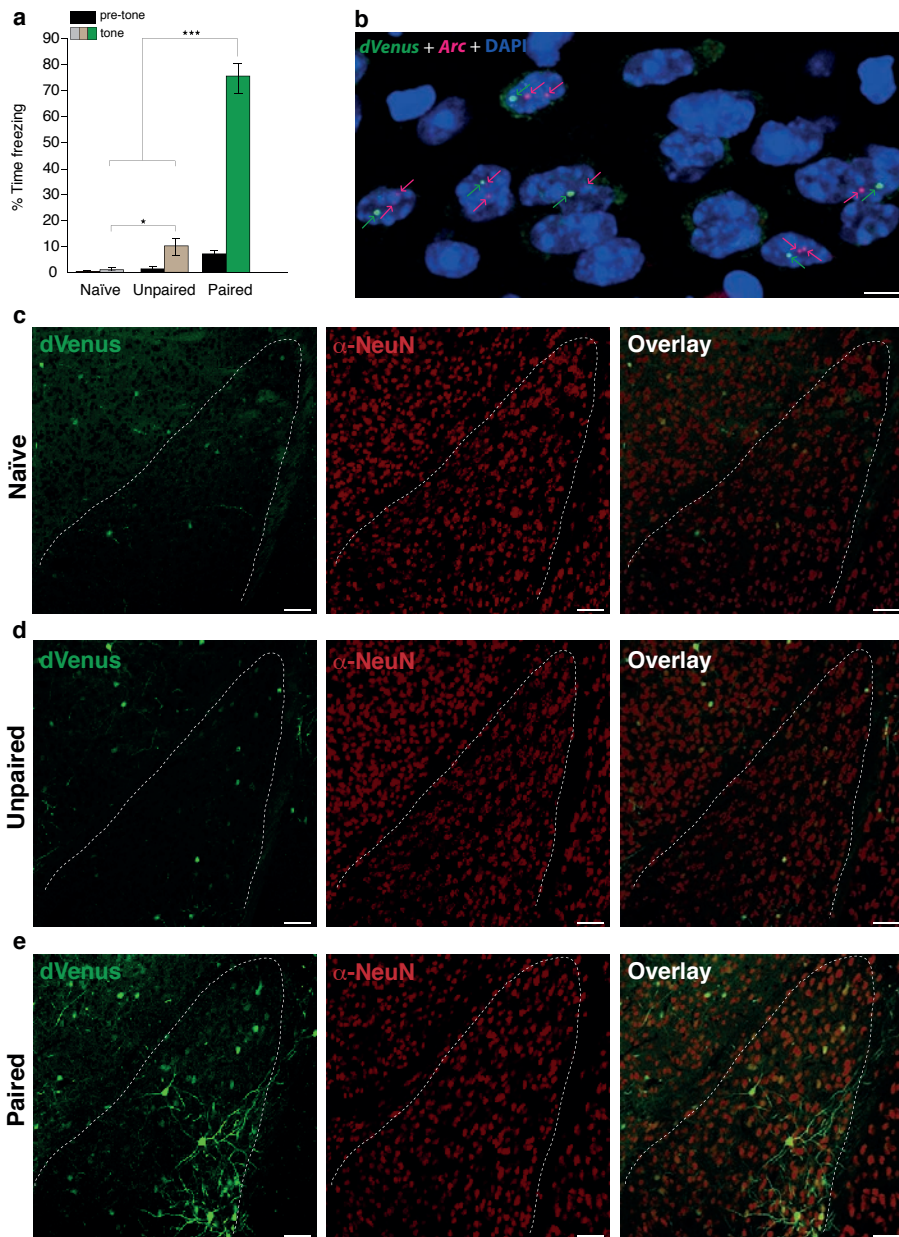


Fig. 1: Fear conditioning induces learning-specific activation of *Arc-dVenus* in the lateral amygdala (LA). (a) Tone-induced freezing in naïve mice, and those receiving either paired or unpaired presentations of tone and shock ($n=8$ mice/group). One-way ANOVA, $F=107.07$, $P<0.001$. $*P<0.05$, $***P<0.001$. (b) *Arc-dVenus* reporter and endogenous *Arc* RNA intra-nuclear foci (indicated by arrows) are highly co-localized. Scale bar, 5 μm . (c-d) *Arc-dVenus*⁺ expression in the LA of mice from naïve (c), unpaired (d) and paired (e) conditions sacrificed 5h post-training. Dotted lines indicate LA boundaries. Scale bar, 50 μm . (f and g) Matching the cell-type specificity of endogenous *Arc* expression, *Arc-dVenus*⁺ neurons in the LA uniformly express the glutamatergic marker *Tbr1* ($n=1900$ cells; f), but not the GABAergic marker *GAD67* ($n=1140$ cells; g). Scale bar, 10 μm .

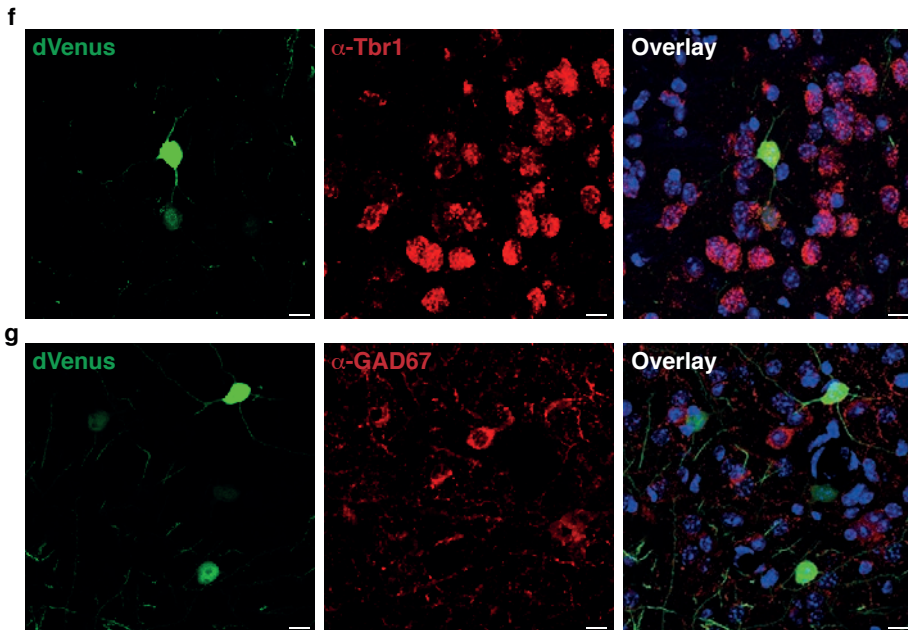


Fig 1: (Continued)

to naïve ($P < 0.0001$) and unpaired ($P < 0.001$) conditions (Fig. 2c). Together, our findings indicate that the induction of *Arc*-dVenus expression in the LA during fear conditioning is highly specific for associative learning, compared to non-associative sensory stimulation.

In order to further explore the relationship between the strength of learning, percentage of *Arc*-dVenus⁺ neurons, and dVenus fluorescence intensity, we used independent groups of mice trained with 1, 3, or 9 CS-US pairings. Stereological analysis demonstrated an asymptotic percentage of *Arc*-dVenus⁺ neurons beyond 3 CS-US pairings, which closely paralleled the CS-evoked freezing curve (Supplementary Figure 2, A and B). Notably however, despite a similar strength of conditioning and percentage of *Arc*-dVenus⁺ neurons, mice receiving 9 CS-US pairings had a significantly increased dVenus fluorescence intensity compared to mice receiving only 3 CS-US pairings (Supplementary Figure 2, C-E). Therefore, successive CS-US pairings do not recruit cells randomly within the LA, but instead result in a highly overlapping re-activation of a similar neuronal subpopulation.

Recent models of memory formation have hypothesized that at any given time, a limited subset of neurons exist in an *a priori* primed state, which could serve to preferentially bias their allocation into a newly encoded associative memory trace^{13,15–17,31,48,49}. Therefore, we considered the possible mechanisms by which cellular activation in the LA could transform the *Arc*-dVenus fluorescence intensity curve from the baseline (naïve) state to the distribution observed after fear conditioning (Fig. 2c). In particular, the rightward shift in the *Arc*-dVenus fluorescence intensity distribution could have resulted from two non-mutually exclusive possibilities: a) In Fig. 2b, we observed a ~50% increase in the number of *Arc*-dVenus⁺ neurons in the LA following paired training. Accordingly, if these newly *Arc*-dVenus⁺ neurons are predominantly of high fluorescence intensity, the resulting cumulative probability curve would shift to the right. b) A second possibility is that baseline *Arc*-dVenus⁺ neurons are preferentially recruited during fear conditioning. Prior to conditioning, ~10% of LA neurons are *Arc*-dVenus⁺, and thereby represent the fluorescence intensity distribution of the baseline (naïve) group. During fear conditioning, activation of these baseline *Arc*-dVenus⁺ neurons would necessarily increase their fluorescence level and consequently shift the overall population distribution to the right. Therefore, in order to distinguish between these possibilities, we examined the absolute frequency histograms of fluorescence intensity, which fully account for the difference in the overall percentage of *Arc*-dVenus⁺ neurons (Fig. 2d). Notably, the fluorescence intensity distribution remained significantly right-shifted despite having fully accounted for the increased percentage of *Arc*-dVenus⁺ neurons, and consistent with a model of neuronal selection during fear conditioning in which baseline *Arc*-dVenus⁺ neurons are preferentially recruited into the memory trace.

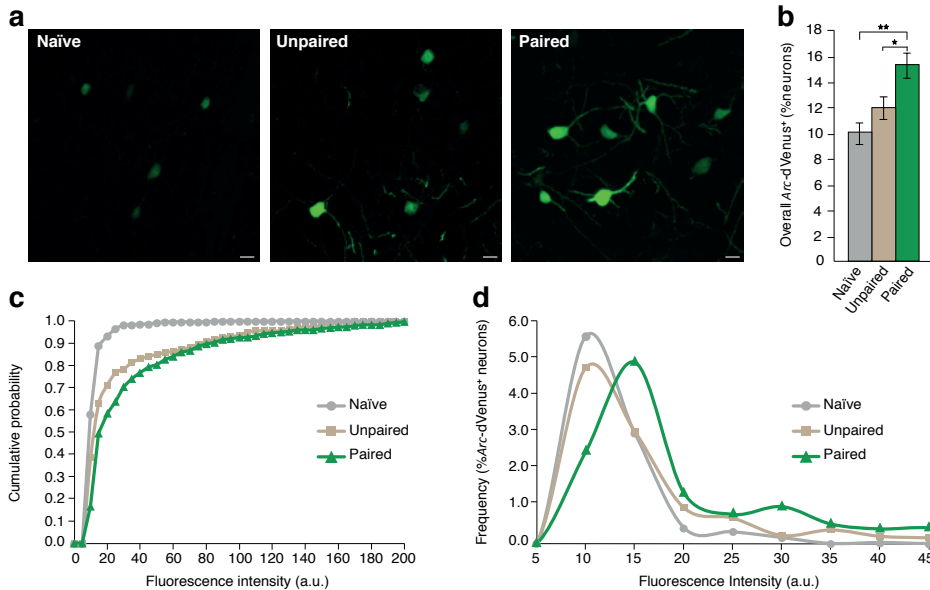


Fig. 2: *Arc*-dVenus expression is selectively induced by fear learning. (a) Native dVenus fluorescence from naïve, unpaired and paired mice at 5h post-training. Scale bar, 10 μ m. (b) Stereological quantification of *Arc*-dVenus⁺ neurons in naïve, unpaired, and paired conditions. Paired training significantly increases the percentage of *Arc*-dVenus⁺ cells compared to naïve and unpaired controls. In contrast, a similar percentage of *Arc*-dVenus⁺ cells is observed between naïve and unpaired conditions (Naïve: $n=7$ mice, Unpaired: $n=7$ mice, Paired: $n=6$ mice). One-way ANOVA, $F=8.59$, $P<0.01$. (c) Cumulative distribution of *Arc*-dVenus fluorescence intensity. Fluorescence intensity is significantly higher in mice receiving paired fear conditioning, compared to naïve and unpaired controls. Kolmogorov-Smirnov: Naïve vs. Paired, $D=0.48$, $P<0.0001$; Unpaired vs. Paired, $D=0.24$, $P<0.001$. (d) Frequency histograms of *Arc*-dVenus fluorescence intensity. X-axis is truncated at 45 a.u. (Panels C and D: bin size, 5 a.u.). * $P<0.05$, ** $P<0.01$, *** $P<0.001$

Preferential recruitment of neurons with enhanced intrinsic excitability

To further examine the hypothesis that baseline *Arc*-dVenus⁺ neurons are preferentially recruited during fear learning, we made use of the differential half-life of endogenous *Arc*⁵⁰ compared to dVenus³². Endogenous *Arc* is nearly undetectable in naïve mice⁴⁷, and peaks in the LA at 1h after fear conditioning, specifically marking neurons that were activated during conditioning (Supplementary Figure 3). In contrast, baseline *Arc*-dVenus⁺ neurons remain easily detectable over a 1h period given that the in vivo half-life of *Arc*-dVenus fluorescence is 3h³². Therefore, at 1h after fear conditioning, a high percentage of *Arc*-dVenus⁺ neurons with co-localized expression of endogenous *Arc* would confirm that baseline *Arc*-dVenus⁺ neurons are preferentially recruited during fear conditioning. In contrast, a low rate of

co-localized expression would suggest that the baseline *Arc*-dVenus⁺ population has no *a priori* bias towards activation. Indeed, consistent with a model of preferential recruitment, 92.6% of *Arc*-dVenus⁺ neurons from mice undergoing paired training were co-localized with endogenous *Arc*, compared to only 10.2% in naïve mice (Fig. 3a-e; $P < 0.0001$). Mice receiving unpaired training also showed recruitment of baseline *Arc*-dVenus⁺ neurons, although the co-localization was significantly lower than in mice receiving paired training ($P < 0.05$). Lastly, *c-Fos* activation was also highly co-localized with *Arc*-dVenus at 1h post-training (Supplementary Figure 4), demonstrating that this finding is not simply restricted to *Arc*. Together, these data indicate that baseline *Arc*-dVenus expression represents a unique molecular marker for LA neurons that are preferentially recruited during fear memory encoding.

Given that *Arc*-dVenus⁺ neurons are preferentially recruited during fear conditioning, their defining electrophysiological properties might offer unique insights into the physiological mechanisms underlying associative memory encoding. Passive membrane properties and single AP characteristics of *Arc*-dVenus⁺ and neighbouring *Arc*-dVenus⁻ neurons demonstrated no two-way interactions of *Arc*-dVenus status and training condition (Supplementary Table 1). Furthermore, there were no overall main effects of *Arc*-dVenus status. However, three parameters demonstrated overall main effects of training condition: membrane resistance ($F_{2,104} = 5.52$, $P < 0.01$), AP threshold ($F_{2,95} = 8.37$, $P < 0.001$), and AP half-width ($F_{2,95} = 6.03$, $P < 0.01$) (Supplementary Table 1). Post-hoc pairwise comparisons across training conditions demonstrated that membrane resistance was significantly lower in mice receiving paired training compared to naïve mice ($P < 0.01$), with no significant differences of either condition in comparison to mice receiving unpaired training. AP threshold was significantly more depolarized in mice from the paired ($P < 0.01$) and unpaired ($P < 0.01$) condition, compared to naïve mice. Lastly, AP half-width was significantly narrower in mice receiving paired training, compared to naïve ($P < 0.05$) or unpaired ($P < 0.01$). Importantly, these main effects of training condition are independent of whether the recorded neurons were *Arc*-dVenus⁺ or *Arc*-dVenus⁻, and therefore reflect global experience-dependent changes in the LA.

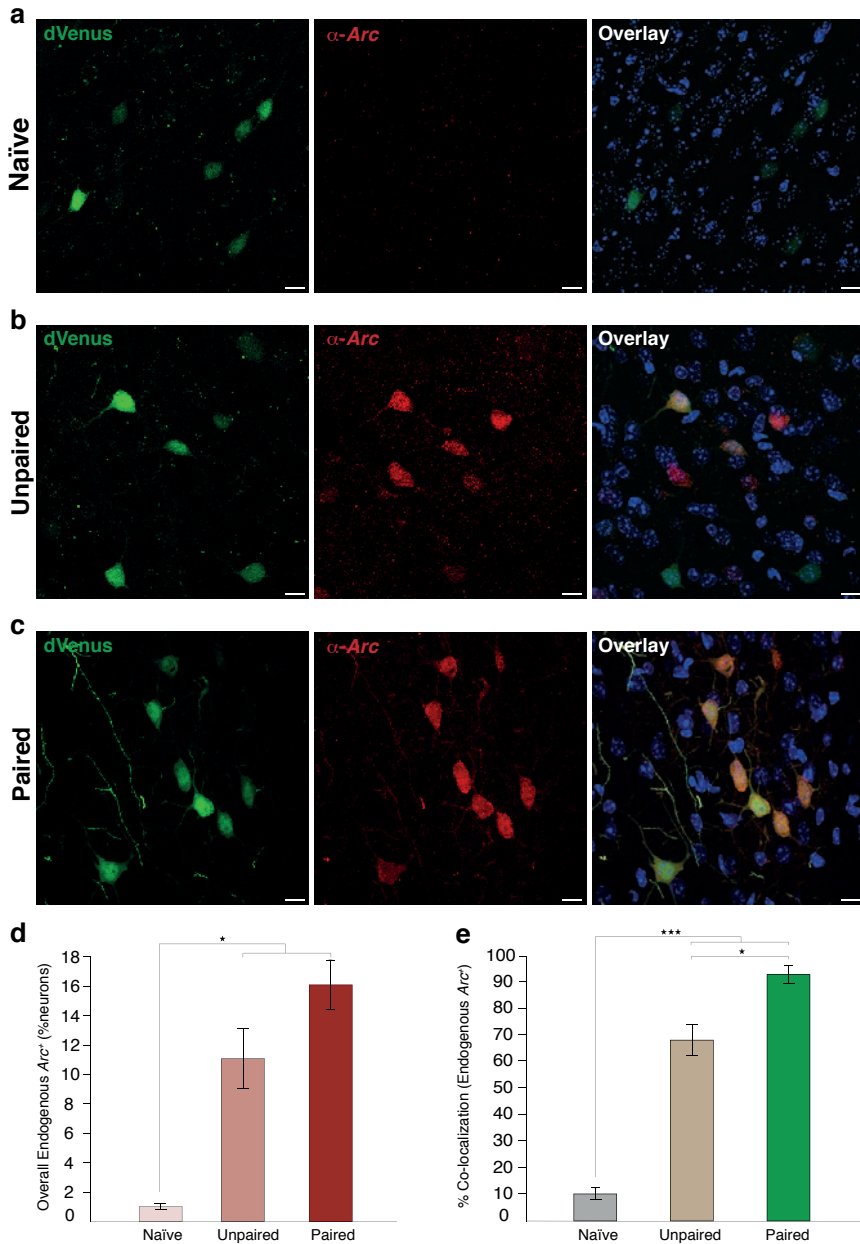


Fig. 3: Baseline *Arc*-dVenus⁺ neurons are preferentially recruited during fear conditioning. (a-c) Representative images of *Arc*-dVenus and endogenous *Arc* co-localization at 1h post-training. Scale bar, 10 μ m. (d) Overall percentage of LA neurons expressing endogenous *Arc* in naïve, unpaired and paired conditions. Paired and unpaired training induce an increase in the number of neurons expressing endogenous *Arc*. One-way ANOVA, $F=25.03$, $P<0.001$. (e) Endogenous *Arc* is preferentially localized to *Arc*-dVenus⁺ neurons in mice receiving paired conditioning, compared to naïve or unpaired controls. Two-way ANOVA, group x *Arc*-dVenus interaction, $F=94.12$, $P<0.0001$. * $P<0.05$, ** $P<0.01$, *** $P<0.001$

Intrinsic excitability has been widely hypothesized as a candidate mechanism for neuronal recruitment during associative learning¹⁵⁻¹⁷. However, no previous studies have been able to directly address this hypothesis under entirely physiological conditions. Therefore, we performed targeted whole-cell recordings from *Arc-dVenus*⁺ neurons and their non-activated *Arc-dVenus*⁻ neighbours. Consistent with the hypothesis that increased excitability might support their preferential recruitment into the fear memory trace, baseline *Arc-dVenus*⁺ neurons had significantly higher intrinsic excitability than their non-activated neighbours (Fig. 4). Moreover, *Arc-dVenus*⁺ neurons from both the paired and unpaired conditions displayed a similar increase in excitability, the magnitude of which was independent of learning or sensory stimulation. Accordingly, *Arc-dVenus*⁺ neurons also displayed higher instantaneous action potential (AP) frequencies than neighbouring *Arc-dVenus*⁻ neurons (Supplementary Figure 5). Notably however, no differences were observed in AP amplitude or duration across spike trains (Supplementary Figures 6 and 7). Taken together, these findings suggest that enhanced excitability cannot account for the encoding of a fear memory, but rather is highly consistent with a model for neuronal selection during learning regulated by intrinsic excitability.

Synaptic plasticity is highly localized to Arc-dVenus⁺ neurons during fear conditioning, and postsynaptically mediated

The encoding of auditory fear memories is thought to occur through selective potentiation of glutamatergic synaptic inputs to the LA^{5,6,10-12}. However, previous studies investigating auditory fear conditioning-induced synaptic modifications have been performed without knowledge of whether recorded neurons were part of the memory trace. Therefore, the *Arc::dVenus* mice represented a unique opportunity to examine whether learning-induced synaptic potentiation would be preferentially localized to *Arc-dVenus*⁺ neurons, as predicted by a model of sparse memory encoding.

We recorded excitatory postsynaptic currents (EPSCs) evoked by stimulation of thalamic afferents to LA neurons. In both naïve and unpaired conditions, similar EPSC amplitudes were observed in *Arc-dVenus*⁺ and neighbouring *Arc-dVenus*⁻ neurons (Fig. 5a,b).

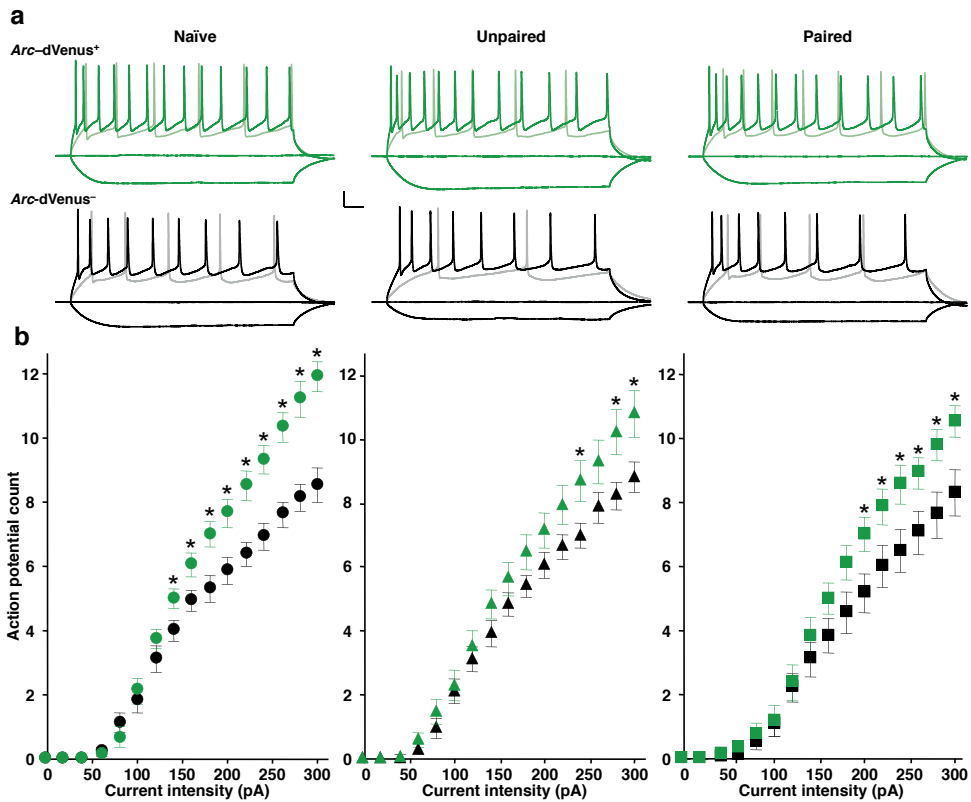


Fig. 4: *Arc-dVenus*⁺ neurons exhibit increased excitability. (a) Superimposed current-clamp recordings with -100, 0, +140, +300 pA sustained current injection at a holding membrane potential of -75 mV. *Arc-dVenus*⁺ neurons (top) fire more APs than non-activated neighbors (bottom) in naïve, unpaired and paired conditions. Scale bars: 20 mV, 50 ms. (b) Plot of the mean AP count versus current injection intensity for naïve (left), unpaired (center), and paired (right) conditions. *Arc-dVenus*⁺ neurons (naïve: $n=15$, unpaired: $n=17$, paired: $n=16$; green) show higher excitability compared to neighboring *Arc-dVenus*⁻ neurons (naïve: $n=16$, unpaired: $n=17$, paired: $n=18$; black). Naïve: $n=12$ mice, Unpaired: $n=6$ mice, Paired: $n=8$ mice. Repeated measures ANOVA, *Arc-dVenus* x current intensity interaction: naïve, $F=14.06$, $P<0.001$; unpaired, $F=3.75$, $P<0.05$; paired, $F=3.55$, $P<0.05$. * $P<0.05$

In contrast, paired conditioning induced a robust and highly-specific potentiation of thalamic afferent synapses, selectively in *Arc*-dVenus⁺ neurons (Fig. 5a,b). Therefore, *Arc* expression defines the LA neuronal ensemble onto which synaptic plasticity is highly localized during fear conditioning.

We next sought to determine whether the site of plasticity for the enhancement in glutamatergic synaptic transmission during auditory fear conditioning was pre- or postsynaptic. If fear conditioning differentially modifies the neurotransmitter release probability onto *Arc*-dVenus⁺ versus *Arc*-dVenus⁻ neurons, such a change should be evident by a decrease in the paired-pulse ratio for glutamatergic inputs onto *Arc*-dVenus⁺ neurons compared to neighboring *Arc*-dVenus⁻ neurons. Therefore, we performed paired-pulse stimulation of thalamic afferents across a range of interstimulus intervals from 25 to 300 ms (Fig. 5c,d). Notably, *Arc*-dVenus⁺ and *Arc*-dVenus⁻ neurons showed similar paired-pulse ratios across all interstimulus intervals examined, making it unlikely that the learning-induced synaptic potentiation of *Arc*-dVenus⁺ neurons was presynaptic in origin.

Alternatively, we measured the ratio of α -amino-3-hydroxy-5-methyl-4-isoxazole-propionic acid (AMPA) to NMDA currents, a widely used measure that is highly sensitive to postsynaptically-mediated plasticity of glutamatergic transmission, including long-term potentiation^{6,51}. Indeed, consistent with a postsynaptic locus of plasticity, fear conditioning induced a significant increase in the AMPA/NMDA current ratio in *Arc*-dVenus⁺ neurons compared to their *Arc*-dVenus⁻ neighbors (Fig. 5e,f). Taken together, our findings demonstrate that learning-induced synaptic potentiation is postsynaptically-mediated and selectively localized onto the sparse population of *Arc*-expressing neurons.

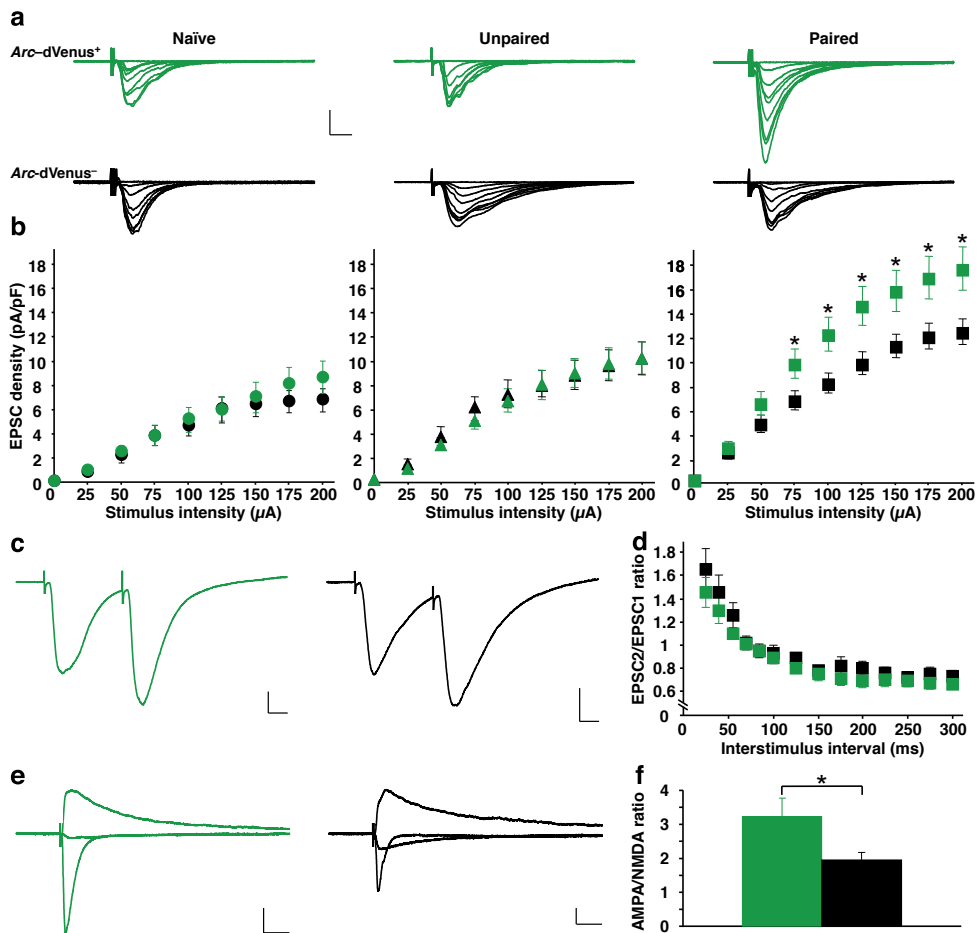


Figure 5: Synaptic potentiation is learning-specific and highly localized to *Arc*⁺ neurons. (a) Superimposed averages (5 traces) of EPSCs evoked via thalamic input stimulation (0 to 200 μ A, 25 μ A increments) at a holding membrane potential of 70 mV. Stimulus artifacts are truncated. *Arc-dVenus*⁺ neurons (top) display strongly potentiated evoked EPSCs specific to the paired (right) versus naïve (left) or unpaired (center) conditions. Scale bars: 200 pA, 10 ms. (b) Input-output curves for naïve (left), unpaired (center), and paired (right) conditions. In the naïve and unpaired conditions, EPSCs recorded from *Arc-dVenus*⁺ (naïve: $n=13$, unpaired: $n=19$; green) and *Arc-dVenus*⁻ (naïve: $n=14$, unpaired: $n=18$; black) neurons are similar. In contrast, EPSCs are selectively potentiated in *Arc-dVenus*⁺ neurons in the paired condition ($n=34$, green) compared to neighbouring *Arc-dVenus*⁻ neurons ($n=34$, black), across all stimulus intensities >50 μ A. Naïve: $n=12$ mice, Unpaired: $n=12$ mice, Paired: $n=21$ mice. Repeated measures ANOVA, stimulus intensity \times *Arc-dVenus* interaction: naïve, $F=0.88$, $P=0.39$; unpaired, $F=0.28$, $P=0.69$; paired, $F=5.26$, $F<0.01$. (c) Averages (5 traces) of EPSC pairs (normalized to the 1st EPSC) with a 45 ms interstimulus interval from *Arc-dVenus*⁺ (left) and *Arc-dVenus*⁻ (right) neurons of mice receiving paired conditioning. Scale bars: 100 pA, 10 ms. (d) Paired-pulse ratios were similar between *Arc-dVenus*⁺ ($n=14$, green) and *Arc-dVenus*⁻ ($n=16$, black) neurons from 15 mice. Repeated measures ANOVA, stimulus intensity \times *Arc-dVenus* interaction, $F=1.08$, $P=0.33$. (e) Evoked EPSCs (average of 5 traces) at 70, 0 and +40 mV holding membrane potentials, scaled to the +40 mV peak amplitude. *Arc-dVenus*⁺ (left) and *Arc-dVenus*⁻ (right) neurons from mice receiving paired conditioning. Scale bars: 100 pA, 40 ms. (f) AMPA/NMDA ratio is significantly increased in *Arc-dVenus*⁺ ($n=24$, green) compared to neighbouring *Arc-dVenus*⁻ ($n=26$, black) neurons from 15 mice. * $P < 0.05$

DISCUSSION

The elucidation of the physiological mechanisms underlying memory encoding remains a considerable technical challenge, due to the sparseness of neuronal representations. Therefore, we used a novel *Arc* reporter mouse^{32,45,52} to permit visual identification and neurophysiological interrogation of neurons with recent activation. Using this powerful approach for exploring learning-specific alterations in neuronal physiology, we now demonstrate that fear conditioning-induced glutamatergic synaptic potentiation in the LA is preferentially localized to *Arc*⁺ neurons, thereby confirming the sparse encoding hypothesis and identifying *Arc* as a *bona fide* molecular marker of the LA fear memory trace. Furthermore, we show that baseline differences in neuronal excitability are highly predictive of the ensemble of neurons selectively recruited into the fear memory trace.

We found that the potentiation of glutamatergic synaptic transmission from the thalamic input pathway was postsynaptically-mediated, given the highly significant enhancement in AMPA/NMDA ratio from mice receiving paired training, in the absence of changes in the presynaptically-mediated paired-pulse ratio. These findings are consistent with the comprehensive series of previous studies reporting a postsynaptically-mediated plasticity of the thalamic input pathway^{5,6,9,53}, although a minority of reports have also suggested the contribution of a presynaptic mechanism¹². Nonaka et al. (2014) recently used the *Arc::dVenus* mice to examine neuronal recruitment and synaptic plasticity following contextual conditioning in the basolateral amygdala (BLA)⁵². Similar to our findings, they observed a preferential recruitment of *Arc-dVenus*⁺ neurons evident in both the learning and non-associative conditions. Moreover, a presynaptically-mediated potentiation of cortical-BLA synaptic transmission was observed selectively in *Arc-dVenus*⁺ neurons, as evidenced by an increase in mEPSC frequency and a decrease in paired-pulse ratio. Taken together, these findings demonstrate that the induction of *Arc* IEG activation is a highly reliable marker for identifying the limited subset of neurons recruited to the fear memory trace and defined by pathway-specific alterations in synaptic transmission.

Previous studies demonstrating postsynaptically-mediated plasticity of the thalamic input pathway to the LA using whole-cell patch-clamp recordings were performed in randomly chosen LA neurons without knowledge of their *Arc* expression^{5,6}. Our findings now extend these results by demonstrating that potentiation of glutamatergic synaptic transmission occurs disproportionately onto *Arc*⁺ neurons. However, this also raises an important question regarding the *Arc*⁻ population, which presumably constitute a substantial proportion of the recorded neurons. Notably, although not statistically significant, there was a strong trend for increased synaptic transmission within the *Arc*⁻ population in mice receiving paired training, compared to the unpaired and naïve groups (Fig. 5b). Moreover, there are two notable aspects of our experimental design that may also be important to consider. First, we performed the electrophysiological recordings directly following training without intervening memory testing, given the increasing literature demonstrating that retrieval of newly learned associations modifies synaptic physiology^{12,54–57}. Furthermore, given the highly divergent CS-evoked freezing responses between the paired and unpaired groups, electrophysiological recordings would have always been confounded by the impact of their differential fear responses during the intervening test session.

Second, we chose a behavioural training protocol that did not result in overtraining (Supplementary Figure 2). In contrast, previous studies of thalamic-LA synaptic transmission demonstrating postsynaptically-mediated plasticity have used stronger conditioning protocols. With more robust training, it is possible that changes in thalamic-LA synaptic transmission might have occurred outside the *Arc*⁺ population. Alternatively, the *Arc*⁺ population might have constituted a significantly larger proportion of LA neurons than we have observed, for which random sampling would have yielded the observed effects despite the learning-specific changes in thalamic-LA synaptic transmission being largely restricted to the *Arc*⁺ population, however this latter possibility is inconsistent with our finding of an asymptotic percentage of *Arc*⁺ neurons beyond 3 CS-US pairings.

In addition to learning-induced plasticity, we also observed that neurons with baseline elevation of intrinsic excitability are preferentially recruited into the fear memory trace. Previous studies using viral-mediated overexpression of CREB have proposed intrinsic excitability as a candidate cellular mechanism for neuronal selection during

fear learning in the LA^{15–17,58}. However, it remained unknown to what extent these findings recapitulated the endogenous physiological mechanism. Our present results add compelling evidence that intrinsic excitability is indeed a highly influential cellular mechanism underlying recruitment of individual LA neurons during fear memory encoding. Interestingly, studies in both vertebrate and invertebrate species have demonstrated robust and enduring learning-induced alterations in neuronal excitability^{59–66}. Our findings provide strong support for the hypothesis that neurons with baseline elevation of intrinsic excitability are preferentially recruited into the memory trace, and may serve to bind together experiences acquired closely together in time. Moreover, we speculate that the recent elegant studies using targeted manipulations of IEG-defined memory traces are influencing neuronal selection during learning precisely through modulation of neuronal excitability^{30,31}.

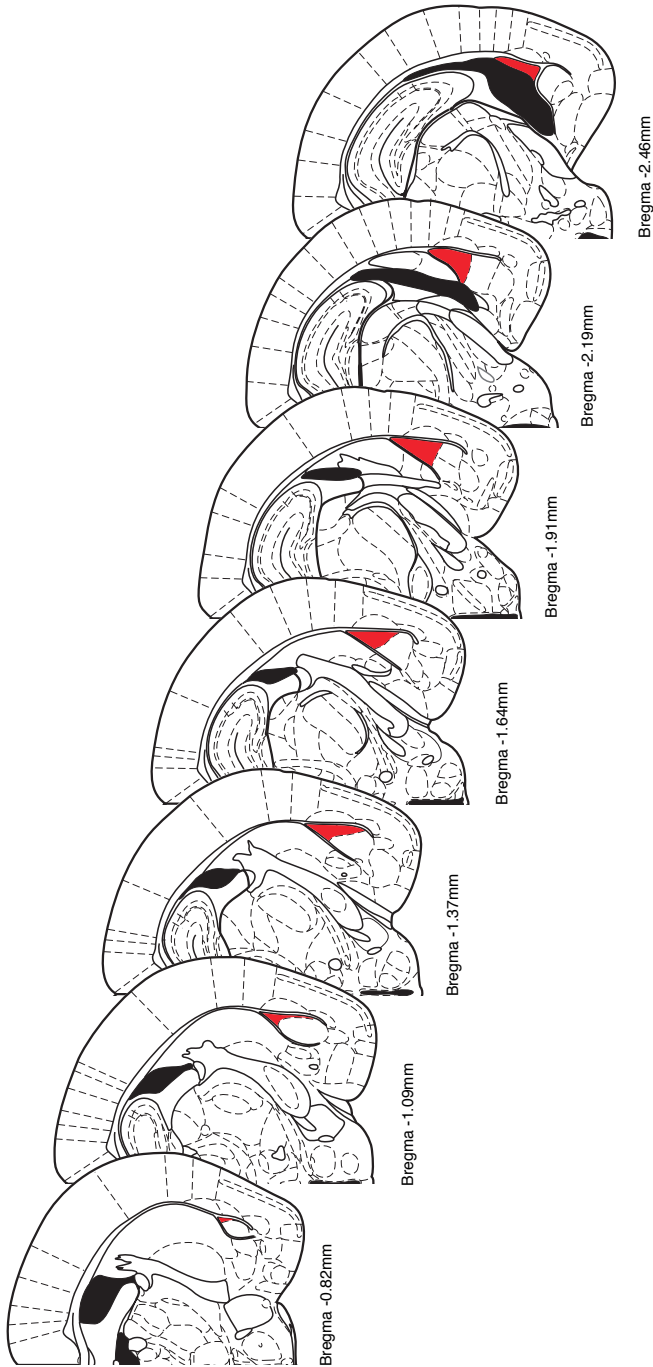
We observed an asymptotic percentage of *Arc*-dVenus⁺ neurons beyond 3 CS-US pairings, despite a further increase in dVenus fluorescence intensity in mice receiving 9 CS-US pairings. Therefore, neuronal selection during fear learning appears to be constrained by the intrinsic microcircuitry of the LA, leading to re-activation of a similar neuronal subpopulation upon successive CS-US pairings throughout the training session. Given the extensive inhibitory network within the LA, a feed-forward inhibitory microcircuitry is a well-suited candidate for mediating this outcome^{67,68}. Previous studies have demonstrated unique mechanisms of inhibitory interneuron plasticity within the LA that are likely to function critically in both neuronal selection and fear memory encoding^{17,67–71}. Future studies using multicellular recordings will be required to more precisely define the local microcircuit connectivity and cell-type specific mechanisms of plasticity.

Our experiments utilized two independent control groups: a) Unpaired: mice receiving explicitly unpaired CS and US presentations but matched with the paired condition regarding the number and specifications of the CS and US, context exposure, and handling; and b) Naïve: mice that were truly naïve to any experimental manipulations in that they had no context exposures, nor any handling beyond their standard housing conditions. Our rationale for this design was that the unpaired condition would provide the ideal control for handling, context exposure, and the influence of CS and US stimuli independent of auditory fear conditioning. However,

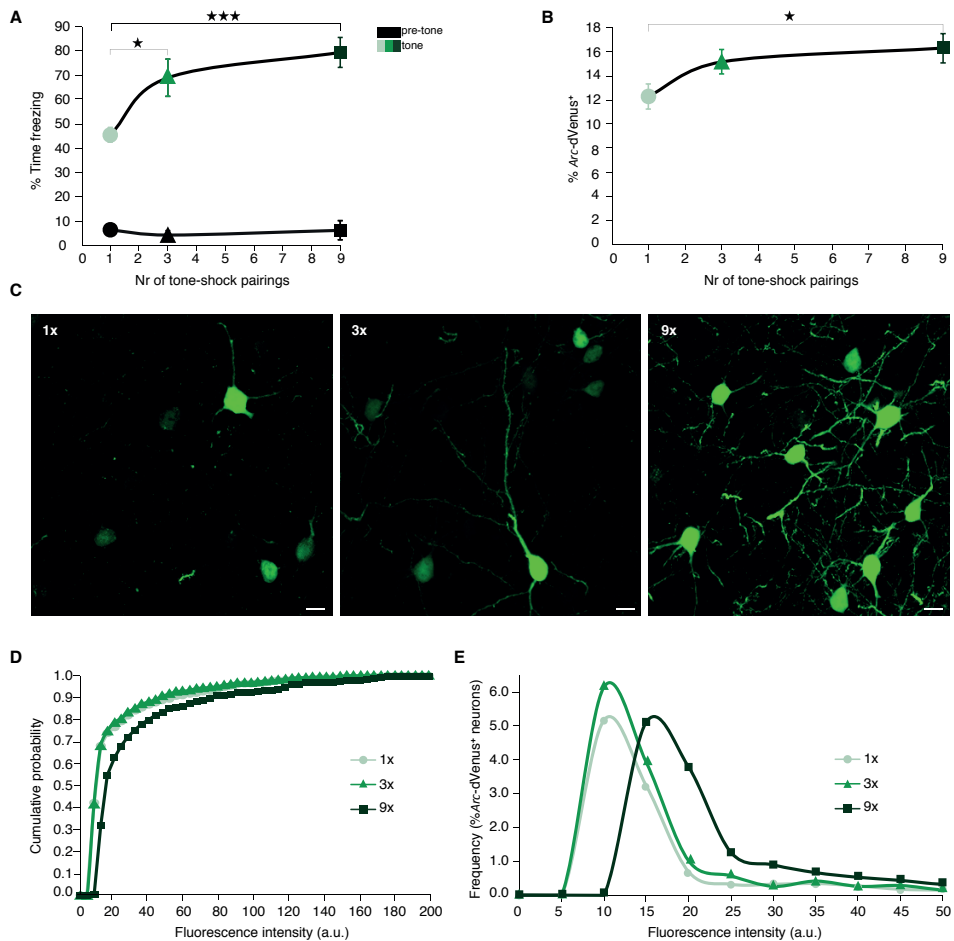
any differences observed between the naïve and unpaired groups remain difficult to precisely attribute etiologically, as these effects could be due to the handling, context exposure, CS and/or US stimuli. Moreover, mice receiving unpaired training undergo contextual conditioning. Differences in the naïve and unpaired groups were observed exclusively in experiments examining dVenus fluorescence intensity (Fig. 2, c & d) and neuronal recruitment (Fig. 3), in which the effect size was in both cases smaller than observed in the paired condition. No differences were observed in electrophysiological recordings comparing dVenus⁺ and dVenus⁻ neurons between the naïve and unpaired conditions. Rather, the only electrophysiological difference observed between naïve and unpaired mice regarded AP threshold (Supplementary Table 1), an effect that was independent of dVenus status. Therefore, learning-specific changes in synaptic plasticity cannot be accounted for by handling, context exposure, or the unpaired presentation of CS and US stimuli. In contrast, neuronal recruitment in the LA appears to occur independently of auditory fear learning, and mediated by one or more of the stimuli distinguishing the unpaired and naïve groups. Given the function of the LA in assigning emotional valence, we would hypothesize that the strong recruitment in the unpaired condition likely results from the stress sensitization of the US stimuli, but future studies will be required to examine this in further detail.

Taken together with previous findings, we propose a model of fear learning in which non-associative neuronal selection and Hebbian synaptic encoding of the learned association are distinct physiological processes: intrinsic excitability determines neuronal selection, while learning-related encoding is governed by synaptic plasticity.

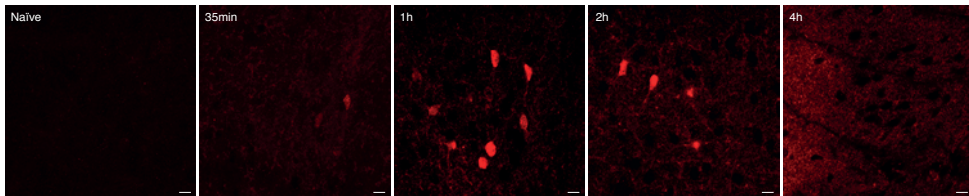
SUPPLEMENTARY FIGURE/TABLE



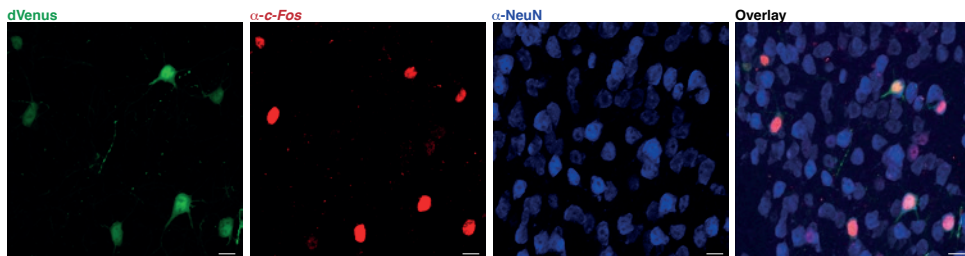
Supplementary Figure 1: Serial sections of LA for confocal stereology. Stereological analysis was performed systematically at 160 μm intervals across the entire rostro-caudal extent of the LA using coronal brain sections (red). Bregma coordinates are shown based upon the *in vivo* grid, prior to tissue processing. Modified from Paxinos and Franklin⁷²



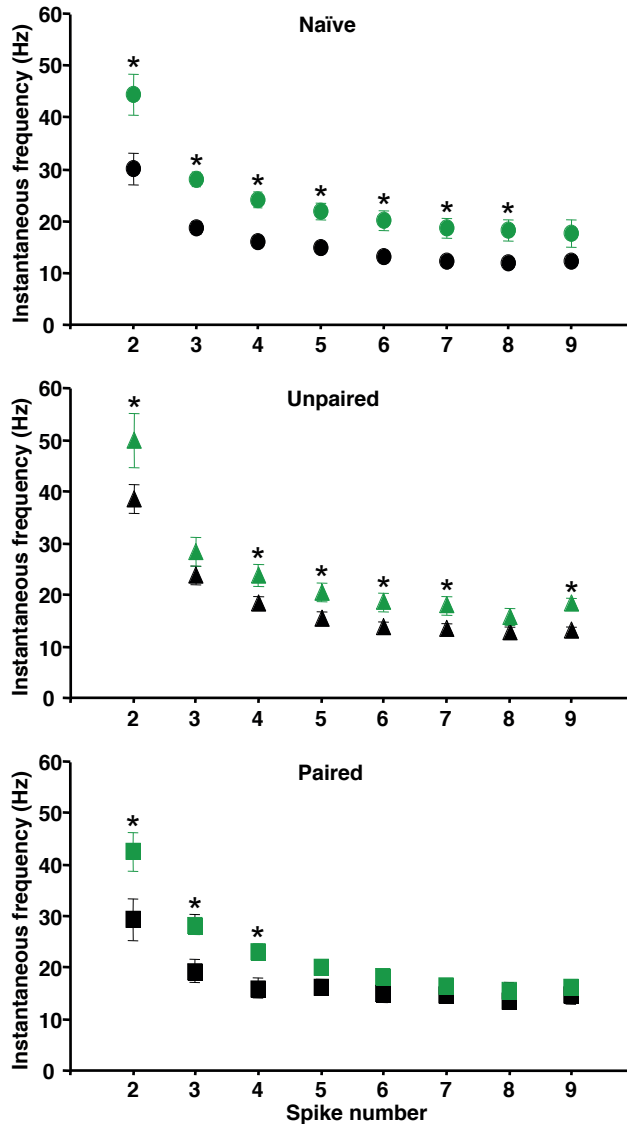
Supplementary Figure 2: Influence of the strength of conditioning on *Arc-dVenus* expression. (A) Tone-induced freezing in mice trained with 1, 3, or 9 CS-US pairings (Naïve: $n=8$ mice, Unpaired: $n=7$ mice, Paired: $n=8$ mice). One-way ANOVA, $F=9.34$, $P<0.001$. (B) Stereological quantification of *Arc-dVenus*⁺ neurons (Naïve: $n=6$ mice, Unpaired: $n=6$ mice, Paired: $n=6$ mice). One-way ANOVA, $F=3.65$, $P<0.05$. (C) Native dVenus fluorescence at 5h post-training. Scale bar, 10 μm . (D) Cumulative distribution of *Arc-dVenus* fluorescence intensity. Fluorescence intensity is significantly higher in mice receiving 9 CS-US pairings, compared to mice receiving only 1 or 3. Kolmogorov-Smirnov: 1 vs. 9, $D=0.23$, $P<0.01$; 3 vs. 9, $D=0.25$, $P<0.01$. (E) Frequency histograms of *Arc-dVenus* fluorescence intensity. X-axis is truncated at 50 a.u. (Panels D and E: bin size, 5 a.u.). * $P<0.05$, *** $P<0.001$



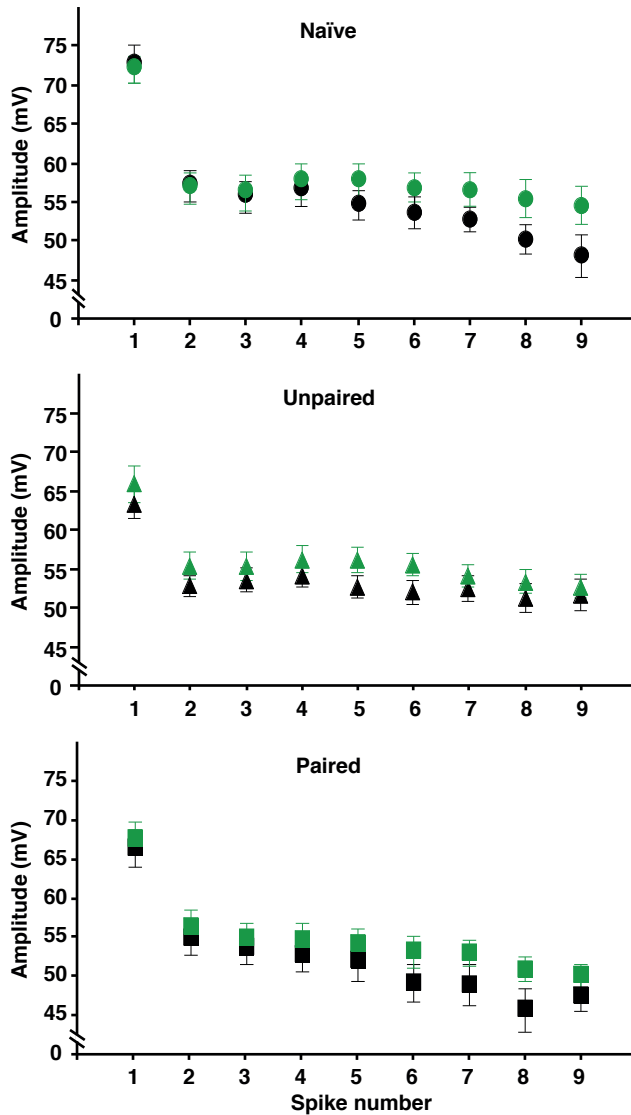
Supplementary Figure 3: Time course of endogenous *Arc* activation in the LA following fear conditioning. Representative images of endogenous *Arc* expression at multiple time points after paired conditioning. Endogenous *Arc* expression is higher at 1h after fear conditioning compared to other time points and to naïve mice. Scale bar, 10 μ m



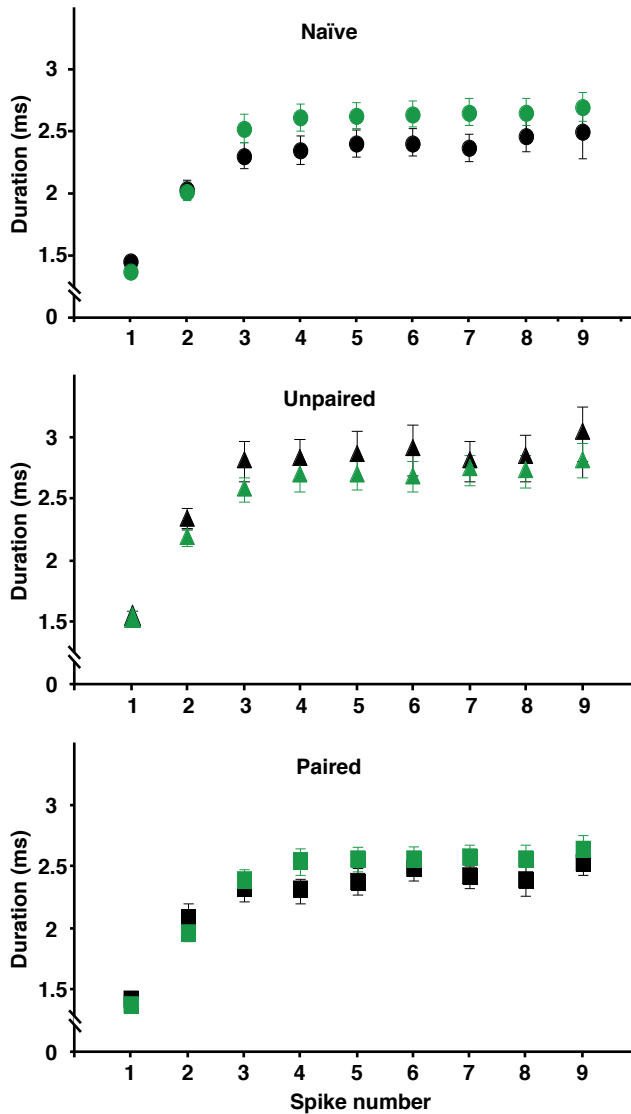
Supplementary Figure 4: Co-localization of *Arc*-dVenus and endogenous *c-Fos*. Endogenous *c-Fos* and *Arc*-dVenus expression are highly co-localized in the LA at 1h following paired conditioning. Scale bar, 10 μ m.



Supplementary Figure 5: *Arc-dVenus*⁺ neurons display higher instantaneous AP frequencies during spike trains. Plot of the mean AP instantaneous frequencies from the maximal number of evoked AP for naïve (top), unpaired (middle) and paired (bottom) conditions. *Arc-dVenus*⁺ neurons (naïve: *n*=15, unpaired: *n*=17, paired: *n*=16; filled symbols) show higher AP instantaneous frequencies compared to neighboring *Arc-dVenus*⁻ neurons (naïve: *n*=16, unpaired: *n*=17, paired: *n*=18; open symbols). Naïve: *n*=12 mice, Unpaired: *n*=6 mice, Paired: *n*=8 mice. **P* < 0.05.



Supplementary Figure 6: *Arc*-dVenus⁺ neurons have the same AP amplitude during spike trains. Plot of the mean AP amplitude from the maximal number of evoked AP for naïve (top), unpaired (middle) and paired (bottom) conditions. *Arc*-dVenus⁺ neurons (naïve: $n=15$, unpaired: $n=17$, paired: $n=16$; filled symbols) and *Arc*-dVenus⁻ neighbors (naïve: $n=16$, unpaired: $n=17$, paired: $n=18$; open symbols) have similar AP amplitude. Naïve: $n=12$ mice, Unpaired: $n=6$ mice, Paired: $n=8$ mice.



Supplementary Figure 7: *Arc-dVenus*⁺ neurons have similar AP duration during spike trains. Plot of the mean AP half-width from the maximal number of evoked AP for naïve (top), unpaired (middle) and paired (bottom) conditions. *Arc-dVenus*⁺ neurons (naïve: $n=15$, unpaired: $n=17$, paired: $n=16$; filled symbols) and *Arc-dVenus*⁺ neighbors (naïve: $n=16$, unpaired: $n=17$, paired: $n=18$; open symbols) have the same AP duration. Naïve: $n=12$ mice, Unpaired: $n=6$ mice, Paired: $n=8$ mice.

	n	Membrane resistance (MΩ)	Membrane capacitance (pF)	Resting membrane potential (mV)	AP threshold (mV)	AP peak amplitude (mV)	AP antipeak amplitude (mV)	AP half-width (ms)
Naïve Arc-dVenus⁺	15	290.5 ± 61.7	53.1 ± 5.8	-59.5 ± 0.9	-35.2 ± 1.4	71.0 ± 3.1	-21.4 ± 1.4	1.29 ± 0.02
Naïve Arc-dVenus⁻	16	225.1 ± 18.8	54.4 ± 5.0	-63.3 ± 2.0	-35.8 ± 1.1	75.1 ± 3.0	-19.6 ± 1.3	1.32 ± 0.03
Unpaired Arc-dVenus⁺	16	216.0 ± 15.4	55.0 ± 3.6	-63.9 ± 1.5	-31.4 ± 1.3	64.5 ± 3.0	-21.9 ± 1.1	1.33 ± 0.03
Unpaired Arc-dVenus⁻	17	232.1 ± 17.4	61.0 ± 6.1	-64.1 ± 1.2	-30.5 ± 1.3	66.7 ± 2.6	-22.0 ± 1.1	1.32 ± 0.02
Paired Arc-dVenus⁺	16	190.7 ± 7.2	61.6 ± 5.4	-65.4 ± 1.2	-30.2 ± 1.4	66.0 ± 2.7	-24.8 ± 1.0	1.21 ± 0.03
Paired Arc-dVenus⁻	18	213.5 ± 12.5	55.1 ± 2.6	-62.4 ± 1.2	-30.5 ± 1.6	70.1 ± 1.7	-22.5 ± 1.2	1.25 ± 0.03

Supplementary Table 1: Passive membrane properties and single AP characteristics. *Arc-dVenus⁺* and *Arc-dVenus⁻* neurons displayed similar passive and active membrane properties in naïve, unpaired and paired conditions. Naïve: n=12 mice, Unpaired: n=6 mice, Paired: n=7 mice.

References

1. Rescorla, R. A. Pavlovian conditioning and its proper control procedures. *Psychol Rev* **74**, 71–80 (1967).
2. LeDoux, J. E., Cicchetti, P., Xagoraris, A. & Romanski, L. M. The lateral amygdaloid nucleus: sensory interface of the amygdala in fear conditioning. *The Journal of neuroscience : the official journal of the Society for Neuroscience* **10**, 1062–9 (1990).
3. Quirk, G. J., Repa, C. & LeDoux, J. E. Fear conditioning enhances short-latency auditory responses of lateral amygdala neurons: parallel recordings in the freely behaving rat. *Neuron* **15**, 1029–39 (1995).
4. Johansen, J. P., Cain, C. K., Ostroff, L. E. & LeDoux, J. E. Molecular mechanisms of fear learning and memory. *Cell* **147**, 509–24 (2011).
5. Rumpel, S., LeDoux, J., Zador, A. & Malinow, R. Postsynaptic receptor trafficking underlying a form of associative learning. *Science (New York, N.Y.)* **308**, 83–8 (2005).
6. Clem, R. L. & Huganir, R. L. Calcium-permeable AMPA receptor dynamics mediate fear memory erasure. *Science* **330**, 1108–12 (2010).
7. Rodrigues, S. M., Schafe, G. E. & LeDoux, J. E. Intra-amygdala blockade of the NR2B subunit of the NMDA receptor disrupts the acquisition but not the expression of fear conditioning. *J Neurosci* **21**, 6889–96 (2001).
8. Bauer, E. P., Schafe, G. E. & LeDoux, J. E. NMDA receptors and L-type voltage-gated calcium channels contribute to long-term potentiation and different components of fear memory formation in the lateral amygdala. *The Journal of neuroscience : the official journal of the Society for Neuroscience* **22**, 5239–49 (2002).
9. Humeau, Y. *et al.* A pathway-specific function for different AMPA receptor subunits in amygdala long-term potentiation and fear conditioning. *J Neurosci* **27**, 10947–56 (2007).
10. Rogan, M. T., Stäubli, U. V & LeDoux, J. E. Fear conditioning induces associative long-term potentiation in the amygdala. *Nature* **390**, 604–7 (1997).
11. McKernan, M. G. & Shinnick-Gallagher, P. Fear conditioning induces a lasting potentiation of synaptic currents in vitro. *Nature* **390**, 607–11 (1997).
12. Li, Y. *et al.* Learning and reconsolidation implicate different synaptic mechanisms. *Proceedings of the National Academy of Sciences of the United States of America* **110**, 4798–803 (2013).
13. Han, J.-H. *et al.* Neuronal competition and selection during memory formation. *Science (New York, N.Y.)* **316**, 457–60 (2007).
14. Kim, J., Kwon, J.-T., Kim, H.-S., Josselyn, S. a & Han, J.-H. Memory recall and modifications by activating neurons with elevated CREB. *Nat Neurosci* (2013). doi:10.1038/nn.3592
15. Zhou, Y. *et al.* CREB regulates excitability and the allocation of memory to

- subsets of neurons in the amygdala. *Nat Neurosci* **12**, 1438–43 (2009).
16. Silva, A. J., Zhou, Y., Rogerson, T., Shobe, J. & Balaji, J. Molecular and cellular approaches to memory allocation in neural circuits. *Science (New York, N.Y.)* **326**, 391–5 (2009).
 17. Kim, D., Paré, D. & Nair, S. S. Assignment of model amygdala neurons to the fear memory trace depends on competitive synaptic interactions. *The Journal of neuroscience : the official journal of the Society for Neuroscience* **33**, 14354–8 (2013).
 18. Repa, J. C. *et al.* Two different lateral amygdala cell populations contribute to the initiation and storage of memory. *Nature neuroscience* **4**, 724–31 (2001).
 19. An, B., Hong, I. & Choi, S. Long-term neural correlates of reversible fear learning in the lateral amygdala. *J Neurosci* **32**, 16845–56 (2012).
 20. Kawashima, T. *et al.* Functional labeling of neurons and their projections using the synthetic activity-dependent promoter E-SARE. *Nat Methods* **10**, 889–95 (2013).
 21. Benedetti, B. L., Takashima, Y., Wen, J. A., Urban-Ciecko, J. & Barth, A. L. Differential Wiring of Layer 2/3 Neurons Drives Sparse and Reliable Firing During Neocortical Development. *Cereb Cortex* **22**, (2012).
 22. Wang, K. H. *et al.* In vivo two-photon imaging reveals a role of arc in enhancing orientation specificity in visual cortex. *Cell* **126**, 389–402 (2006).
 23. Guzowski, J. F., McNaughton, B. L., Barnes, C. A. & Worley, P. F. Environment-specific expression of the immediate-early gene Arc in hippocampal neuronal ensembles. *Nature neuroscience* **2**, 1120–4 (1999).
 24. Guzowski, J. F. *et al.* Recent behavioral history modifies coupling between cell activity and Arc gene transcription in hippocampal CA1 neurons. *Proceedings of the National Academy of Sciences of the United States of America* **103**, 1077–82 (2006).
 25. Reijmers, L. G., Perkins, B. L., Matsuo, N. & Mayford, M. Localization of a stable neural correlate of associative memory. *Science (New York, N.Y.)* **317**, 1230–3 (2007).
 26. Tayler, K. K., Tanaka, K. Z., Reijmers, L. G. & Wiltgen, B. J. Reactivation of neural ensembles during the retrieval of recent and remote memory. *Current biology : CB* **23**, 99–106 (2013).
 27. Trouche, S., Sasaki, J. M., Tu, T. & Reijmers, L. G. Fear Extinction Causes Target-Specific Remodeling of Perisomatic Inhibitory Synapses. *Neuron* **80**, 1–12 (2013).
 28. Han, J.-H. *et al.* Selective erasure of a fear memory. *Science (New York, N.Y.)* **323**, 1492–6 (2009).
 29. Liu, X. *et al.* Optogenetic stimulation of a hippocampal engram activates fear memory recall. *Nature* **484**, 381–5 (2012).
 30. Garner, A. R. *et al.* Generation of a synthetic memory trace. *Science* **335**,

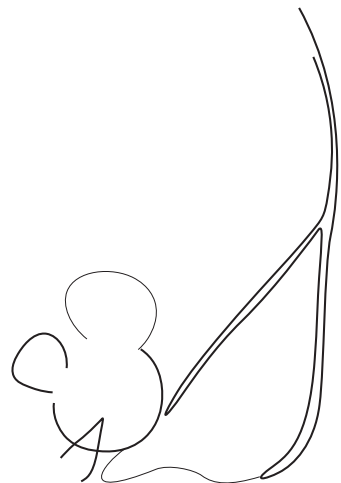
- 1513–6 (2012).
31. Ramirez, S. *et al.* Creating a false memory in the hippocampus. *Science (New York, N.Y.)* **341**, 387–91 (2013).
 32. Eguchi, M. & Yamaguchi, S. In vivo and in vitro visualization of gene expression dynamics over extensive areas of the brain. *NeuroImage* **44**, 1274–83 (2009).
 33. Cain, C. K. & LeDoux, J. E. Escape from fear: a detailed behavioral analysis of two atypical responses reinforced by CS termination. *J Exp Psychol Anim Behav Process* **33**, 451–63 (2007).
 34. Anagnostaras, S. G. *et al.* Automated assessment of pavlovian conditioned freezing and shock reactivity in mice using the video freeze system. *Front Behav Neurosci* **4**, 1–11 (2010).
 35. Hossaini, M., Jongen, J. L. M., Biesheuvel, K., Kuhl, D. & Holstege, J. C. Nociceptive stimulation induces expression of Arc/Arg3.1 in the spinal cord with a preference for neurons containing enkephalin. *Mol Pain* **6**, 43 (2010).
 36. Ben-Ari, Y., Zigmond, R. E., Shute, C. C. & Lewis, P. R. Regional distribution of choline acetyltransferase and acetylcholinesterase within the amygdaloid complex and stria terminalis system. *Brain Res* **120**, 435–44. (1977).
 37. Inberg, S., Elkobi, A., Edri, E. & Rosenblum, K. Taste familiarity is inversely correlated with Arc/Arg3.1 hemispheric lateralization. *The Journal of neuroscience : the official journal of the Society for Neuroscience* **33**, 11734–43 (2013).
 38. Gundersen, H. J. Stereology of arbitrary particles. A review of unbiased number and size estimators and the presentation of some new ones, in memory of William R. Thompson. *J Microsc* **143**, 3–45 (1986).
 39. Gundersen, H. J. & Jensen, E. B. The efficiency of systematic sampling in stereology and its prediction. *J Microsc* **147**, 229–63 (1987).
 40. Schmitz, C. Variation of fractionator estimates and its prediction. *Anat Embryol (Berl)* **198**, 371–97 (1998).
 41. Lang, E. J. & Paré, D. Synaptic responsiveness of interneurons of the cat lateral amygdaloid nucleus. *Neuroscience* **83**, 877–89 (1998).
 42. Mahanty, N. K. & Sah, P. Calcium-permeable AMPA receptors mediate long-term potentiation in interneurons in the amygdala. *Nature* **394**, 683–687 (1998).
 43. Faber, E. S., Callister, R. J. & Sah, P. Morphological and electrophysiological properties of principal neurons in the rat lateral amygdala in vitro. *J Neurophysiol* **85**, 714–23 (2001).
 44. Vazdarjanova, A. *et al.* Spatial Exploration Induces ARC , a Only in Calcium / Calmodulin-Dependent Protein Kinase II-Positive Principal Excitatory and Inhibitory Neurons of the Rat Forebrain. *J Comp Neurol* **329**, 317–329 (2006).

45. Rudinskiy, N. *et al.* Orchestrated experience-driven Arc responses are disrupted in a mouse model of Alzheimer's disease. *Nat Neurosci* **15**, 1422–9 (2012).
46. Waclaw, R. R., Ehrman, L. a, Pierani, A. & Campbell, K. Developmental origin of the neuronal subtypes that comprise the amygdalar fear circuit in the mouse. *J Neurosci* **30**, 6944–53 (2010).
47. Lyford, G. L. *et al.* Arc, a growth factor and activity-regulated gene, encodes a novel cytoskeleton-associated protein that is enriched in neuronal dendrites. *Neuron* **14**, 433–45 (1995).
48. Parsons, R. G. & Davis, M. A metaplasticity-like mechanism supports the selection of fear memories: role of protein kinase a in the amygdala. *J Neurosci* **32**, 7843–51 (2012).
49. Cowansage, K. K., Bush, D. E. A., Josselyn, S. A., Klann, E. & Ledoux, J. E. Basal variability in CREB phosphorylation predicts trait-like differences in amygdala-dependent memory. *Proc Natl Acad Sci U S A* **1–6** (2013). doi:10.1073/pnas.1304665110
50. Soulé, J. *et al.* Balancing Arc synthesis, mRNA decay, and proteasomal degradation: maximal protein expression triggered by rapid eye movement sleep-like bursts of muscarinic cholinergic receptor stimulation. *The Journal of biological chemistry* **287**, 22354–66 (2012).
51. Liao, D., Hessler, N. A. & Malinow, R. Activation of postsynaptically silent synapses during pairing-induced LTP in CA1 region of hippocampal slice. *Nature* **75**, 400–4 (1995).
52. Nonaka, A. *et al.* Synaptic Plasticity Associated with a Memory Engram in the Basolateral Amygdala. *Journal of Neuroscience* **34**, 9305–9309 (2014).
53. Humeau, Y. *et al.* Dendritic spine heterogeneity determines afferent-specific Hebbian plasticity in the amygdala. *Neuron* **45**, 119–31 (2005).
54. Ben Mamou, C., Gamache, K. & Nader, K. NMDA receptors are critical for unleashing consolidated auditory fear memories. *Nature neuroscience* **9**, 1237–9 (2006).
55. Rao-Ruiz, P. *et al.* Retrieval-specific endocytosis of GluA2-AMPA receptors underlies adaptive reconsolidation of contextual fear. *Nature neuroscience* **14**, 1302–8 (2011).
56. Hong, I. *et al.* AMPA receptor exchange underlies transient memory destabilization on retrieval. *Proceedings of the National Academy of Sciences of the United States of America* **110**, 8218–23 (2013).
57. Fukushima, H. *et al.* Enhancement of fear memory by retrieval through reconsolidation. *eLife* **3**, e02736 (2014).
58. Yiu, A. P. *et al.* Neurons Are Recruited to a Memory Trace Based on Relative Neuronal Excitability Immediately before Training. *Neuron* **83**, 722–735 (2014).

59. Brons, J. F. & Woody, C. D. Long-term changes in excitability of cortical neurons after Pavlovian conditioning and extinction. *J Neurophysiol* **44**, 605–15 (1980).
60. Alkon, D. L. Calcium-mediated reduction of ionic currents: a biophysical memory trace. *Science* **226**, 1037–45 (1984).
61. Moyer, J. R., Thompson, L. T. & Disterhoft, J. F. Trace eyeblink conditioning increases CA1 excitability in a transient and learning-specific manner. *J Neurosci* **16**, 5536–46 (1996).
62. Antonov, I., Antonova, I., Kandel, E. R. & Hawkins, R. D. The contribution of activity-dependent synaptic plasticity to classical conditioning in *Aplysia*. *J Neurosci* **21**, 5536–46 (2001).
63. Saar, D. & Barkai, E. Long-term modifications in intrinsic neuronal properties and rule learning in rats. *Eur J Neurosci* **17**, 2727–2734 (2003).
64. Santini, E., Quirk, G. J. & Porter, J. T. Fear conditioning and extinction differentially modify the intrinsic excitability of infralimbic neurons. *J Neurosci* **28**, 4028–36 (2008).
65. McKay, B. M., Matthews, E. A., Oliveira, F. A. & Disterhoft, J. F. Intrinsic neuronal excitability is reversibly altered by a single experience in fear conditioning. *J Neurophysiol* **102**, 2763–70 (2009).
66. Sehgal, M., Ehlers, V. L. & Moyer, J. R. Learning enhances intrinsic excitability in a subset of lateral amygdala neurons. *Learning & memory (Cold Spring Harbor, N.Y.)* **21**, 161–70 (2014).
67. Bissière, S., Humeau, Y. & Lüthi, A. Dopamine gates LTP induction in lateral amygdala by suppressing feedforward inhibition. *Nature neuroscience* **6**, 587–92 (2003).
68. Polepalli, J. S., Sullivan, R. K. P., Yanagawa, Y. & Sah, P. A specific class of interneuron mediates inhibitory plasticity in the lateral amygdala. *The Journal of neuroscience : the official journal of the Society for Neuroscience* **30**, 14619–29 (2010).
69. Bauer, E. P. & LeDoux, J. E. Heterosynaptic long-term potentiation of inhibitory interneurons in the lateral amygdala. *The Journal of neuroscience : the official journal of the Society for Neuroscience* **24**, 9507–12 (2004).
70. Szinyei, C., Narayanan, R. T. & Pape, H.-C. Plasticity of inhibitory synaptic network interactions in the lateral amygdala upon fear conditioning in mice. *The European journal of neuroscience* **25**, 1205–11 (2007).
71. Wolff, S. B. E. *et al.* Amygdala interneuron subtypes control fear learning through disinhibition. *Nature* **509**, 453–8 (2014).
72. Paxinos, G. & Franklin, K. B. J. *The Mouse Brain in Stereotaxic Coordinates, Deluxe 2nd edition.* (Academic Press, 2001).

Chapter 3
***Novel fear learning-dependent activity of
Arc in the ventrolateral subregion of lateral
amygdala***

Hosseini B, Jaarsma D, Suzuki L, Stedehouder J, Ruigrok T,
Slump DE, Rao-Ruiz P, Kushner SA



Novel fear learning-dependent activity of Arc in the ventrolateral subregion of lateral amygdala

Hosseini B¹, Jaarsma D², Suzuki L¹, Stedehouder J¹, Ruigrok T², Slump DE¹, Rao-Ruiz P¹, Kushner SA¹

¹Department of Psychiatry, Erasmus University Medical Center, Dr. Molewaterplein 50, 3015 GE Rotterdam, The Netherlands

² Department of Neuroscience, Erasmus Medical Centre, Dr. Molewaterplein 50, 3015 GE Rotterdam, The Netherland

ABSTRACT

Sparse populations of neurons are recruited during the consolidation of fear memory in the lateral amygdala (LA). Induction of immediate early gene (IEGs) transcription distinguishes these individual neurons that undergo recent learning-induced modifications. Here, we identified a discrete subpopulation of *Arc positive neurons* in the ventrolateral subnucleus of the lateral amygdala (LaVL). Our results indicate that these explicit neuronal substrates express *Arc* specifically during new learning and not during retrieval or relearning.

INTRODUCTION

The fear-conditioning paradigm, where an animal learns to associate a previously neutral conditioned stimulus (CS) to an aversive unconditioned stimulus (US) has been widely used to study the neurobiological basis of learning and memory across species¹. A large body of evidence points to the basolateral complex of the amygdala, comprising of the lateral amygdala (LA), basal amygdala (BA) and basomedial nuclei (BM), as being critical to the consolidation and maintenance of fear memories²⁻⁸.

Intriguingly only a sparse subset of neurons within the LA, consisting of dorsal (dLA) and ventral (vLA) subregions, is recruited to the consolidation of memory, and these collectively form a memory-trace⁹⁻¹¹. These limited numbers of cells are capable of

learning related plasticity and are both necessary and sufficient to evoke memory recall¹². Visualization of Immediate Early Gene (IEG) activity, such as that of the proto-oncogene *c-Fos* and the activity-regulated cytoskeleton-associated protein (*Arc*), has been widely used to identify the composition of fear memory-traces in different brain regions¹²⁻¹⁷. Using these molecular tags, sparse populations of LA, particularly dLA, neurons have been causally linked to fear memory consolidation, with tagged memory-trace cells exhibiting persistent modification of synaptic strength in the hours following conditioning¹⁸⁻²². While the activation profile of memory-trace cells within the dLA has been well defined, the identity and distribution of neuronal ensembles involved in different phases of fear conditioning in the vLA remains relatively unknown.

Recorded single-cell activity in the dLA and vLA after learning, indicates that these subregions may contribute differently to the initiation and storage of memory respectively¹¹. Additionally, activated neurons in the basal nucleus of the amygdala are reportedly reactivated during retrieval¹². This raises the interesting question of whether memory-trace neurons in different subregions of the amygdala are differently engaged during distinct phases of memory processing. Furthermore, it is not known whether the neurons recruited to a specific memory are reactivated when animals undergo a subsequent learning experience.

Here we aim to systematically identify memory-trace neurons in the vLA and elucidate if they are differentially involved in the encoding, relearning and retrieval of fear memory. To this end, we make use of a fluorescence-based reporter of *Arc* that provides a precise molecular tag for neurons that undergo learning related changes²³. We have previously shown that this system enables the identification and physiologic characterization of cells participating in the dLA fear memory trace²⁴. In this study, we identify a subset neurons in the ventrolateral nucleus of the LA (LaVL), that express *Arc* selectively during the consolidation, but not retrieval, of novel fear memories, when there is a prominent difference between expectancy and actual experience.

MATERIALS AND METHOD

Animals

Arc::dVenus mice were backcrossed more than 10 generations into C57BL/6J. Mice were maintained on a 12 h light/dark cycle with food and water available *ad libitum*.

All experiments were performed during the light phase, using adult mice (postnatal weeks 8-11). Mice were single-housed for 5 days prior to the start of experiments. All experiments were approved by Dutch Ethical Committee and in accordance with the Institutional Animal Care and Use Committee (IACUC) guidelines. The behavioral protocols and fluorescence intensity analyses were done using 3-4 *Arc::dVenus* mice/group.

Auditory fear conditioning

Fear conditioning was performed using a Med Associates Standard Fear Conditioning chamber (30.5 cm × 24.1 cm × 21.0 cm) with a stainless-steel electrifiable grid floor, enclosed within a large sound-attenuating box. Video images were recorded using a progressive scan CCD video camera with a visible light filter suitable for near-infrared imaging.

Behavioral experiments

Home-cage (HC): Mice in naïve (home-cage) group received no exposure to the training context, they remained in their standard housing conditions until immediately prior to perfusion for confocal imaging.

Fear conditioning (FC): All mice were habituated to the conditioning chamber, 24 h prior to the training session, unless specified. Habituation sessions consisted of a 30 min exposure to the training context without any tone or shock presentations. On the day of conditioning, mice received one of the following fear-conditioning protocols:

Paired protocol: Animals were placed in the conditioning chamber for 180 s, followed by a series of three co-terminating presentations of a tone CS (30s, 5KH, 85 dB) and scrambled foot-shock unconditioned stimulus (US) (2 s, 0.75mA). The inter-trial

interval between tone-shock presentations was 210 s.

Weak conditioning protocol: Animals were placed in the conditioning chamber for 180 s, followed by a series of three co-terminating presentations of a tone CS (30s, 5KH, 85 dB) and scrambled foot-shock unconditioned stimulus (US) (2 s, 0.25mA). The intertrial interval between tone-shock presentations was 210 s.

White noise and new context protocol: Mice were placed in the conditioning chamber for 180 s, followed by a series of three co-terminating presentations of a tone CS (30s, 10KH, 85 dB) and scrambled foot-shock unconditioned stimulus (US) (2 s, 0.75mA). The inter-trial interval between tone-shock presentations was 210 s. The grid floor of the original context was replaced with a different new configuration.

Immediate shock protocol: No habituation session was applied for the immediate shock protocol. The 3 US (2 s interstimulus interval), were delivered immediately upon placement in the chamber.

No shock protocol: Mice were exposed to the conditioning context with the total duration of 810 s without receiving any US and CS stimulations.

Cue test protocol: Mice were put in a different context than the one they received the auditory fear conditioning training the day before. The tone started after 120 s of baseline and lasted for 180 s.

Context test: Mice were put for 300 s in the same context that they received the auditory fear conditioning protocol the day before.

Fox odor experiment: The procedure started by pre-exposing the *Arc::dVenus* mice to separate cages each for 30 minutes on two consecutive days. During the habituation sessions filter papers without fox odor were placed into the cages. On day three, the animals brought separately to the experimental room where they were put into the cages that they had experienced the habituation sessions. After 120 seconds of baseline recording, a piece of filter paper with 35ul 2,5-Dihydro-2,4,5-Trimethylthiazoline (TMT) was placed inside the cage. The test procedure lasted for approximately 30 minutes per animal and was recorded. Animals were sacrificed

5 hours after they exhibited freezing behaviors.

Immunofluorescence

After deep anesthesia induced by intra-peritoneal injection of pentobarbital (50 mg kg⁻¹), mice were transcardially perfused with saline, followed by 4% paraformaldehyde. Brains were dissected and post-fixed in 4% paraformaldehyde for 2 h at 4 °C. After post-fixation, the brains were transferred into 10% sucrose phosphate buffer (PB 0.1 M, pH 7.3) and stored overnight at 4 °C. Embedding was performed in a 10% gelatin+10% sucrose block, with fixation in 10% paraformaldehyde+30% sucrose solution for 2 h at room temperature and immersed in 30% sucrose at 4 °C. Forty micrometer coronal sections were collected serially (rostral to caudal) using a freezing microtome (Leica, Wetzlar, Germany; SM 2000R) and stored in 0.1M PB. Free-floating sections were incubated in sodium citrate (10mM) at 80 °C for 1 h and rinsed with tris-buffered saline (TBS, pH 7.6). Sections were pre-incubated with a blocking TBS buffer containing 0.5% Triton X-100 and 10% normal horse serum (NHS; Invitrogen, Bleiswijk, The Netherlands) for 1 h at room temperature. Sections were incubated in a mixture of primary antibodies, in TBS buffer containing 0.4% Triton X-100 and 2% NHS for 72 h at 4 °C. The following primary antibodies were used: mouse anti-NeuN (1:2000, Millipore, Hertfordshire, UK; MAB377), goat anti-choline acetyltransferase (1:200, Millipore AB144P, mouse anti-Arc (C-7, 1:200, Santa Cruz sc-17839, Heidelberg, Germany), rabbit anti-c-Fos (ab-5, 1:10000, Millipore PC38). Sections were washed with TBS, and incubated with corresponding Alexa-conjugated secondary antibodies (1:200, Invitrogen) and cyanine dyes (1:200, Sanbio, Uden, The Netherlands) in TBS buffer containing 0.4% Triton X-100, 2% NHS for 2 h at room temperature. For some experiments, nuclear staining was performed using DAPI (1:10000, Invitrogen). Sections were washed with PB 0.1M and mounted on slides, cover slipped with Vectashield H1000 fluorescent mounting medium (Vector Labs, Peterborough, UK), and sealed.

Confocal imaging

Stained LA images were acquired using a Zeiss LSM 700 confocal microscope (Carl Zeiss, Oberkochen, Germany) equipped with Zeiss Plan- Apochromat Å~ 10/0.45, Å~ 20/0.8 and Å~ 40/1.3 (oil immersion) objectives. Native dVenus, Cy3, Alexa647

and DAPI were imaged using the excitation wavelengths of 488, 555, 639 and 405 nm, respectively. Native dVenus fluorescence intensity was quantified using ImageJ (NIH, 1.42q) with the Multi Measure plug-in. The mean fluorescence intensity of *Arc*-dVenus⁺ neurons was determined by drawing a region of interest around the LaVL subregion.

Statistical analysis

Significance of observations was established by a two-tailed t test or analysis of variance followed by Tukey's *post hoc* test. Data are expressed as mean \pm s.e.m. Significance threshold was set at $P=0.05$ for all statistical comparisons.

RESULTS

We used *Arc::dVenus* transgenic mice in our study, where the destabilized Venus fluorescent protein (dVenus) is expressed under the control the *Arc* promoter. Using this mouse line, we are able to monitor *Arc* expression with a longer half-life after fear conditioning (4-7 hours)^{23,24} compared to that of the endogenous *Arc* (1hour)²⁵ without interfering with its function. This method enables optimal detection of *Arc* expression by visualizing native fluorescence of the dVenus reporter.

1. Learned aversive associations trigger the activation of a discrete population of cells in the LaVL

Fear conditioning results in the formation of a robust fear memory) (Fig. 1A,B)²⁴. At the cellular level, besides activation of the dLA fear memory trace, a discrete cluster-shaped ensemble of *Arc*-dVenus⁺ cells was detected in the ventrolateral nucleus of the LA (LaVL) of mice after fear conditioning (Fig. 1A, C, D and Fig .2). This activation was most pronounced with significantly increased levels of dVenus intensity in mice that associated the CS to the US (fear conditioned, FC) when compared to naïve home-cage (HC) controls or mice that received the CS but not the US (No shock, NS) (Fig, 1C, D), indicating that these cells are specifically involved in the formation of an associative fear memory. The LaVL ensemble was visualized up to 5 h after conditioning, with lower activity 24 h later (Fig. 3A, B). Furthermore, dVenus reporter fluorescence co-localized with endogenous expression of the IEGs, *Arc* and *c-Fos*, validating the activation of this LaVL subpopulation

after fear conditioning (Fig. 3C).

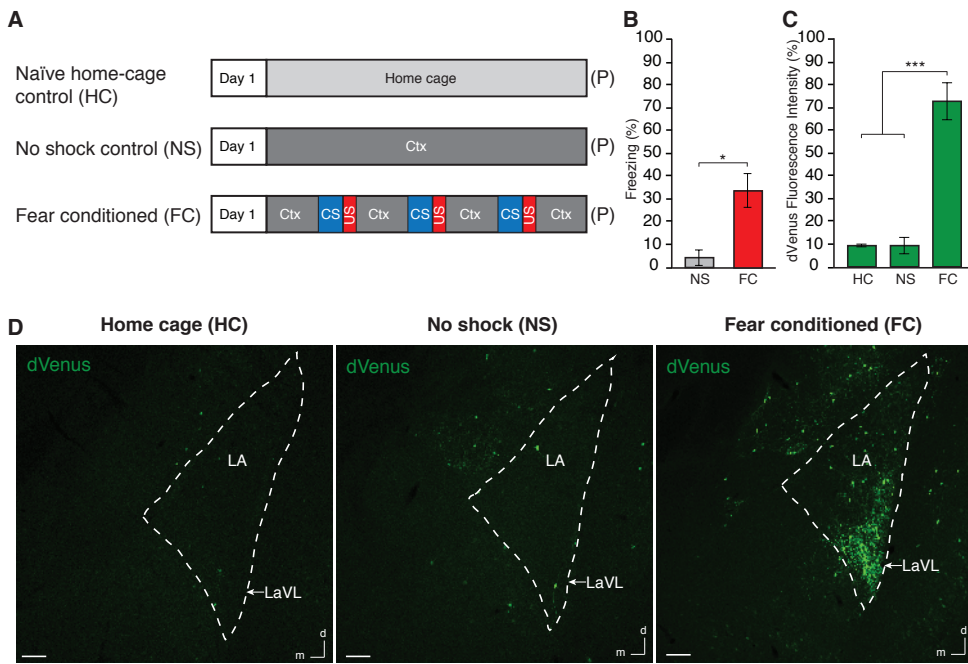


Figure 1. Learned aversive associations trigger the activation of a discrete population of cells in the LaVL. (A) Behavioural set up. Control mice were either naïve to the experimental conditions (home cage, HC), or were put in a fear-conditioning context without receiving any sensory stimulation (No-shock group, NS). Fear conditioned mice (FC) received 3 CS (tone) and US (foot-shock) associations. Mice were perfused 5 hrs after. (B) No shock controls exhibit very low levels of freezing during conditioning while fear conditioned mice exhibit a robust fear response to the context after the third CS-US paired training ($n=4$ mice/group). Two-tailed t-test, $P<0.05$. * $P<0.05$. (C) dVenus fluorescence intensity in the LaVL region is significantly higher in the FC group compared to the control conditions ($n=3$ mice/group). One-way analysis of variance, $F=26.867$, $P<0.001$. *** $P<0.001$. All data points show mean \pm s.e.m. (D) Representative images indicating fear conditioning results in the activation of a memory trace with *Arc*-dVenus expression in the LA and the LaVL, when compared to naïve and no shock groups. Scale bar, 100 μ m. d, dorsal; m, medial; (P), perfusion.

Next, in order to confirm that this observed activity in the LaVL was induced by learned associations to the aversive stimulus and not due to innate fear, we performed a fox odor experiment (Fig. 4A). It is well established that animals show fear and freezing behaviors when exposed to the threat of a predator, namely, fox odor (2,5-Dihydro-2,4,5- Trimethylthiazoline (TMT)²⁶. Our results show that animals were threatened and exhibited freezing behavior (Fig. 4B) while sensing this odor in the environment they were placed in. However, there was no significant *Arc*-dVenus induction in either the LA or the LaVL (Fig. 4C, D) confirming that innate fear does not drive the activation of cells in the LA.

2. No activation of Arc in the LaVL ensemble after retrieval

Animals were fear conditioned and underwent a retrieval session 24 h later (Fig. 5A). While the subjects exhibited a robust fear response to the auditory CS, as measured by their freezing levels (Fig. 5B), we observed very low activation of the *Arc*-dVenus expressing ensemble in the LaVL, as measured by levels of dVenus intensity (Fig. 5C, D). This result indicates that the retrieval of fear memory does not reactivate *Arc* expression in the LaVL memory trace.

3. The LaVL ensemble does not express Arc after repeated training

Albeit not being reactivated by retrieval of memory, we next examined whether retraining the animals once the original fear memory was consolidated, would trigger the activation of *Arc* expression in the LaVL ensemble. Animals were subjected to a second identical conditioning trial 24 hours after the first (Fig. 5A). Measured *Arc*-dVenus expression was very low in the LaVL after this training session (Fig. 5C, D), even though animals exhibited robust freezing behavior (Fig. 5B), suggesting that *Arc* is not activated in the LaVL engram when the second learning experience is identical to the first. We next questioned whether this pattern of activation was specific to *Arc* expression, or if these neurons in the LaVL were incapable of reactivation once they were recruited to a memory trace.

To this end, endogenous *Arc* and *c-Fos* expression was examined in the LaVL of mice that were re-conditioned a day after the first conditioning session. *Arc* expression was recorded 1 h after animals were re-exposed to the same fear conditioning paradigm on day 2.

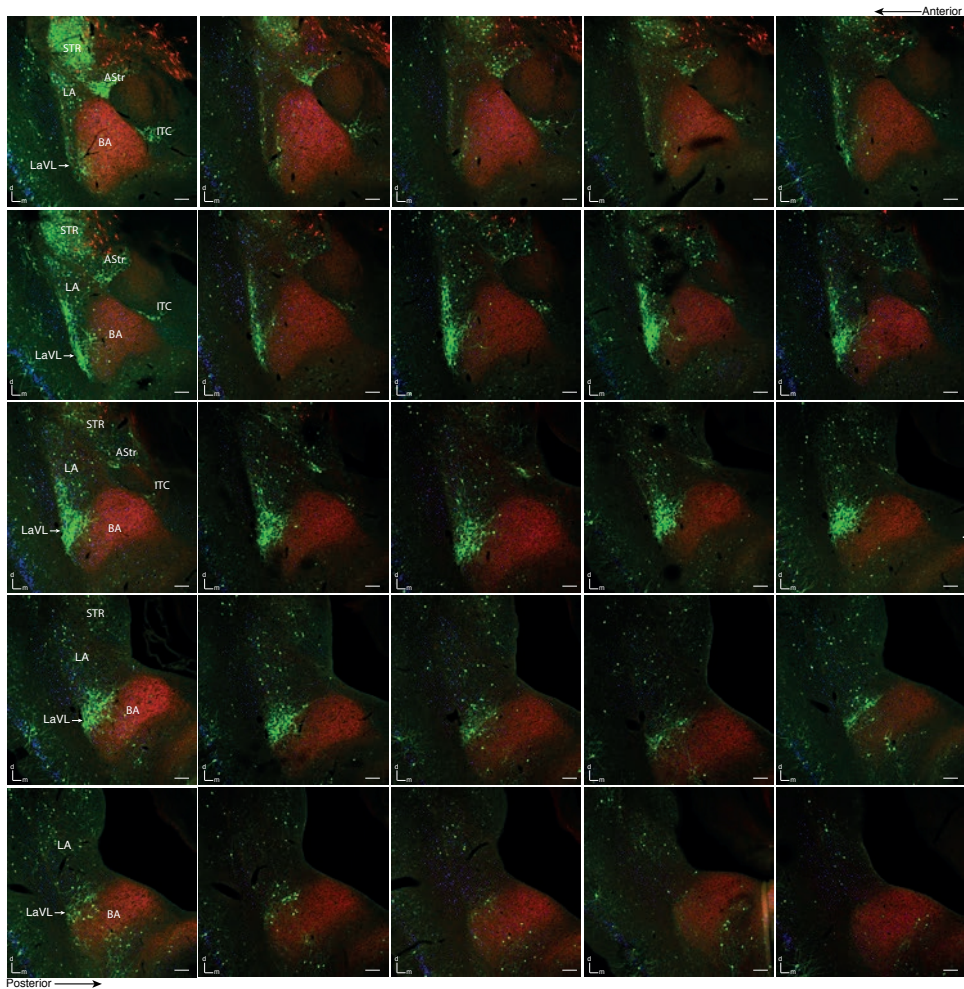


Figure 2. Serial collection of amygdala sections showing the extent of *Arc*-dVenus activity in the LaVL. Serial coronal sections of one hemisphere were collected from a mouse brain that was trained with 3 times CS and US pairings and perfused 5 h later. dVenus expression in the LaVL was observed between bregma -1.37 mm (top left corner image) and -2.46 mm (bottom right corner image). Distinct dVenus activity was also observed in the AStr, STR and ITC subregions. Red: choline acetyltransferase (ChAT) antibody, which marks the basal amygdala (BA), and was used to precisely distinguish the LA from the BA. dVenus: green. AStr: amygdalostratial transition area, STR: Striatum, ITC: intercalated cells of the amygdala, LaVL: ventrolateral lateral amygdala, LA: lateral amygdala, BA: basal amygdala. Scale bar, 100 μ m. d, dorsal; m, medial.

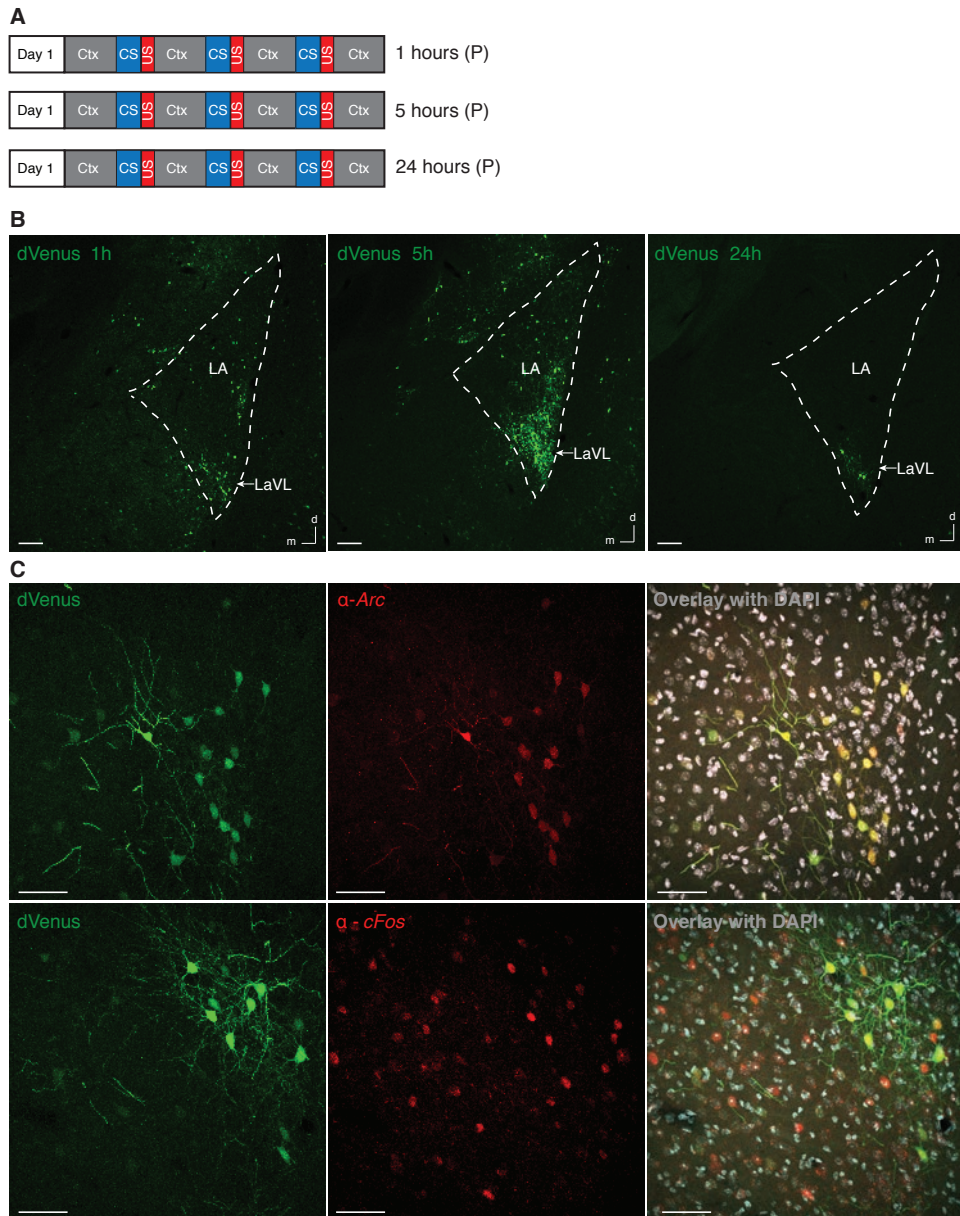


Figure 3. Characterization of *Arc*-dVenus activity after fear conditioning. (A) Behavioral setup. Mice received 3 times CS and US pairings and were perfused at 1, 5, and 24 h post-training. (B) dVenus expression is robust up to 5 hrs after conditioning, with less activity 24 h later. Scale bar, 100 μ m. d, dorsal; m, medial. (C) endogenous *Arc*⁺ cells showed high co-localization with dVenus⁺ cells at 1 h post-training. Endogenous *c-Fos* expression high co-localized with dVenus⁺ cells at 2 h post- fear conditioning training. Scale bar, 50 μ m. (P), perfusion.

The expression of endogenous *Arc* after fear conditioning on the second day reflected what we observed reporter dVenus activity. An emphatic decrease in endogenous *Arc* expression was found on the second day in the LaVL (Fig. 6). However, unlike endogenous *Arc*, the expression of *c-Fos* was higher than *Arc*-dVenus in the LaVL after retraining (Fig. 6), showing no difference when compared to *c-Fos* expression after the initial learning on day 1 (Fig. 3C). These results imply that unlike *Arc*, *c-Fos* is expressed after relearning, suggesting that neurons in the LaVL are capable of being reactivated every time a learning experience occurs.

Next, we tested whether subtle changes in US and CS contingencies during retraining could induce the expression of *Arc* in the LaVL ensemble

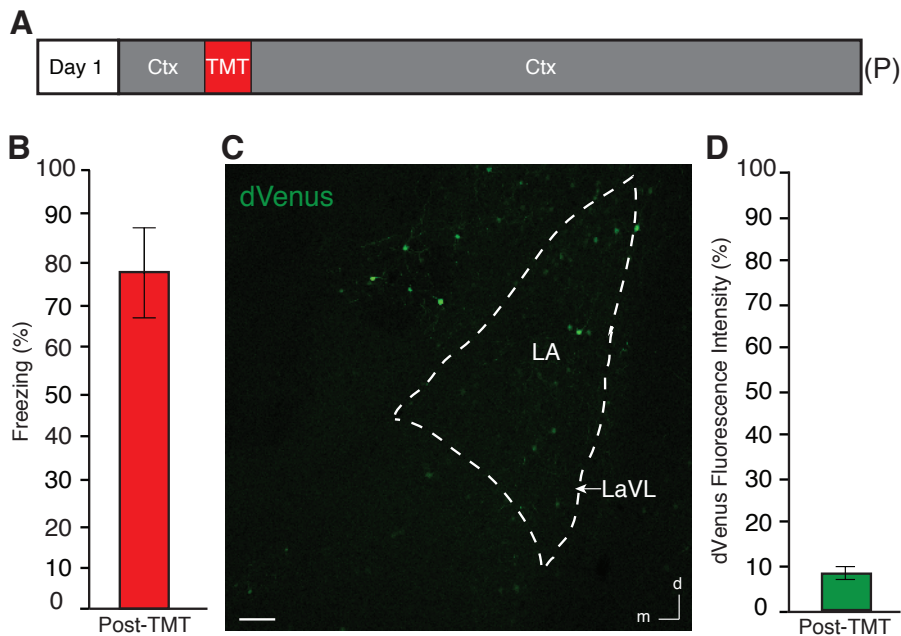


Figure 4. Innate fear does not induce *Arc*-dVenus activity in the LaVL. (A) Mice were exposed to fox odor (TMT) and perfused 5 h later. (B) Animals exhibited high freezing behaviour after being exposed to fox odor. (C) Representative image of mice that were exposed to fox odor with no strong activity in the LaVL. (D) No significant dVenus fluorescence intensity was detected in the LaVL. All data points show mean \pm s.e.m. Scale bar, 100 μ m. d, dorsal; m, medial. (P), perfusion

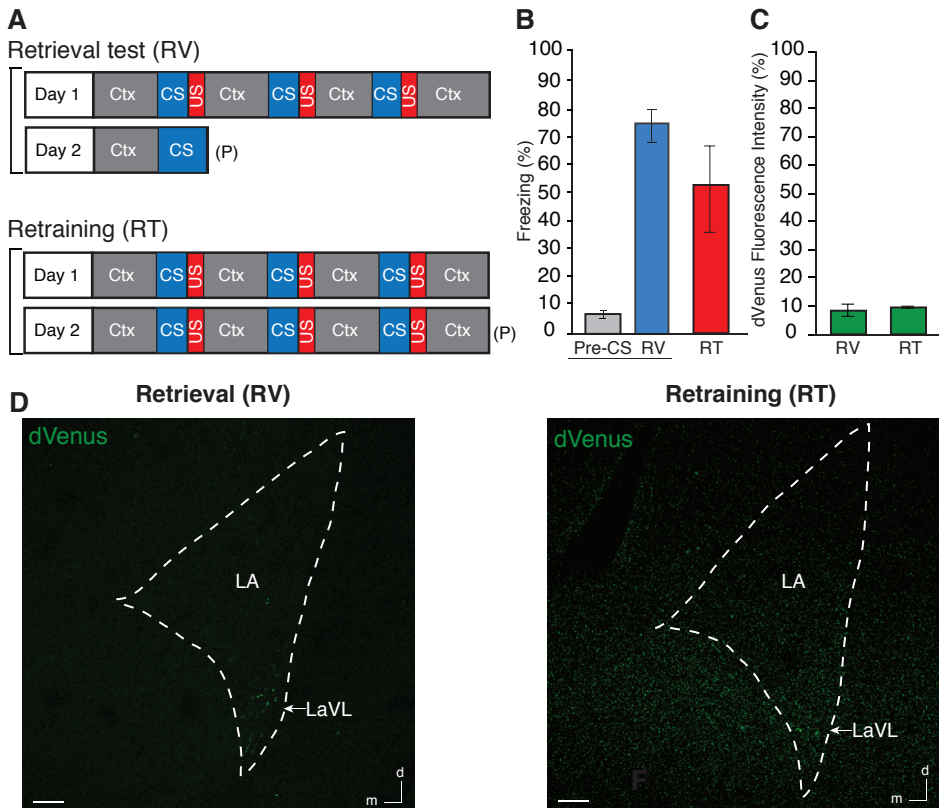


Figure 5. No significant expression of *Arc*-dVenus in the LaVL after retrieval or retraining. (A) Behavioral setup. Mice were fear conditioned on day 1, 24 h later they were cue tested and perfused 5 hrs later (upper panel). Mice were fear conditioned with 3 CS-US pairings on day 1, 24 h later the animals were retrained using the same experimental setup and were perfused 5 h later (lower panel). (B) Robust freezing behaviour during the auditory tone interval of the cue test, and after the last US presentation during retraining. (C) No significant dVenus fluorescence intensity was detected in the LaVL after retrieval and retraining. (D) Representative images indicating low dVenus expression in the LA and LaVL after retrieval and retraining. All data points show mean \pm s.e.m. Scale bar, 100 μ m. d, dorsal; m, medial. (P), perfusion.

3.1 No significant activation of *Arc*-dVenus in the LaVL ensemble with US variability during retraining

Animals were retrained 24 hours after initial conditioning using a stronger protocol on day 2 (Fig. 7A). Mice received either a single CS-US pairing or a less intense US on the first day, while receiving three shocks or more intense shocks on the second day. Even though animals exhibited freezing behavior (Fig. 7B), these variations to the US on day 2 induced low *Arc*-dVenus expression in the LaVL (Fig. 7C, D). This indicates that increasing the intensity or number of the US does not result in

a mismatch between expectation and actual experience or the formation of a new memory that generates *Arc* expression in LaVL.

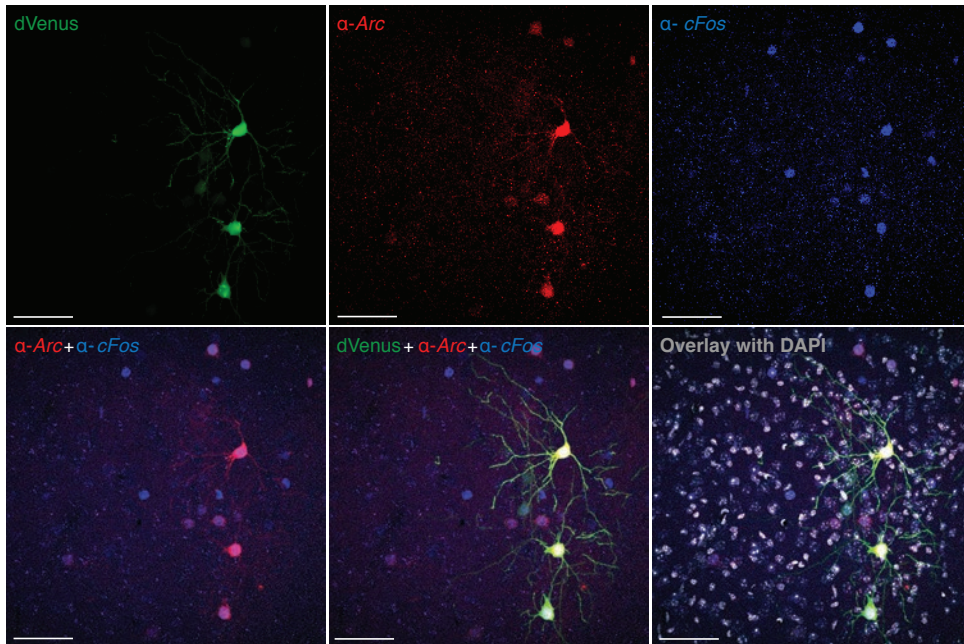


Figure 6. *Arc*-dVenus activity and endogenous *Arc* expression show decay after retraining. Mice were fear conditioned, retrained 24 h later and perfused 1 h post retraining on day 2. Endogenous *Arc*⁺ and dVenus⁺ cells show decreasing in their expression after retraining, while endogenous *c-Fos*⁺ cells show higher expression than the endogenous *Arc* and *Arc*-dVenus⁺ cells. Scale bar, 50 μ m. d, dorsal; m, medial. Red: endogenous *Arc*, blue: endogenous *c-Fos*, green: dVenus, grey: DAPI.

3.2 No significant activation of *Arc*-dVenus in the LaVL ensemble with CS variability during retraining

The components of the auditory and contextual CS stimuli were changed on the second day of training, wherein the tone was replaced with white noise, and the original context was replaced with a new one (Fig. 7A). Though the mice exhibited no fear response when first placed in the new context on day 2, they did show a robust fear response to the first presentation of the white noise (Fig. 7B). Furthermore, no significant *Arc*-dVenus expression was observed in the LaVL (Fig. 7C, D). Taken together, these results indicate that the subjects did not distinguish between the auditory stimulus on day 1 and the white noise on day 2. Thus, the animals did not

discriminate between the experiences on day 1 and 2 and neurons in the LaVL did not have a significant *Arc* expression.

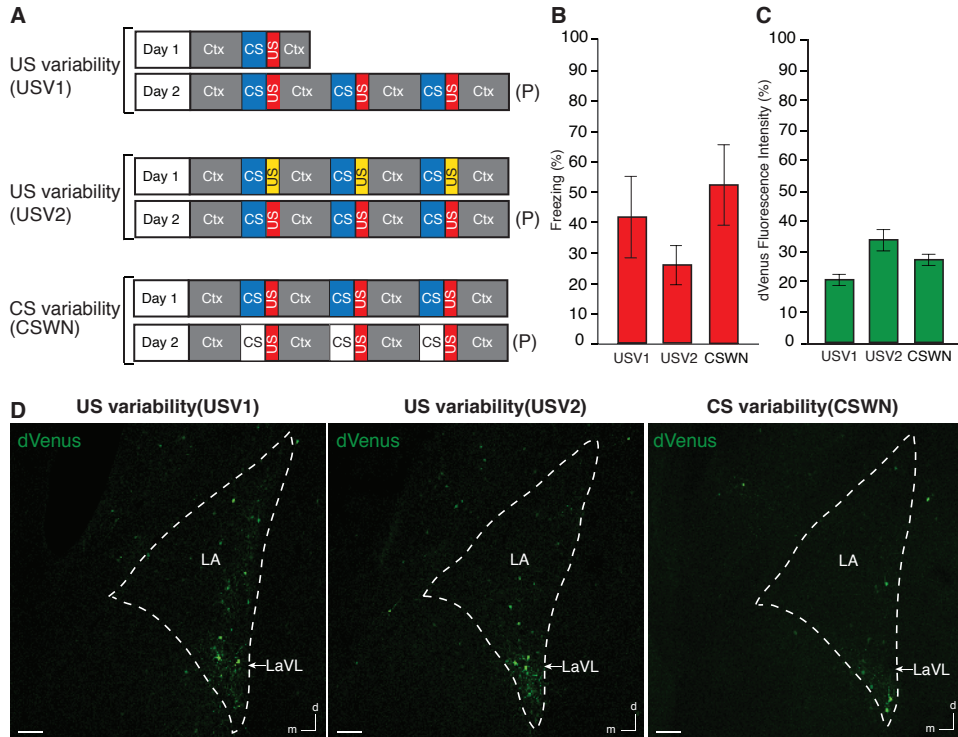


Figure 7. No activation of *Arc*-dVenus in the LaVL ensemble with US or CS variability during retraining. (A) Behavioral setup. Two US variability experiments were performed. In the first one (US variability experiment (USV1)), mice were fear conditioned with one CS-US pairing on day 1, and 24 h later were fear conditioned with three pairings of CS and US and perfused 5 h later. In the second US variability experiment (USV2), animals were fear conditioned with weaker US stimulations on day 1 (0.25mA), and received more intense US stimulations on day 2 (0.75mA). Animals were perfused 5 h later. In the CS variability group (CSWN), mice received 3 CS (tone) and US pairings on day 1 and 3 white noise (WN) CS paired with a US in a new context on day 2. Animals were perfused 5 hrs later. (B) All three USV1, USV2 and CSWN groups exhibited robust freezing after the last US on day 2. (C) No significant dVenus fluorescence intensity was detected in the LaVL after the second day of training. (D) Representative images indicating very low dVenus expression was observed in the LA and LaVL after the second day of training. All data points show mean \pm s.e.m. Scale bar, 100 μ m. d, dorsal; m, medial. (P), perfusion

4. Effect of longer interval between the two FC trainings

We next asked whether the inability of LaVL neurons to express *Arc* after retraining is because these cells have a longer refractory period to evoke *Arc* expression. In order to test this, we increased the inter-training-interval to 14, 30, and 60 days (Fig. 8A, B). Overall, very low induction of *Arc*-dVenus was observed in the

LaVL compared to the first day of training (Fig. 8C, D). However, we observed a small increase in *Arc*-dVenus⁺ intensity with time (Fig. 8C), albeit not reaching the same level as initial activation, when the interval between the first and second fear conditioning training became longer. These results, together with the previous results (*c-Fos* expression), demonstrate that the LaVL ensemble, once activated, may indeed be refractory to the expression of *Arc*, a phenomenon that may display partial recovery with the passage of time.

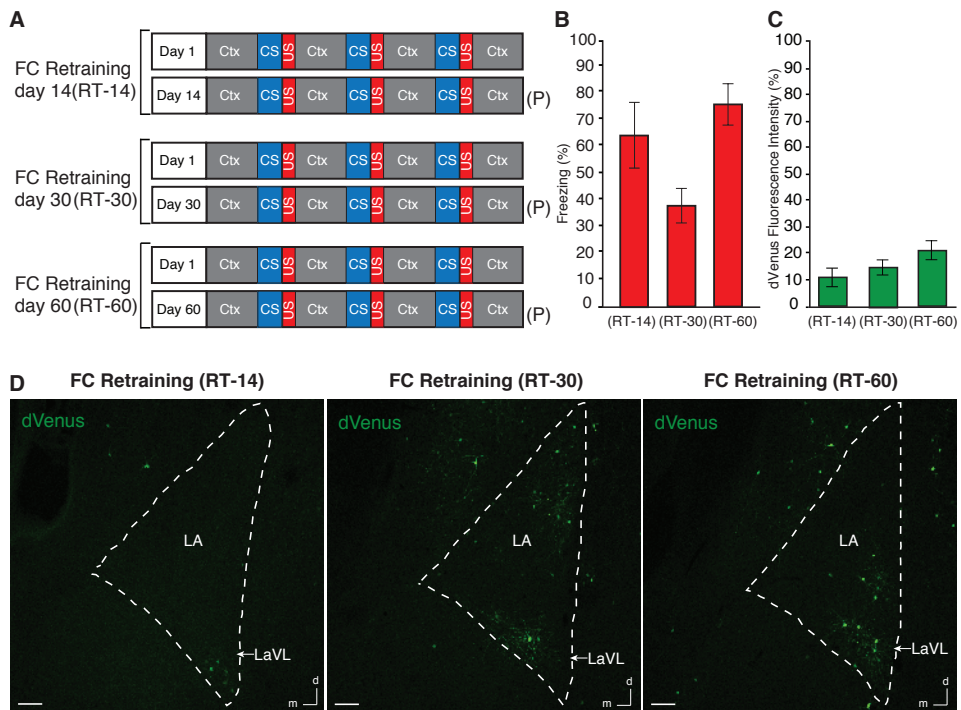


Figure 8. Effect of longer time intervals between the two FC trainings. (A) Behavior setup. Mice were fear conditioned and retrained after 14, 30 and 60 days and perfused 5 h after the second training. (B) High freezing behaviour after the last US during the the second fear conditioning training. (C) No overall high dVenus activity in the LaVL was detected in all three groups, however, with increasing interval between the first and second FC trainings, an ascending pattern of dVenus activity was observed in the LaVL. (D) Representative images indicating an overall reduction of dVenus expression in the LaVL in all the three paradigms. All data points show mean \pm s.e.m. Scale bar, 100 μ m. d, dorsal; m, medial. (P), perfusion.

5. *Arc*-dVenus expression in the LaVL is due to novel learning

Since the LaVL ensemble is not activated after repeated training sessions, we hypothesized that the expression of *Arc* is exclusive to the formation of novel fear memories.

In order to test this hypothesis, animals were exposed to a new experience on the second day, and we investigated whether this change in experience resulted in the formation of a novel memory that drives *Arc*-dVenus expression.

On day 1, animals underwent an immediate shock conditioning paradigm, wherein they received the US immediately upon placement in the conditioning chamber (Fig. 9A).

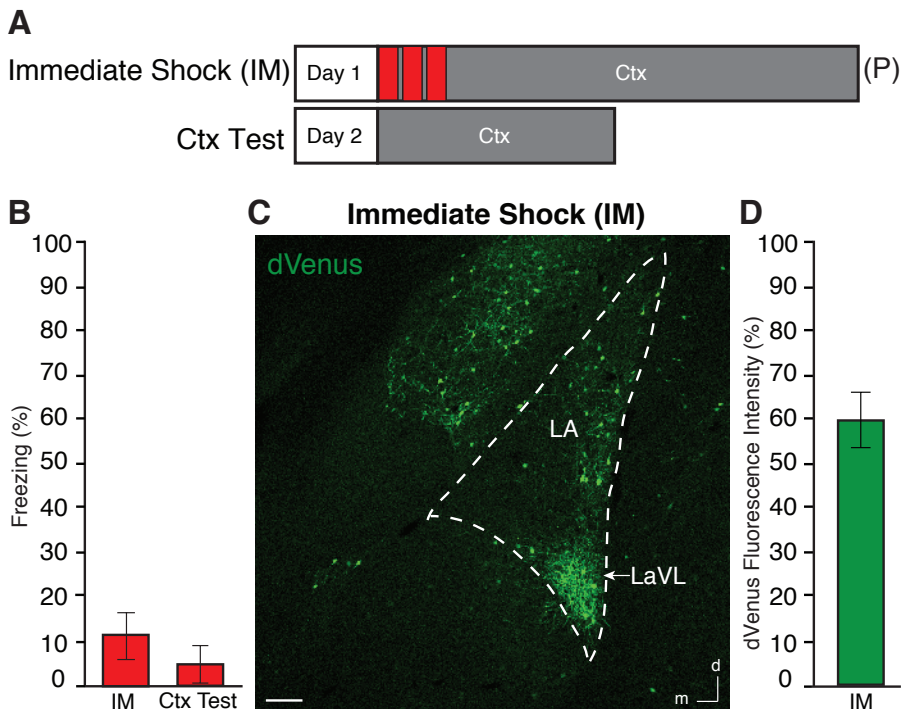


Figure 9. Expression of *Arc*-dVenus in the LaVL after the immediate shock paradigm. (A) Behavior setup. Mice received 3 consecutive foot-shocks immediately upon placement in the conditioning chamber, and were either perfused 5 h later or underwent a retrieval session 24 h later. (B) No freezing behaviour to the context was observed after US presentations during training or during a context retrieval test 24 h later. (C) Representative image indicating robust activation in the LA and LaVL after the immediate shock paradigm. (D) A significant high dVenus activity was detected in the LaVL. All data points show mean \pm s.e.m. IM, immediate shock; Ctx, context; (P), perfusion.

In this protocol animals do not form an overt memory to the conditioning context²⁷, even though they receive the aversive US. However, it is possible that an aversive memory is formed to other environmental stimuli present at the time of conditioning²⁸. We hypothesized that if this is the case 1) IS training will result in the activation of the LaVL ensemble, 2) Fear conditioning the mice a day after IS training will

result in the formation of a novel memory that activates *Arc*-dVenus⁺ neurons in the LaVL and 3) If the IS animals are pre-exposed to the context, it will result in an associative CS-US fear memory, and any subsequent fear conditioning will not induce *Arc* expression.

In line with this, we observed that IS training resulted in a significant activation of neurons in the LaVL (Fig. 9C, D), even though the US was not associated to the auditory and contextual CS (Fig. 9B). Furthermore, fear conditioning the animals to the context a day after IS training (Fig. 10A) resulted in activation of cells in the LaVL (Fig. 10C, G), indicating that a new US associated fear memory is formed which differs significantly from the memory formed on day 1 after IS training (Fig. 10B). Finally, pre-exposure to the context on day 1, followed by IS training on day 2 (Fig. 10D) attenuates the observed activation of cells after FC on day 3 (Fig. 10F, G). This strongly suggests that pre-exposure to the context prior to IS training results in a CS-US fear memory (Fig. 10E), which does not differ to the one formed after FC. Overall, we observed the highest *Arc*-dVenus activity in the LaVL in the group that experienced fear conditioning training for the first time, while the novelty of the second fear training experience relative to the initial one determined the strength of the LaVL activity after the subsequent fear learning experience (Fig. 10H). Together, these experiments conclusively show that *Arc* is expressed in the LaVL only when there is a prominent difference between expectation and actual experience.

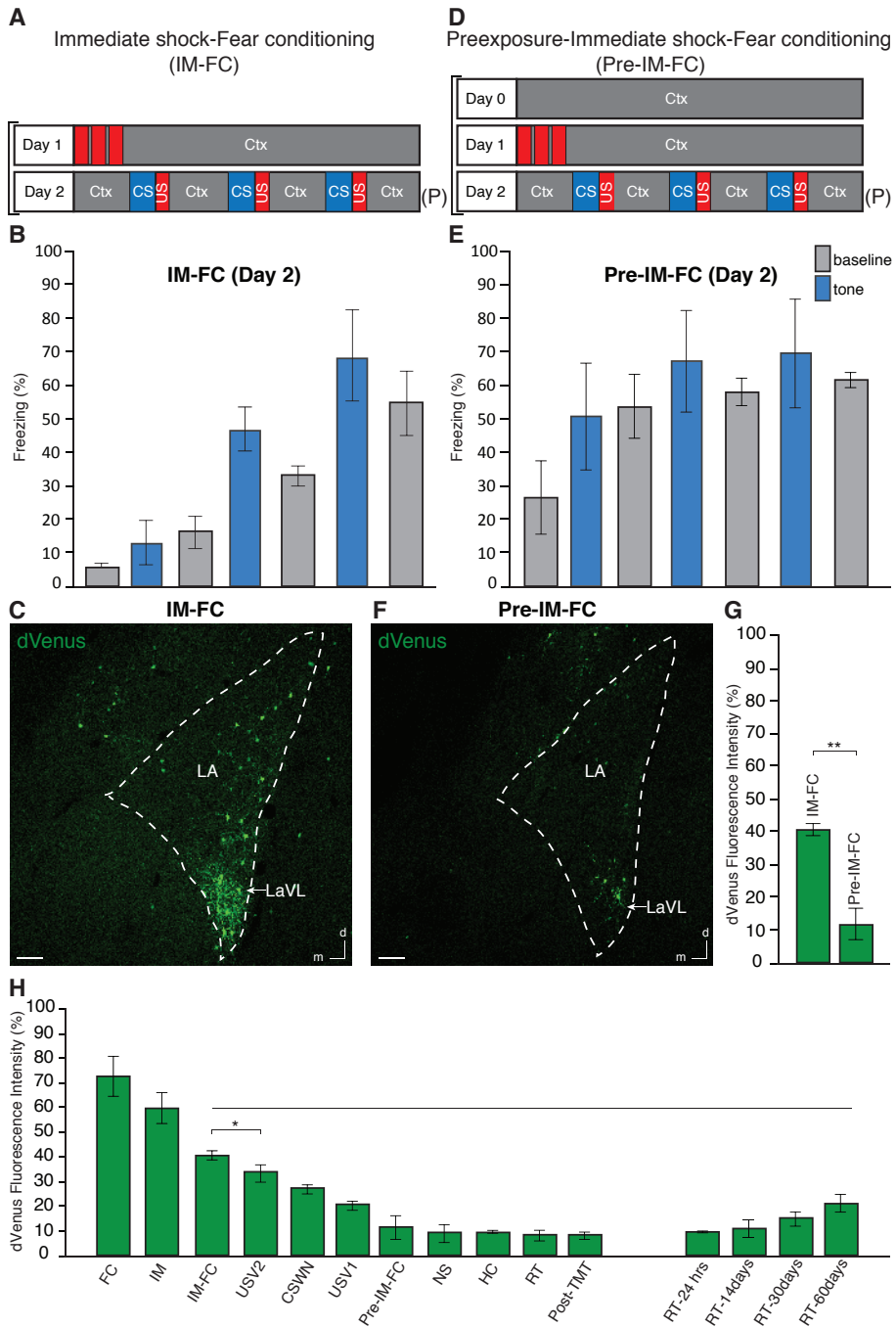


Figure 10. *Arc*-dVenus expression in the LaVL is due to novel learning. (A) Behavior setup. Mice received the immediate shock protocol on day 1, and were fear conditioned with 3 CS-US pairings on day 2. (B) Low freezing was observed on day 2 immediately upon placement in the fear conditioning chamber. (Continue in the next page)

(Fig 10-Continued) This fear response increased during training as a CS-US fear memory began to form. **(C)** Representative image indicating dVenus⁺ cells that were expressed in the La and LaVL after fear conditioning on day 2. **(D)** Behavior setup. Mice were pre-exposed to the context for 30 min on day 1, prior to immediate shock training on day 2 and fear conditioning on day 3. **(E)** Pre exposure rescues the immediate shock deficit, with mice exhibiting freezing behaviour to the context and tone upon placement in the conditioning chamber on day 3, prior to receiving the first US during fear conditioning. This fear response increased during training. **(F)** Representative image indicating no significant dVenus induction was observed in the LA and LaVL after fear conditioning on day 3. **(G)** dVenus fluorescence intensity in the LaVL was significantly higher in the IM-FC group compared to the preexposure-IM-FC group, ($n=3$ mice/group). Two-tailed t-test, $P<0.01$. $**P<0.01$. **(H)** Overall comparison of dVenus fluorescence intensity across all the experimental conditions indicating a significant reduction in the dVenus activity in the LaVL from IM-FC to the right side of the graph, ($n=3$ mice/group). One-way analysis of variance, $F=26.867$, $P<0.05$. $*P<0.05$. All data points show mean \pm s.e.m. Scale bar, 100 μ m. d, dorsal; m, medial; (P), perfusion.

DISCUSSION

Elucidating the distribution of neuronal activity patterns in subregions of the LA after fear conditioning is critical to understanding whether neurons in these different regions are recruited to the fear memory engram differently. In our study we report that an *Arc* based fluorescent reporter identifies a discrete ensemble of LaVL neurons activated after aversive fear learning, but not innate fear. Furthermore, this ensemble of neurons encoding memory is not activated by retrieval or retraining. Finally, our findings indicate that the LaVL ensemble expresses *Arc* exclusively when the learning experience is novel and unexpected to the animals.

The data presented here builds on previous studies reporting the activation of a discrete subpopulation of neurons in the LaVL after fear conditioning^{29,30}. These studies, using a variety of markers for neuronal activity and learning, identified principle-neuron-like cell activation in the LaVL that did not alter after memory recall^{18,30,31}. However, to our knowledge, our study provides the first comprehensive description of the conditions under which neurons in the LaVL are activated, as measured by *Arc* expression, after fear conditioning.

We show that the LaVL ensemble, which is strongly activated after fear conditioning, cannot express *Arc* after retrieval or retraining. It could be argued that these neurons possess a longer refractory period to evoked *Arc* expression, which prevents the expression of this protein after retrieval or retraining. Indeed, in line with this, we show that repeated exposure to the same experience 24 h apart, results in the expression of *c-Fos* but not *Arc* in the LaVL ensemble, indicating that these cells

do get activated, and are unable to express *Arc*. This is further evidenced by the observation that these neurons begin to express *Arc* if the interval between the two conditioning sessions is increased.

Our study reveals that neurons in the LaVL uniquely express *Arc* after a new learning experience, when there is a prominent difference between the expectancy and the actual experience. This finding is supported by previous studies which demonstrate that unexpected US presentations induces significantly higher IEG activity in LA neurons than an expected US stimulation³². Furthermore, US-evoked depolarization of neurons in the LA have been shown to decrease during the CS-US pairings³³. Our results are in line with the prediction error interpretation extracted from the Rescorla–Wagner model³⁴. At the start of conditioning, the US is novel and unexpected, resulting in a prediction error and high-evoked activity in the LaVL. During the conditioning as the CS comes to predict the shock, the US becomes expected resulting in low prediction error and lower activity in the LaVL.

It has been widely reported that when the aversive stimulation is given immediately upon placement in the conditioning chamber, fear conditioning to the conditioned stimuli is completely absent³⁵. This is normally measured as a lack of fear responding/freezing of the animals during retrieval to the defined CS. Although we could replicate this finding at the behavioral level, we observed robust activation of the LaVL ensemble at the cellular level. This activation cannot be attributed to the presentation of foot-shocks alone, since no expression of *Arc* is observed in response to foot-shocks during repeated fear conditioning training. Thus, the most parsimonious explanation consistent with these findings would be that the animals do form an associative memory, albeit not to the auditory or contextual CS.

We postulate that LaVL neurons are not exclusively activated by the association of the US to the auditory and contextual CS presented in the conditioning chamber, but also respond to the association of the shock to other environmental cues present around the time of training, such as transport, handling or placement cues²⁸. This results in the formation of an aversive memory that is distinct from the conditioned CS-US fear memory, and is encoded, in part, by neurons in the ventrolateral nucleus of the lateral amygdala. In line with this, we show that repeated fear conditioning

with the same protocol does not activate the LaVL ensemble while these neurons do express *Arc* if animals are fear conditioned a day after IS training. Taken together, this convincingly demonstrates that the memory induced by the immediate shock experiment is different from the one formed after fear conditioning. Finally, as described previously³⁶, pre-exposing the animals to the context before IS training, results in an association of the immediate shocks to the auditory and contextual CS. This attenuates the observed activation of LaVL neurons when animals are fear conditioned a day after receiving IS. These experiments elegantly demonstrate that novel learning resulting from a prominent difference between expectancy and actual experience activates *Arc* in a subset of LaVL cells.

It remains unknown whether *Arc* activation after a new experience, occurs in the same neurons that were recruited during the initial experience, or whether a new subset of neurons is recruited after the animals are exposed to a new experience/learning paradigm, resulting in formation of a new memory. Our results indicate the latter, since we observe *Arc* expression only when the experience is novel (IS followed by fear conditioning), and not when the animals are fear conditioned after the IS deficit is rescued by pre-exposure to the CS. We hypothesize that DNA methylation might be the potential intracellular mechanism silencing *Arc* transcription, after its robust induction to the initial fear learning training. New learning would then recruit a new subset of neighboring cells, and the original cells would still remain methylated and refractory to *Arc* expression. More studies are yet to be done to confirm and elaborate the exact processes involved in intra- and intercellular regulatory mechanisms of old and new fear memories.

Taken together, we show that novel fear learning results in distinct *Arc* activity within the LaVL. This activation is optimal only when the prediction error is high with a prominent difference between expectation and actual experience.

References

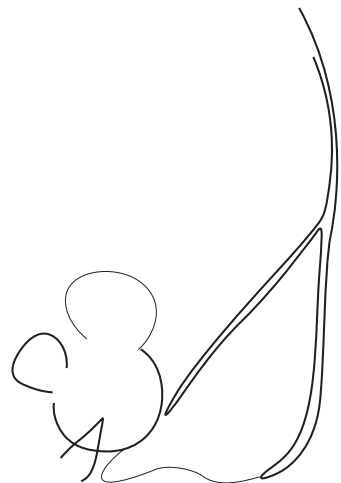
1. Johansen, J. P. *et al.* Molecular Mechanisms of Fear Learning and Memory. *Cell* **147**, 509–524 (2011).
2. LeDoux, J. E. Emotion circuits in the brain. *Annual review of neuroscience* **23**, 155–84 (2000).
3. Fendt, M. & Fanselow, M. S. The neuroanatomical and neurochemical basis of conditioned fear. *Neuroscience and biobehavioral reviews* **23**, 743–60 (1999).
4. Davis, M. Neurobiology of fear responses: the role of the amygdala. *The Journal of neuropsychiatry and clinical neurosciences* **9**, 382–402 (1997).
5. Maren, S. Neurotoxic basolateral amygdala lesions impair learning and memory but not the performance of conditional fear in rats. *The Journal of neuroscience : the official journal of the Society for Neuroscience* **19**, 8696–703 (1999).
6. Davis, M. The role of the amygdala in fear and anxiety. *Annual review of neuroscience* **15**, 353–75 (1992).
7. Maren, S. Neurobiology of Pavlovian fear conditioning. *Annual review of neuroscience* **24**, 897–931 (2001).
8. Duvarci, S. & Pare, D. Amygdala microcircuits controlling learned fear. *Neuron* **82**, 966–80 (2014).
9. Rumpel, S., LeDoux, J., Zador, A. & Malinow, R. Postsynaptic receptor trafficking underlying a form of associative learning. *Science (New York, N.Y.)* **308**, 83–8 (2005).
10. Kim, J., Kwon, J.-T., Kim, H.-S., Josselyn, S. a & Han, J.-H. Memory recall and modifications by activating neurons with elevated CREB. *Nat Neurosci* (2013). doi:10.1038/nn.3592
11. Repa, J. C. *et al.* Two different lateral amygdala cell populations contribute to the initiation and storage of memory. *Nature neuroscience* **4**, 724–31 (2001).
12. Reijmers, L. G., Perkins, B. L., Matsuo, N. & Mayford, M. Localization of a stable neural correlate of associative memory. *Science (New York, N.Y.)* **317**, 1230–3 (2007).
13. Guzowski, J. F., McNaughton, B. L., Barnes, C. A. & Worley, P. F. Environment-specific expression of the immediate-early gene Arc in hippocampal neuronal ensembles. *Nature neuroscience* **2**, 1120–4 (1999).
14. Guzowski, J. F. *et al.* Recent behavioral history modifies coupling between cell activity and Arc gene transcription in hippocampal CA1 neurons. *Proceedings of the National Academy of Sciences of the United States of America* **103**, 1077–82 (2006).
15. Tayler, K. K., Tanaka, K. Z., Reijmers, L. G. & Wiltgen, B. J. Reactivation of neural ensembles during the retrieval of recent and remote memory. *Current biology : CB* **23**, 99–106 (2013).

16. Trouche, S., Sasaki, J. M., Tu, T. & Reijmers, L. G. Fear Extinction Causes Target-Specific Remodeling of Perisomatic Inhibitory Synapses. *Neuron* **80**, 1–12 (2013).
17. Han, J.-H. *et al.* Neuronal competition and selection during memory formation. *Science (New York, N.Y.)* **316**, 457–60 (2007).
18. Schafe, G. E. & LeDoux, J. E. Memory consolidation of auditory pavlovian fear conditioning requires protein synthesis and protein kinase A in the amygdala. *The Journal of neuroscience : the official journal of the Society for Neuroscience* **20**, RC96 (2000).
19. Fanselow, M. S. & Poulos, A. M. The neuroscience of mammalian associative learning. *Annual review of psychology* **56**, 207–34 (2005).
20. Maren, S. Synaptic mechanisms of associative memory in the amygdala. *Neuron* **47**, 783–6 (2005).
21. Davis, M. & Whalen, P. J. The amygdala: vigilance and emotion. *Molecular psychiatry* **6**, 13–34 (2001).
22. Kim, J. J. & Jung, M. W. Neural circuits and mechanisms involved in Pavlovian fear conditioning: a critical review. *Neuroscience and biobehavioral reviews* **30**, 188–202 (2006).
23. Eguchi, M. & Yamaguchi, S. In vivo and in vitro visualization of gene expression dynamics over extensive areas of the brain. *NeuroImage* **44**, 1274–83 (2009).
24. Gouty-Colomer, L. A. *et al.* Arc expression identifies the lateral amygdala fear memory trace. *Molecular psychiatry* **21**, 364–75 (2016).
25. Soulé, J. *et al.* Balancing Arc synthesis, mRNA decay, and proteasomal degradation: maximal protein expression triggered by rapid eye movement sleep-like bursts of muscarinic cholinergic receptor stimulation. *The Journal of biological chemistry* **287**, 22354–66 (2012).
26. Janitzky, K., Prellwitz, O., Schwegler, H., Yanagawa, Y. & Roskoden, T. 2,5-Dihydro-2,4,5-Trimethylthiazoline (TMT)-Induced Neuronal Activation Pattern and Behavioral Fear Response in GAD67 Mice. *Journal of Behavioral and Brain Science* **05**, 318–331 (2015).
27. Landeira-Fernandez, J., DeCola, J. P., Kim, J. J. & Fanselow, M. S. Immediate shock deficit in fear conditioning: effects of shock manipulations. *Behavioral neuroscience* **120**, 873–9 (2006).
28. Bevins, R. A., Rauhut, A. S., McPhee, J. E. & Ayres, J. J. B. One-trial context fear conditioning with immediate shock: The roles of transport and contextual cues. *Animal Learning & Behavior* **28**, 162–171 (2000).
29. Wilson, Y. M. & Murphy, M. A discrete population of neurons in the lateral amygdala is specifically activated by contextual fear conditioning. *Learning & Memory* **16**, 357–361 (2009).

30. Trogrlic, L., Wilson, Y. M., Newman, A. G. & Murphy, M. Context fear learning specifically activates distinct populations of neurons in amygdala and hypothalamus. *Learning & Memory* **18**, 678–687 (2011).
31. Besnard, A., Laroche, S. & Caboche, J. Comparative dynamics of MAPK/ERK signalling components and immediate early genes in the hippocampus and amygdala following contextual fear conditioning and retrieval. *Brain structure & function* **219**, 415–30 (2014).
32. Furlong, T. M., Cole, S., Hamlin, A. S. & McNally, G. P. The role of prefrontal cortex in predictive fear learning. *Behavioral neuroscience* **124**, 574–86 (2010).
33. Johansen, J. P., Tarpley, J. W., LeDoux, J. E. & Blair, H. T. Neural substrates for expectation-modulated fear learning in the amygdala and periaqueductal gray. *Nature neuroscience* **13**, 979–86 (2010).
34. Rescorla, R. A. & Wagner, A. R. “A theory of Pavlovian conditioning: Variations in the effectiveness of reinforcement,.” **Vol. 2**, (1972).
35. Fanselow, M. S. Conditioned fear-induced opiate analgesia: a competing motivational state theory of stress analgesia. *Annals of the New York Academy of Sciences* **467**, 40–54 (1986).
36. Fanselow, M. S. Factors governing one-trial contextual conditioning. *Animal Learning & Behavior* **18**, 264–270 (1990).

Chapter 4
***Modulation of cerebellar-dependent
associative learning by the amygdala***

Boele HJ, Hosseini B, Medina JF, Kushner SA, De Zeeuw CI



Modulation of cerebellar-dependent associative learning by the amygdala

Boele HJ¹, Hosseini B², Medina JF³, Kushner SA², De Zeeuw CI^{1,4}

¹Erasmus MC Rotterdam, Department of Neuroscience

²Erasmus MC Rotterdam, Department of Psychiatry

³Baylor College of Medicine, Department of Neuroscience

⁴Netherlands Institute for Neuroscience, Royal Academy of Arts and Sciences, Amsterdam

ABSTRACT

Recent studies suggest that eye-blink conditioning is not solely dependent on the cerebellum, introducing the amygdala as another brain region involved in the acquisition of conditioned eyelid responses. In the current study, we investigated the role of somatostatin⁺ (SOM⁺) neurons in the lateral subdivision of central nucleus of the amygdala (CeL) during eye-blink conditioning. Our results indicate that activation of these SOM⁺ neurons in the CeL results in faster acquisition and distinct enhancements of conditioned eyelid response amplitudes. Herewith, we provide the first evidence that the amygdala plays an important role in the modulation of cerebellar-dependent associative learning.

INTRODUCTION

The amygdala is crucially involved in the formation and retrieval of fear-memories¹⁻⁴. However, recent evidence also indicates that the amygdala might modulate the formation of memories in other brain areas, like the cerebellum⁵. One of the best models to study cerebellar learning is eye-blink conditioning. During eye-blink conditioning an association is learned between an unconditioned stimulus (US) that elicits a reflexive eye-blink, usually an air puff, and a conditional stimulus (CS) that predicts the onset of the US, usually a tone. Repeated pairing of CS and US at fixed time-intervals of several hundreds of milliseconds will gradually lead to acquisition

of eyelid conditioned responses (CRs), that is, the animal will learn to close its eye in response to the CS. It is well established that for eye-blink conditioning the memory trace is formed in the cerebellum. The US is transmitted by climbing-fibers originating in the inferior-olive (IO) and the CS by mossy-fibers originating in the pontine nuclei (PN) to Purkinje-cells in specific microzones in the cerebellar cortex^{3,6-11}. During CS-US pairings these Purkinje-cells will learn to associate the CS with the instructive US and acquire a timed suppression in their simple-spike firing¹²⁻¹⁵. As such, they provide a timed disinhibition of the cerebellar nuclei (CN), which then ‘command’ eyelid-muscles to contract. Although the cerebellum is both necessary and sufficient for learning the association between the eye puff US and tone CS, evidence is accumulating that the amygdala could play a modulatory role in this task, probably by regulating the saliency of the CS-related signals sent to the cerebellum^{5,10,16}. Support for this hypothesis comes from inactivation experiments that mimic the behavioral impairments observed when the saliency of the CS is reduced: (1) If the amygdala is inactivated during conditioning, the rate of learning slows down^{10,17-20}, and (2) if the amygdala is inactivated after conditioning, performance deteriorates⁵. Here, we ask the reciprocal question: Can amygdala stimulation be used to boost the saliency of the CS and enhance learning and performance? To selectively stimulate amygdalar output, we used an optogenetic approach to control somatostatin-containing neurons (SOM⁺) in the lateral subdivision of the central amygdala (CeL). These SOM⁺ neurons in the CeL generate fear responses, including freezing behavior²¹. Based on the assumption that activation of the amygdala can enhance CS saliency^{5,10}, we hypothesize that stimulating these SOM⁺ neurons during eye-blink conditioning the time of the CS will induce faster learning than in control mice.

METHODS

Surgery for experiments with optogenetic stimulation

For all experiments we used 15-24 week old mice (male and female, *Som-IRES-cre*²¹⁻²³, n=10, individually housed, food ad libitum, 12:12 light/dark cycles). Mice were anesthetized with initially 5% isoflurane (PCH) and with 2% during stereotactical surgery. Body temperature was kept constant at 37° Celsius. Mice were placed into

a stereotactical frame (Stoelting, Chicago laboratory supply) and head was fixed in a standard mouse stereotaxic head-holding device, using stub ear bars to prevent eardrum perforation. Next, mice were subcutaneously injected with bupivacaine hydrochloride (2.5mg/ml), Rimadyl (50mg/ml), and Temgesic (0.3mg/ml). A sagittal scalp incision of 2-3 cm length was performed. Next, we carefully removed the exposed periosteum and roughened the surface of the skull using an etchant gel (Kerr, Bioggio, Switzerland). A craniotomy was made to reach the CeL bilaterally (bregma -1.2mm, lateral 2.72mm, ventral (depth) 4.1mm). After this, a small messing block (1.0 x 0.4 x 0.3 mm) with 1 screw-thread and 2 additional pinholes was placed on the skull using Optibond primer and adhesive (Kerr, Bioggio, Switzerland) and Charisma (Heraeus Kulzer, Armonk, NY, USA). The surgical placement of this so-called pedestal allowed for head-fixation during the experiments. Injection was done using AAV5/Flex-hChR2-GFP or AAV5/EF1a-DIO-eYFP viruses (0.5 μ l per hemisphere, infusion speed 0.05 μ l/ minute) (Fig. 1A-D). The virus was injected using a glass micropipette controlled by a syringe. The micropipette was slowly lowered to the target site and remained for 5 min before the start of the injection. After finishing the injection, the micropipette was kept for 5 min and withdrawn slowly out of the skull. Optical fibers (diameter 1.25 μ m) were implanted bilaterally (ventral 3.6mm) (total length 5mm, THORLABS, USA) (Fig. 1A-D). The optical fiber implant was secured to the skull using adhesive cement, a mixture of simplex rapid powder and liquid (Kendent). After the surgery, mice were allowed to recover for 3 weeks in the stable before all subsequent experiments. All fiber placements and viral injection sites were confirmed histologically.

Behavioral conditioning setup and stimuli

All behavioral experiments were conducted using head-fixed mice that were placed on top of a cylindrical treadmill on which they were allowed to walk freely. The treadmill consisted of a foam roller (diameter 15cm, width 12cm; Exervo, TeraNova EVA) with a horizontal metal rod through the axis that was connected with a ball bearing construction to two solid vertical metal poles. A horizontal messing bar was fixated to the same vertical poles at 3-5 cm above the treadmill. Mice were head-fixed to this bar using 1 screw and 2 pins, thereby ensuring perfect head-fixation (for further details, see²⁴). This entire setup was placed in a sound- and light-isolating chamber.

National Instruments (NI-PXI) processors were used to control experimental parameters and to acquire the eyelid position signal.

Eyelid movements were recorded with the magnetic distance measurement technique (MDMT), which makes use of an NVE GMR magnetometer, positioned above the upper left eyelid, that measures movements of a minuscule magnet (1.5x0.7x0.5mm) that is placed on the lower eyelid of the animal with superglue (cyanoacrylate). This way, MDMT allows high spatio-temporal detection of eye-blink kinematics (For details, see²⁵).

The CS during acquisition training was a 10 kHz tone coming from a speaker on the back plane of the conditioning chamber. Depending from the type of experiment (see: *behavioral training protocol*) the tone intensity was set at 70, 80, or 90 dB and the tone duration was set at 50 or 280 ms. The US consisted of a weak air-puff applied to the eye (30-40 psi, 30 ms duration), which was controlled by an API MPPI-3 pressure injector, and delivered via a 27.5 gauge needle that was perpendicularly positioned at about 0.5 cm from the center of the left cornea. The optogenetic stimulation was a bilateral 470 nm LED light controlled by a Thorlabs four channel LED driver (DC4100) delivered via a hub (DC4100-HUB) to fiber coupled LEDs (M470F3), which were connected to the optic cannula's with core patch cables. Depending from the type of experiment (see: *behavioral training protocol*) the optogenetic stimulation intensity was set at 0, 5, 20, or 35 mW/mm² and the optogenetic stimulation duration was set at 50, 150, 250, or 300 ms (Fig 1E).

To absolutely make sure that the animal would not detect the 470 nm light used for optogenetic stimulation either through light leakage from the connector between optic cannula and optic fiber or by light leakage through the brain resulting in retinal activation²², we used an 470 nm continuous ambient light in the behavioral setup during training and used two continuous extra LEDs (Thorlabs, M470F3), which were directed at the eyes of the mouse. In addition, we put a black sleeve around the connector between the optic cannula and optic fiber to minimize light leakage at this point.

Behavioral training protocol

The full training consisted of 3 daily habituation sessions with baseline measurements, 10 daily acquisition sessions, and 6 probe session after training. During the first habituation session, mice were placed in the setup for 30-45 minutes, during which the air puff needle (for US delivery) and NVE chip (for MDMT recording) were positioned properly to the animal's head but no stimuli were delivered. During the second and third habituation session, each animal received 5 weak puff trials and 20-40 tone CS-only trials as a baseline measure. For each individual animal we established that the 80dB 280 ms tone CS did not elicit any reflexive eyelid closures but only a small alpha startle response (for details, see¹⁰). During the acquisition phase (Results: Experiment 1), animals received 100 paired Opto-CS-US trials. The interval between the onset of CS and that of US was set at 250 ms. Because of the inherent delay in the delivery of air puff of 14 ms, we triggered the air puff at 236 ms after CS onset so that it would hit the cornea exactly at 250 ms after CS onset. The optogenetic stimulation was delivered during all paired Opto-CS-US trials always started 50 ms before CS onset and ended at US onset (total duration 300 ms). During acquisition we used the 'high intensity' of 35 mW/mm². The inter-trial interval was set according to the following constraints: at least 10 seconds had to elapse, the eyelid had to be open below a predetermined threshold, and eyelid position had to be stable for at least 1 second for a trial to begin. After the acquisition phase we tested the animals performance during 6 so called probe session, in which we presented probe trials (trials without US) in between the normal Opto-CS-US trials with combinations of the tone CS and optogenetic stimulation at slightly different durations and intensities as the ones we used during the acquisition phase. The ratio of the normal Opto-CS-US trials and new probe trials was always 4:1. During probe session 1-3 (Results: Experiment 2) we tested the effects of CS tone intensity on the CR expression and the potential modulating effects of amygdala stimulation on the CS saliency. Therefore, we presented probe trials, which consisted of the CS tone at three different intensities (70, 80, and 90 dB) combined with four different optogenetic stimulation intensities (0, 5, 20, or 35 mW/mm²). During probe session 4-6 (Results: Experiment 3) we tested the effects of different durations of the tone CS and optogenetic stimulation on the kinetic profile of the eye-blink CRs.

For this, we used CS tones at durations of 50 or 280 ms and optogenetic stimulations of 50, 150, 250 or 300 ms, starting at different onsets respectively to CS onset. During all sessions, the experimenter carefully inspected threshold and stability parameters and adjusted them if necessary. All experiments were performed at approximately the same time of day by the same experimenter.

Analysis of behavioral data

Individual eye-blink traces were analyzed automatically with custom computer software (LabVIEW or MATLAB) in a five-step process. First, trials with significant activity in the 500 ms pre-CS period were regarded as invalid for further analysis. Second, trials were normalized by aligning the 500 ms pre-CS baselines and calculating the averaged unconditioned response (UR) amplitude in Volts per session. The voltage corresponding with a full closure was further used in the analysis of the eye-blink traces as the 100% value reflecting full eyelid closure (± 1 mm movement), and other values like CR amplitude were expressed relative to this 100% value. Third, in these valid, normalized trials eyelid movements larger than 5% of the 500 ms pre-CS period and a latency to onset between 50-250 ms and a latency to peak of 100-255 ms (both relative to CS onset) were considered as conditioned responses (CRs). Fourth, based on this trial-by-trial analysis we calculated for each session per mouse (1) the percentage of eye-blink CRs, (2) the averaged amplitude in the CS-US interval (based on all valid trials and not thus only for trials in which a CR was present), and (3) timing parameters like latency to CR onset and latency to CR peak time relative to CS onset (based on only these trials wherein a CR is present). Fifth, we calculated group averages (mutants vs. wildtypes) for the same parameters (1-3) and determined statistically significant differences using non-parametric tests because of the small sample size. Data was considered statistically significant if $P < 0.05$.

Immunofluorescence and confocal imaging

After deep anesthesia induced by intra-peritoneal injection of pentobarbital (50mg/kg), mice were transcardially perfused with saline, followed by 4% paraformaldehyde (PFA). Brains were dissected and post-fixed in 4% PFA for 2h at 4°C. After post-fixation, the brains were transferred into 10% sucrose phosphate buffer

(PB 0.1M, pH 7.3) and stored overnight at 4°C. Embedding was performed in a 10% gelatin + 10% sucrose block, with fixation in 10% PFA+30% sucrose solution for 2h at room temperature and immersed in 30% sucrose at 4°C. 40 µm coronal sections were collected serially (rostral to caudal) using a freezing microtome (Leica, SM 2000R) and stored in 0.1M PB. Nuclear staining was performed using DAPI (1:10000, Invitrogen). Sections were washed with PB 0.1M and mounted on slides, cover slipped with Vectashield H1000 fluorescent mounting medium (Vector Labs), and sealed. Stained brain images were acquired using a Zeiss LSM 700 confocal microscope (Carl Zeiss) equipped with Zeiss Plan-Apochromat 10x/0.45, 20x/0.8, and 40x/1.3 (oil immersion) objectives. Native AAV5/EF1a-DIO-hChR2-eYFP and AAV5/EF1a-DIO-eYFP virus expressions and DAPI were imaged using the excitation wavelengths of 488 and 405 nm, respectively. Confocal images including tile-scanned images were acquired using 10x/0.45 objective. So far, we did no detailed quantification of the projections of CeL SOM⁺ neurons to the various brain stem nuclei (*Results: Experiment 4*).

RESULTS

Experiment 1: What is the effect of optogenetic stimulation of SOM⁺ neurons in the CeL during the tone CS on the rate of acquisition in eye-blink conditioning?

Som-IRES-cre mice injected with either AAV5/EF1a-DIO-hChR2-eYFP (mouse n = 4, red trace), hereafter called CeL SOM⁺ stimulated mice, or a control construct AAV5/EF1a-DIO-eYFP (mouse n = 6, blue trace), hereafter called control mice, were trained in an eye-blink conditioning paradigm for 10 consecutive daily sessions. Each session consisted of 100 paired Opto-CS-US trials, the interval between CS and US was 250 ms, and the interval between trials was 10 ±2 seconds, tone CS intensity was 80dB and optogenetic stimulation started 50ms before CS onset and ended at US onset (total duration 300 ms). CeL SOM⁺ stimulated mice showed faster acquisition in terms of CR percentage ($p < .05$, Wilcoxon matched-pair signed-rank test) (Fig. 2A). Moreover, after ten days of training CeL SOM⁺ stimulated mice showed CRs with bigger amplitudes than control mice (Fig. 2B). Control mice showed normal timing of their eye-blink CRs, i.e. the peak of the CR coincides with the onset of the expected US, which means that the eyelid is maximally closed at

the moment that the eye-puff would be delivered. However, CeL SOM⁺ sometimes seemed to ‘overshoot’ with a peak time slightly (± 30 ms) later than the onset of the expected US (see also Fig. 3, 4, not further statistically investigated for now).

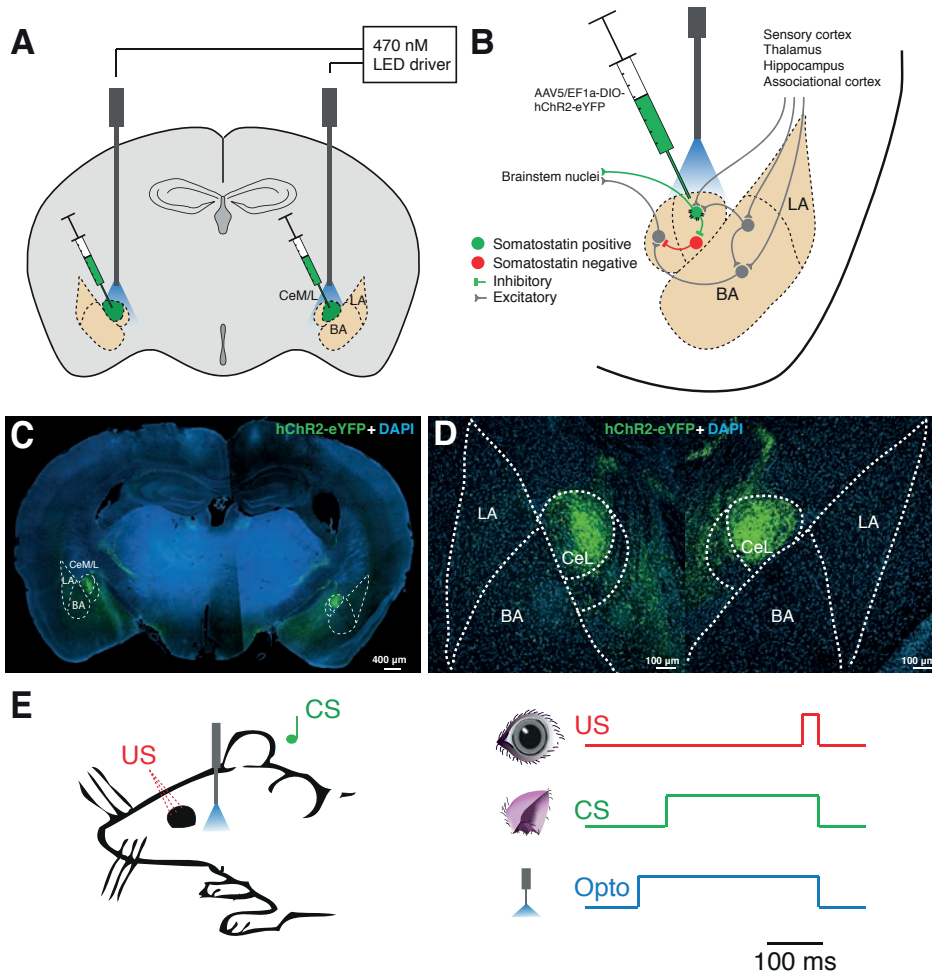


Fig 1. The experimental paradigm to study the effect of SOM⁺ cells on eye-blink conditioning responses. The *Som-IRES-cre* mice were used in these experiments. (A) A schematic diagram showing the experimental optogenetic design. AAV5/EF1a-DIO-hChR2-eYFP virus was expressed in SOM⁺ neurons in CeL (shown in green) by viral infection. Optic fibers were chronically implanted bilaterally in CeL and were connected to 470 nm laser source. (B) A schematic illustration of the amygdala complex showing the SOM⁺ cells in CeL receive sensory input from the cortical and thalamic regions, and major glutamatergic input from the basolateral amygdala (LA +BA). The SOM⁺ cells locally inhibit the non-SOM⁺ in CeL causing disinhibition of the CeM. CeL regulates the brainstem nuclei through direct and indirect pathways. (C) A representative overview image of a brain coronal section showing the SOM⁺ neurons in CeL infected with AAV5/EF1a-DIO-hChR2-eYFP virus. (D) Representative zoomed images of amygdala complex in left and right hemispheres showing the SOM⁺ neurons in CeL infected with AAV5/EF1a-DIO-hChR2-eYFP virus. (E) A schematic behavioral paradigm showing mice receive CS (tone) associated with US (corneal air puff) combined with optogenetic stimulation. LA: lateral amygdala, BA: Basal amygdala

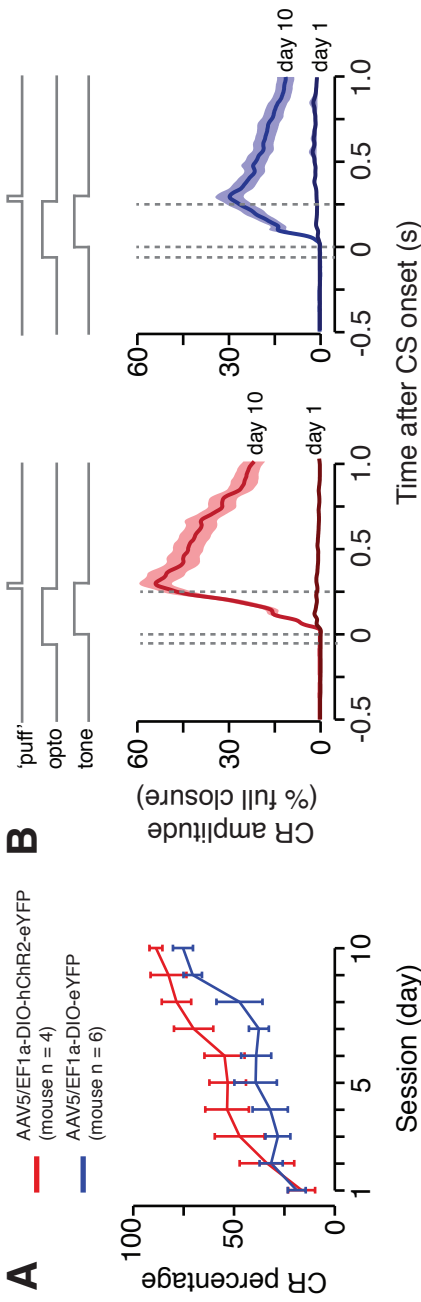


Fig. 2 Optogenetic stimulation of SOM⁺ neurons in the CeL during the CS period results in faster and better learning. (A) *Som-ires-cre* mice injected with either AAV5/EF1a-DIO-hChr2-eYFP (mouse n = 4, red trace) or a control construct AAV5/EF1a-DIO-eYFP (mouse n = 6, blue trace) were trained in an eye-blink conditioning paradigm for 10 consecutive daily sessions. Each session consisted of 100 paired Opto-CS-US trials, the interval between CS and US was 250 ms, and the interval between trials was 10 ± 2 seconds, tone CS intensity was 80dB and optogenetic stimulation started 50ms before CS onset and ended at US onset (total duration 300 ms). Mice in which SOM⁺ CeL neurons were optogenetically stimulated during training show significantly faster acquisition in terms of CR percentage. (B) After ten days of training SOM⁺ CeL stimulated mice show CRs with bigger amplitudes than control mice. Note that the peak of the CR in CS only trials coincides with the onset of the expected eyepeff US. The CR amplitude is expressed as a percentage of the full eyelid closure (full closure = 100%). Depicted traces show the average of the average of *all* traces per mouse for session 1 and 10. All trials were presented without eyepeff US, but the expected eyepeff is depicted in the plots. Error bars denote mean ± SEM.

Experiment 2: What is the effect of the CS tone intensity on the CR expression and could amygdala stimulation modulate the saliency of the CS?

Eyelid CR amplitudes are determined by the intensity of the CS. In control mice a CS intensity lower (70dB) than the one used during training (80 dB) results in smaller CR amplitudes, whereas a higher CS intensity (90dB) results in bigger CRs (Fig. 3, lower panels). In contrast, mice in which the SOM⁺ CeL neurons were optogenetically stimulated during the CS showed for all CS intensities a strong potentiating effect of amygdala stimulation, i.e. a stronger amygdala stimulation resulted in bigger CRs. Interestingly, a tone CS without amygdala stimulation even resulted in a complete absence of properly *timed* CRs. Note that a 70dB tone alone did not elicit any CRs in CeL SOM⁺ stimulated mice and that titration of the optogenetic stimulation (low, medium, high intensity) could boost them to levels almost as high as the amplitudes of CRs at 80 or 90 dB tone intensity (Fig. 3, upper panels), suggesting that amygdalar stimulation could indeed increase the saliency of the CS. Furthermore, we could find no difference between CR amplitudes for control mice at the different optogenetic stimulation intensities and we therefore can exclude the possibility that mice were able to detect the blue light used for optogenetic stimulation either through the connector between optic fiber and optic cannula or through direct stimulation of retinal photoreceptor by light that penetrates the brain²⁶.

Experiment 3: What is the effect of different durations of the tone CS and optogenetic stimulation on the kinetic profile of eyeblink CRs and is the optogenetic stimulation simply part of the CS?

The kinetic profile of eyelid CRs in mice trained with optogenetic stimulation of CeL SOM⁺ neurons during acquisition was determined by the onset and duration of both CS tone and optogenetic stimulation. If the optogenetic stimulation was kept constant, there was virtually no difference in kinetic profile between eye-blink CRs elicited by a tone of 50 ms or by a tone of 280 ms (Fig. 4A). The timing of the CR peak was mainly determined by the onset of the CS and not by the onset of the optogenetic stimulation. A shorter temporal overlap between optogenetic stimulation and tone CS resulted for both the 50 ms tone (light green traces) and 280 ms tone (light brown traces) in CRs with a smaller amplitude. Also when the tone was kept constant and the onset and duration of the optogenetic stimulation were varied, a

shorter temporal overlap between CS tone and optogenetic stimulation resulted in smaller CRs (Fig. 4B). Here again, the timing of the CR peak seemed to be mainly determined by the tone and not by the optogenetic stimulation.

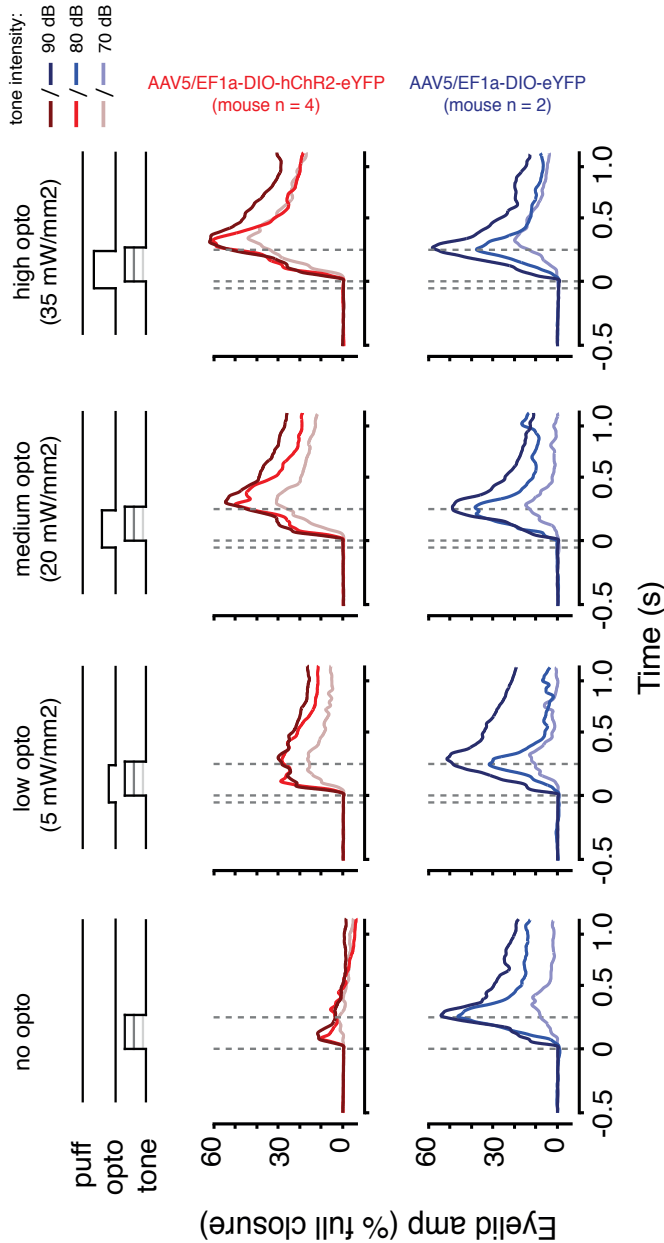


Fig. 3 Eyelid CR amplitudes are determined by the intensity of the CS, which can be modulated by optogenetic stimulation of SOM⁺ neurons in the CeL during the CS-US interval. In control mice a CS intensity lower (70dB, light blue trace) than the one used during training (80 dB, blue trace) results in smaller CR amplitudes, whereas a higher CS intensity (90dB, dark blue trace) results in bigger CRs. Note that the peak of the CR in CS only trials is *timed* in such a manner that its peak coincides with the onset of the expected eye-puff US. In contrast, mice in which the SOM⁺ CeL neurons are optogenetically stimulated during the CS show for all CS intensities a strong potentiating effect of amygdala stimulation, i.e. a stronger amygdala stimulation results in bigger CRs. Interestingly, a tone CS without amygdala stimulation even results in a complete absence of properly timed CRs. Note that a 70dB tone alone does not elicit any CRs in CeL SOM⁺ stimulated mice and that titration of the optogenetic stimulation (low, medium, high intensity) can boost them to levels almost as the CRs for an 80 or 90 dB tone. In addition, there is virtually no difference between an 80 and 90 dB tone. Also compare the CR amplitudes at a 70dB tone for control animals with CeL SOM⁺ stimulated animals. Since there are no differences between CR amplitudes for control mice at the different optogenetic stimulation intensities, we can exclude that mice could detect the blue light used for optogenetic stimulation either through the connector between optic fiber and optic cannula or through direct stimulation of retinal photoreceptor by light that penetrates the brain

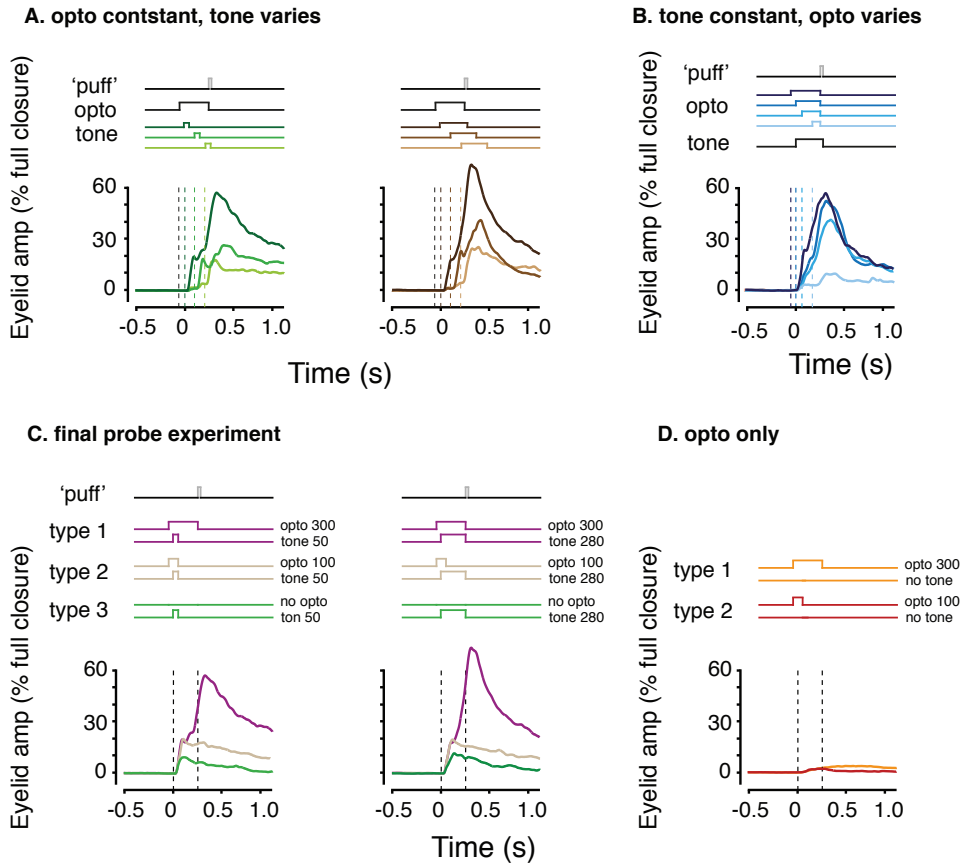


Fig. 4. The kinetic profile of eyelid CRs in mice trained with optogenetic stimulation of CeL SOM⁺ neurons during acquisition is determined by the onset and duration of both CS tone and optogenetic stimulation. (A) If the optogenetic stimulation is kept constant, there is virtually no difference between a CS tone of 50 ms (green traces) and a CS tone of 280 ms (brown traces). The timing of the CR peak is mainly determined by the onset of the CS tone and not by the onset of the optogenetic stimulation. A shorter temporal overlap between optogenetic stimulation and tone CS results for both the 50 ms tone (light green traces) 280 ms tone (light brown traces) in CRs with a smaller amplitude. **(B)** Also when the tone is kept constant and the onset and duration of the optogenetic stimulation changes, a shorter temporal overlap between CS tone and optogenetic stimulation results in smaller CRs. Here again, the timing of the CR peak seems to be mainly determined by the tone and not by the optogenetic stimulation. **(C)** The final probe experiment was designed to illustrate that the optogenetic stimulation of CeL SOM⁺ neurons is not simply part of the CS. Normally, a short version of the CS used during training, e.g. 50 ms instead of 280 ms, will result in normal CRs. Thus, if the optogenetic stimulation is part of the CS (complete CS = tone+opto), one would expect that a short a short tone (50 ms) with a short optogenetic stimulation (100 ms) will result in normal CRs. As expected, trial type 1 (purple) shows that a short tone with a long optogenetic stimulation (left trace) results in CRs, which are almost as big as CRs elicited by a long tone with long optogenetic stimulation (right trace). However, a short optogenetic stimulation with both a short tone (type 2, left beige trace) and a long tone (type 2, right beige trace) results in CRs with only a very small amplitude, suggesting that the optogenetic stimulation is not part of the CS. For comparison, also CS tone only trials (type 3, green traces) are plotted. **(D)** Optogenetic stimulation of CeL SOM⁺ neurons alone after conditioning results in only very minimal eyelid movements.

One might argue that the optogenetic stimulation of SOM⁺ neurons in the CeL was simply part of the CS and that therefore a removal of this stimulation would result in an incomplete CS and thus a different CS than the one the animals were trained with. Although, we could not completely exclude this possibility, we have indirect evidence that this might not be the case. It is known from behavioral²⁷ and electrophysiological studies²⁸ on eye-blink conditioning that the presentation of a short version of the CS used during training (for instance 50 ms) results in CRs that are indistinguishable from CRs elicited by a CS duration used during training (for instance 280 ms). Based on this knowledge, we designed a probe experiment to investigate whether the optogenetic stimulation of CeL SOM⁺ neurons was simply part of the CS. If the optogenetic stimulation is indeed part of the CS (complete CS = tone 280 ms + opto 300 ms), one would expect that a short tone with a short optogenetic stimulation (probe CS = tone 50 ms + opto 100 ms) results in normal CRs. However, this stimulus resulted in CRs with only very small amplitudes, suggesting that the optogenetic stimulation is not part of the CS (Fig 4C). In contrast, a short tone of 50 ms with long optogenetic stimulation (300 ms) resulted in normal CRs (Fig. 4C). Finally, optogenetic stimulation of CeL SOM⁺ neurons alone after conditioning resulted in only very minimal eyelid movements (Fig. 4D).

Experiment 4: What are the efferents of CeL SOM⁺ neurons in the brainstem?

CeL SOM⁺ neurons projected to various brainstem subregions. We found sparse virus labeling in the periaqueductal gray matter and deep mesencephalic nucleus (Fig. 5A). More pronounced labeling was found in parabigeminal nucleus and caudal parts of the hippocampus (subiculum) (Fig. 5B), parabigeminal nucleus, lateral and medial parabrachial nucleus, and locus coeruleus (Fig. 5C), and nucleus of solitary tract (Fig. 5D). Interestingly, we could not establish direct projections from CeL SOM⁺ neurons to the pontine nuclei, which is the source of mossy fiber input the cerebellum transmitting CS information.

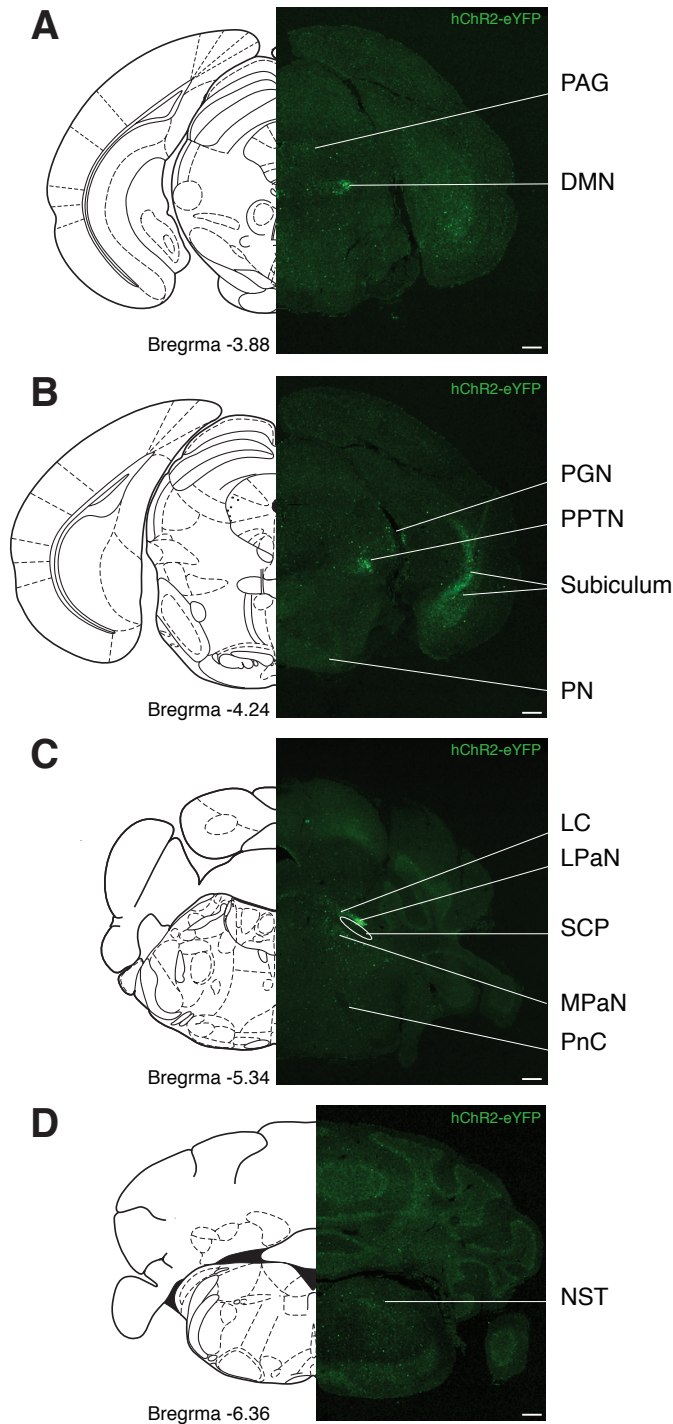


Fig 5. Indirect evidence indicates SOM^+ cells in CeL linked to distinct brainstem subregions.

The *Som-IRES-cre* mice were injected with AAV5/EF1a-DIO-hChR2-eYFP virus in CeL of a mouse brain. A series of representative images of coronal sections of one hemisphere showing the brainstem subregions with virus infected cells. **(A)** Very sparse virus labelling in the PAG and more pronounced labelling in DMN were observed. **(B)** The virus labelling was observed in PGN, PPTN and caudal part of hippocampus (Subiculum) while no labeling was indicated in PN. **(C)** The virus labelling was detected in LC, LPaN and MPaN. Sparse virus labelling was observed in PnC while no labelling was seen in SCP. **(D)** Virus labelling was detected in NST. PAG: Periaqueductal gray matter, DMN: Deep mesencephalic nucleus, PGN: Parabigeminal nucleus, PPTN: Pedunculo potine tegmental nucleus, PN: Pontine nuclei, LC: Locus coeruleus, LPaN: Lateral parabrachial nucleus, MPaN: Medial parabrachial nucleus, SCP: Superior cerebellar peduncle, PnC: Pontine reticular nucleus, caudal part, NST: Nucleus of solitary tract. Scale bar, 400 μ m.

DISCUSSION

Here we show that optogenetic stimulation of SOM⁺ neurons in the CeL during the CS in an eye-blink conditioning paradigm could induce faster CR acquisition and enhance eyelid CR amplitudes. Although the number of animals used so far is relatively small, the behavioral data is very clear and consistent. However, when it comes to an interpretation of our results, things become more complicated. First, it is unclear if optogenetic stimulation of CeL SOM⁺ neurons indeed could increase the saliency of the CS input signals to the cerebellum, as suggested by ourselves in 2010¹⁰ and later anatomically and electrophysiologically confirmed by Siegel et al. (2015)¹⁶ and Farley et al. (2016)⁵, since we could not find direct projections from CeL SOM⁺ neurons to the pontine nuclei, which is the source of mossy fiber input to the cerebellum transmitting the CS information. It still could be possible that CeL SOM⁺ neurons project via the medial division of the central nucleus (CeM) to the pontine nuclei, however, small retrograde tracer injections in the pontine nuclei indicate found only very sparse labeling in the CeM/CeL regions²⁹. Careful inspection of the tracer injections in the mentioned work of Siegel et al. (2015) and Farley et al. (2016), tells us that their injections were very large and not restricted to the amygdalar complex but also labeling neurons in adjacent brain structures and fibers in descending tracts (cerebral peduncle). Therefore, better quantifications are needed of both CeL SOM⁺ neuronal projections to the pontine nuclei but one should also make small anterograde tracer injections that are restricted to the different parts of the amygdalar central nucleus and *small* retrograde tracer injections in the pontine nuclei. Other, more indirect behavioral, evidence that the amygdala is not simply enhancing the saliency of the CS signals transmitted to the cerebellum, comes from our experiment 3. This experiment shows that a short amygdala stimulation of 100 ms during a short CS tone of 50 ms is not sufficient to get proper eyelid CRs. Although this experiment 3 was designed to test the hypothesis if the amygdala stimulation was simply part of the CS by presenting a short version of the complete CS (short opto (100 ms) + short tone (50)), this experimental outcome also indicates that a potential enhancement of the saliency of the short tone CS is not enough to get normal eye-blink CRs. Therefore, we carefully conclude now that the amygdala stimulation during the CS is not simply boosting the saliency of the tone CS.

The optogenetic stimulation also does not seem part of the CS. As mentioned, it is known from behavioral²⁷ and electrophysiological²⁸ studies on eye-blink conditioning that a short version of the CS that was used during training is sufficient to get normal eyelid CRs. We show in experiment 3 that short amygdala stimulation (100 ms) during a short CS (50 ms) could not elicit proper CRs whereas long amygdala stimulation (300 ms) during a short CS (50 ms) does result in proper CRs. Moreover, amygdala stimulation alone (either 100 ms or 300 ms) does not elicit CRs at all (Fig. 4D). It could still be possible though that amygdala stimulation increases the animal's general alertness level and therefore results in better CRs. (It is well known amongst students of eye-blink conditioning that a simple trigger that catches the animal's attention just before the presentation of a CS, like a knock on the eye-blink box, always results in a nice CR.)

However, it is also very likely that the amygdala stimulation does not (only) modulate cerebellar input but might also increase cerebellar output via structures like the locus coeruleus, which has major projections to motoneurons in the facial nucleus³⁰. The fact that removal of the optogenetic stimulation during the CS period (Fig. 3) in animals that were trained with Opto-CS-US trials results in only very small CRs (with even a complete absence of the timed component!) also fits with this idea: the Purkinje cells in the cerebellar cortex, which drive the eye-blink CRs, were taught that only a very mild suppression in their simple spike firing was sufficient to get perfect CRs. (Analogy: a leverage, which is increasing our strength enormously, is suddenly removed). To further investigate this option, future experiments should focus on optic stimulation of channelrhodopsin expressing axon terminals in structures like the locus coeruleus instead of cell bodies in the CeL. Other future experiments should test if amygdala stimulation after eye-blink training could also potentiate CR amplitudes.

Acknowledgements

Authors are grateful to S. Dijkhuizen and A.C.H. Ijpelaar for their technical assistance with the behavioral training of the mice.

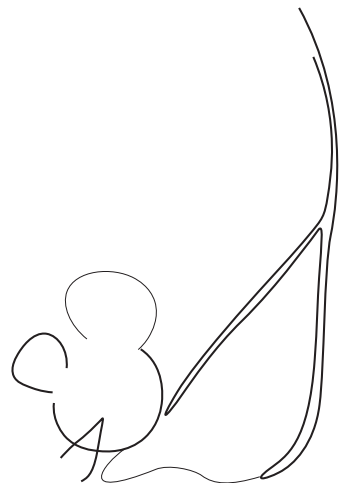
References

1. LeDoux, J.E. Brain mechanisms of emotion and emotional learning. *Curr Opin Neurobiol* **2**, 191-7 (1992).
2. Nader, K., Majidishad, P., Amorapanth, P. & LeDoux, J.E. Damage to the lateral and central, but not other, amygdaloid nuclei prevents the acquisition of auditory fear conditioning. *Learn Mem* **8**, 156-63 (2001).
3. Medina, J.F., Repa, J.C., Mauk, M.D. & LeDoux, J.E. Parallels between cerebellum- and amygdala-dependent conditioning. *Nat Rev Neurosci* **3**, 122-31 (2002).
4. Pare, D., Quirk, G.J. & Ledoux, J.E. New vistas on amygdala networks in conditioned fear. *J Neurophysiol* **92**, 1-9 (2004).
5. Farley, S.J., Radley, J.J. & Freeman, J.H. Amygdala Modulation of Cerebellar Learning. *J Neurosci* **36**, 2190-201 (2016).
6. Yeo, C.H., Hardiman, M.J. & Glickstein, M. Discrete lesions of the cerebellar cortex abolish the classically conditioned nictitating membrane response of the rabbit. *Behav Brain Res* **13**, 261-6 (1984).
7. Mostofi, A., Holtzman, T., Grout, A.S., Yeo, C.H. & Edgley, S.A. Electrophysiological localization of eyeblink-related microzones in rabbit cerebellar cortex. *J Neurosci* **30**, 8920-34 (2010).
8. Freeman, J.H. & Steinmetz, A.B. Neural circuitry and plasticity mechanisms underlying delay eyeblink conditioning. *Learn Mem* **18**, 666-77 (2011).
9. Delgado-Garcia, J.M. & Gruart, A. Building new motor responses: eyelid conditioning revisited. *Trends Neurosci* **29**, 330-8 (2006).
10. Boele, H.J., Koekkoek, S.K. & De Zeeuw, C.I. Cerebellar and extracerebellar involvement in mouse eyeblink conditioning: the ACDC model. *Front Cell Neurosci* **3**, 19 (2010).
11. Yeo, C.H. & Hesslow, G. Cerebellum and conditioned reflexes. *Trends Cogn Sci* **2**, 322-330 (1998).
12. Jirenhed, D.A., Bengtsson, F. & Hesslow, G. Acquisition, extinction, and reacquisition of a cerebellar cortical memory trace. *J Neurosci* **27**, 2493-502 (2007).
13. Ten Brinke, M.M. et al. Evolving Models of Pavlovian Conditioning: Cerebellar Cortical Dynamics in Awake Behaving Mice. *Cell Rep* **13**, 1977-88 (2015).
14. Ohmae, S. & Medina, J.F. Climbing fibers encode a temporal-difference prediction error during cerebellar learning in mice. *Nat Neurosci* **18**, 1798-803 (2015).
15. Halverson, H.E., Khilkevich, A. & Mauk, M.D. Relating cerebellar purkinje cell activity to the timing and amplitude of conditioned eyelid responses. *J Neurosci* **35**, 7813-32 (2015).

16. Siegel, J.J. et al. Trace Eyeblink Conditioning in Mice Is Dependent upon the Dorsal Medial Prefrontal Cortex, Cerebellum, and Amygdala: Behavioral Characterization and Functional Circuitry(1,2,3). *eNeuro* **2** (2015).
17. Lee, T. & Kim, J.J. Differential effects of cerebellar, amygdalar, and hippocampal lesions on classical eyeblink conditioning in rats. *J Neurosci* **24**, 3242-50 (2004).
18. Neufeld, M. & Mintz, M. Involvement of the amygdala in classical conditioning of eyeblink response in the rat. *Brain Res* **889**, 112-7 (2001).
19. Blankenship, M.R., Huckfeldt, R., Steinmetz, J.J. & Steinmetz, J.E. The effects of amygdala lesions on hippocampal activity and classical eyeblink conditioning in rats. *Brain Res* **1035**, 120-30 (2005).
20. Ng, K.H. & Freeman, J.H. Amygdala inactivation impairs eyeblink conditioning in developing rats. *Dev Psychobiol* (2013).
21. Li, H. et al. Experience-dependent modification of a central amygdala fear circuit. *Nat Neurosci* **16**, 332-9 (2013).
22. Yu, K., Garcia da Silva, P., Albeanu, D.F. & Li, B. Central Amygdala Somatostatin Neurons Gate Passive and Active Defensive Behaviors. *J Neurosci* **36**, 6488-96 (2016).
23. Penzo, M.A., Robert, V. & Li, B. Fear conditioning potentiates synaptic transmission onto long-range projection neurons in the lateral subdivision of central amygdala. *J Neurosci* **34**, 2432-7 (2014).
24. Chettih, S.N., McDougale, S.D., Ruffolo, L.I. & Medina, J.F. Adaptive timing of motor output in the mouse: the role of movement oscillations in eyelid conditioning. *Front Integr Neurosci* **5**, 72 (2011).
25. Koekkoek, S.K.E., Den Ouden, W.L., Perry, G., Highstein, S.M. & De Zeeuw, C.I. Monitoring Kinetic and Frequency-Domain Properties of Eyelid Responses in Mice With Magnetic Distance Measurement Technique. *J Neurophysiol* **88**, 2124-2133 (2002).
26. Danskin, B. et al. Optogenetics in Mice Performing a Visual Discrimination Task: Measurement and Suppression of Retinal Activation and the Resulting Behavioral Artifact. *PLoS One* **10**, e0144760 (2015).
27. Boele, H.J., Ten Brinke, M.M. & De Zeeuw, C.I. in *The Neural Codes of the Cerebellum* (ed. Heck, D.) 53-96 (Academic press, 2015).
- Jirenhed, D.A. & Hesslow, G. Time course of classically conditioned Purkinje cell response is determined by initial part of conditioned stimulus. *J Neurosci* **31**, 9070-4 (2011).
29. Mihailoff, G.A., Kosinski, R.J., Azizi, S.A. & Border, B.G. Survey of noncortical afferent projections to the basilar pontine nuclei: a retrograde tracing study in the rat. *J Comp Neurol* **282**, 617-43 (1989).
30. Jones, B.E. & Yang, T.Z. The efferent projections from the reticular formation and the locus coeruleus studied by anterograde and retrograde axonal

transport in the rat. *J Comp Neurol* **242**, 56-92 (1985).

Chapter 5
General Discussion



Summary and scope of the discussion

In this thesis I have focused on the role of the amygdala in two different types of associative conditioning paradigms. First, regarding fear conditioning, the fear memory engram was investigated using fluorescent-reporter based immediate early gene (IEG) expression within the lateral amygdala (LA). Second, for eye-blink conditioning, the function of somatostatin⁺ (SOM⁺) interneurons in the lateral subdivision of the central nucleus (CeL) of the amygdala was studied. Multiple approaches were employed to answer the following questions:

- i. Using confocal imaging and physiological recording methodologies, in chapter 2, I tried to understand how cellular alterations that are induced in a subset of neurons in the LA results in their preferential selection into a fear memory trace. I used the classical auditory fear conditioning paradigm in combination with a novel *Arc* reporter transgenic mouse^{1,2,3} as my main experimental tools. The cells that underwent *Arc* transcription due to the auditory fear learning were visualized, quantified and characterized. Furthermore, their cellular and physiological properties were examined in this study.
- ii. In chapter 3, the distribution pattern of the fear memory engram within subregions of the LA was investigated. We investigated the conditions under which activated neurons optimally express *Arc* and engram activity was detected and monitored through memory encoding, retrieval as well as re-training.
- iii. In chapter 4, we investigated the role of the CeL in the generation of eye-blink conditioned responses (CR). An optogenetic approach enabled us to determine a link between SOM⁺ interneurons located in the CeL, and both the CR as well as the distinct short-latency eyelid response (SLR).

In the following sections, I will discuss the main outcomes of my research in the broader context of neuronal changes in the LA and CeA that contribute to the processing of fear and eye-blink conditioning, respectively.

1. *The amygdala and Pavlovian conditioning*

The amygdala is a brain structure, deep within the medial temporal lobe, consisting of multiple interconnected nuclei which act as an integrative center for emotional behavior⁴. The LA is the key site where multisensory emotional information converges. The LA connects to the central nucleus of amygdala (CeA) through direct and indirect pathways via the basal nucleus of the amygdala (BA) and intercalated masses of the amygdala (ITC). The CeA controls the expression of emotional, defensive, autonomic and endocrine responses⁵.

2. *Fear memory traces in the amygdala*

Enduring physical changes, or engrams, in this brain region are thought to be associated with emotional processing and encoding of both aversive and rewarding Pavlovian memories^{6,7}. The current view is that the engram is formed as a result of enduring alterations of synaptic connectivity between populations of neurons that are active during memory encoding and recruited into the neuronal ensemble^{8,9,10}.

2.1 *Finding and capturing the LA fear memory engram*

Observational studies examining experience-induced changes in neural substrates to reveal the location of the engram have been ongoing for several decades¹¹. Earlier research focused on characterizing learning-induced changes in neurons, such as immediate early gene (IEG) induction^{12–16}, alterations in synaptic strength^{17,18,19}, single and multi-unit recording^{20–23}, and changes in neuronal excitability^{24,25,26}. These studies were successful in detecting the LA engram and roughly estimating the sparse population of neurons recruited to encode a memory^{20–22,27–35}. However, it has been more challenging to monitor engram cells at a time scale of hours after the learning event takes place when the cells are in the consolidation (dormant) state. To overcome this limitation, various neuronal capture strategies take advantage of the observation that IEGs are induced by neural activity and use the IEG promoter to drive transcription of a genetically-encoded fluorescent protein that enables activity-dependent tagging of neuronal populations. The duration of the tagging window (hours to days) is longer than the duration of training experience (typically minutes) enabling in-depth molecular and cellular characterization of memory traces. Using this technology in combination with optogenetics, memory trace neurons in the

LA have been successfully visualized during the encoding, consolidation and retrieval of memories^{36,25}. In particular, optogenetic approaches for the artificial activation of *c-Fos*-defined memory traces have conclusively shown that the identified neurons are necessary and sufficient for memory expression³⁶, demonstrating the validity of this technique in capturing the memory engram. While this molecular-tagging technology has been widely used in the hippocampus, much less is known about the characteristics of the amygdala memory trace. In this thesis, we have tried to fill some of this gap. In chapters 2 and 3, we utilized a fluorescence-based reporter mouse line with a destabilized fluorescent dVenus protein downstream of the IEG *Arc* promoter to label the LA memory engram. Since *dVenus* stimulation-driven expression peaks ~4-5 hrs post-fear training¹, we were able to record neurophysiological alterations that occur during memory consolidation in the hours following the learning event. This time point was 1) long enough to examine the cellular alterations occurring during the consolidation of fear memory, but 2) short enough to capture these changes exclusively, without interference from external unrelated stimulations that may occur with the passage of time. Furthermore, this mouse line enabled us to examine native dVenus expression in a precise population of activated neurons allowing us to detect differences in the intensity of dVenus fluorescence expression across experimental groups. Our observations suggest that LA neurons are probably in different states of activation prior to and after an experience, with the highest intensity observed in animals that consolidate a fear memory when compared to non-learning or home-cage controls. This precise detection and analysis of differences in fluorescence intensity across different experimental conditions (Chapter 2, Fig 2, panels C and D) is not feasible using standard immunohistochemistry due to technical limitations in optimal visualization of protein expression changes across different experimental conditions. Moreover, detecting native dVenus⁺ cells in our study enabled us to specifically target and directly record from cells that went through learning-specific alterations. And moreover to study their physiological properties and compare them with both 1) their neighboring non-activated cells and 2) those of various behavioral control groups in an effort to converge on those mechanisms specifically employed for memory encoding. To the best of our knowledge, our direct recording approach from engram cells under endogenous conditions is the first such study reported in the field, with previous studies recording from either an indiscriminate population of

LA cells or from a random selection of cells virally infected with a plasticity tag^{34,37}. Finally, in Chapter 3, use of the *Arc* promoter in combination with a fluorescent molecular tag permitted us to identify a new and distinct population of neurons in the LaVL that exclusively express *Arc* only upon novel learning when there is a pronounced difference between expectation and actual experience. Taken together, I have used a new molecular tagging technique in my thesis to selectively capture, visualize and characterize the LA fear memory engram. In the following sections, I will discuss the finer characteristics of this LA engram with respect to its allocation, distribution and physiological characteristics.

2.2 Neuronal allocation to a fear memory trace

Multiple studies including my own work have shown that sparse populations of neurons (10-30%) in the LA encode a given fear memory³¹⁻³⁴. Understanding the physiological mechanisms underlying neuronal competition for engram allocation has been a major focus of the field in recent years. A considerable number of previous studies investigated how this neuronal selection takes place and mounting evidence has demonstrated that neurons with higher function of the transcription factor CREB at training are preferentially recruited to the resulting memory trace^{31,38-40}. A seminal study showed that viral overexpression of CREB into a small indiscriminate subset of LA neurons before fear conditioning led to their preferential recruitment into the resulting engram³¹. Additionally, during retrieval, neurons with higher CREB activity were more active than their neighboring cells with lower CREB activity, suggesting this molecule as a key player for neuronal allocation to the engram^{38,40}. This effect was also reported during encoding of hippocampal contextual memory⁴¹. Further experiments using similar experimental techniques demonstrated that cells with higher CREB activity were more excitable than their neighbors, suggesting that intrinsic excitability of neurons is a driving factor that biases recruitment into the memory engram^{24,41,25}. However, this finding was based on artificial manipulation and not from direct physiological characterization of neurons encoding a fear memory. In Chapter 2 of my thesis, we aimed to conclusively test the hypothesis that intrinsic excitability determines neuronal allocation, using a combination of *ex vivo* immunohistochemical neuronal recruitment analysis and whole cell recordings from *Arc*-dVenus⁺ cells and their non-activated neighbors in the LA. We observed that

Arc-dVenus⁺ cells from naïve, unpaired and paired conditions displayed a similar increase in excitability which was independent of learning or sensory stimulation (Figure 4). We thus propose a model for memory trace allocation in which neurons with increased *Arc* expression and neuronal excitability are preferentially recruited to the fear memory trace. This model is supported by the analyses of 1) visually-targeted neuronal recordings in *Arc::dVenus* mice trained with paired versus unpaired fear conditioning, 2) frequency histograms of dVenus fluorescence intensity (Chapter 2, Figure 2D) and 3) strong recruitment of pre-training dVenus⁺ cells into the fear memory network as demonstrated in Figure 3 (Chapter 2). Thus we have provided conclusive evidence that intrinsic excitability is a dominant cellular mechanism that determines whether individual LA neurons are recruited to a memory trace during fear memory encoding.

2.3 Fear memory trace distribution within the LA

The precise numbers and location of LA memory trace neurons across different subregions of the LA has not been well defined thus far. In my thesis I have tried to systematically determine the fear memory trace distribution in the LA during encoding and retrieval. In Chapter 2, we identified and precisely quantified the sparse distribution of *Arc*-dVenus⁺ cells that establish a fear memory trace in the LA, using confocal stereology. Our study indicates that the fear memory network is constrained to a small portion of neurons that are sparsely distributed within the LA (15.17%). This population increased when we increased the strength of the aversive experience during training (from 1 foot-shock to 3 foot-shocks). However, the size of the engram reached an asymptotic percentage, with no increase in the number of cells recruited to the memory trace beyond 3 CS-US pairings, indicating that there is a non-linear relationship between the strength of a memory and the population of the cells that compose a memory trace.

In chapter 3, using the same transgenic mouse line, we showed that along with the sparse distribution of neurons activated by fear learning in the LA, a discrete cluster-like subpopulation of *Arc*-dVenus⁺ cells is activated in the LaVL. This ensemble of neurons was activated specifically after initial learning and not by retrieval of fear memory. Furthermore, we show that the fear memory engram is activated exclusively by learned aversive associations and not by innate fear. Our

results are in line with two previous studies reporting a discrete subpopulation of *c-Fos* activity in the LaVL after contextual fear conditioning^{42,43}. These studies identified principle neuron activation in the LaVL that was context specific and did not alter after memory recall⁴³. Furthermore, by mapping the activity of ERK/MAP kinase after fear conditioning the authors observed an increase in phosphorylated MAPK labeling shortly after auditory fear conditioning in the dorsal lateral amygdala (dLA) and LaVL⁴⁴. Overall, our research along with studies that use different molecular tags, together demonstrate that a unique cluster of cells in the LaVL is activated after fear conditioning, which may be physiologically distinct from trace neurons in the dLA. Furthermore, our work advances previous findings by addressing the conditions under which this subpopulation of cells is activated. Taken together, we have conclusively visualized and quantified the random sparse distribution of memory trace neurons in the LA under different experimental conditions and identified a new population of cells in the LaVL that undergoes subtle changes in activation during the different phases of memory processing. Furthermore, the sparse distribution of a fear memory trace is consistent with earlier findings particular subsets of neurons encode each specific memory as the result of neuronal competition. However, it is important to note that distinct fear memory traces are only formed when their related events occur at distal times resulting in non-overlapping populations of neurons of each memory trace⁴⁵.

2.4 Synaptic plasticity as a mechanism of fear memory trace storage

Experience-dependent alterations of synaptic transmission in the form of Hebbian plasticity are thought to underlie the formation and maintenance of fear memories⁴⁶. Over the years a number of electrophysiological and optogenetic studies have confirmed the nature of synaptic plasticity in the amygdala which takes place as a result of coincident US-evoked depolarization of LA neurons and activation of the same cells by thalamic CS inputs^{7,19,47 37,48,34,49}. For example, at the cellular level, CS-evoked single unit responses exhibit an increase in the LA after fear conditioning⁵⁰ and a potentiation of field responses has been recorded during conditioning¹⁸. Further evidence of this form of plasticity as a mechanism of memory encoding comes from a seminal optogenetic study which demonstrated that substituting the US foot-shock with optogenetic stimulation of LA pyramidal neurons results in the

formation of artificial fear memory⁵¹. However, these studies were indiscriminate in the cells that were recorded or manipulated, and in my thesis I have built on previous work to show that increased synaptic strength underlying fear memory formation occurs in a specific subpopulation of LA neurons identifiable by learning-induced *Arc* transcription. To this end, in Chapter 2, we report that acquisition of associative fear conditioning results in potentiation of the afferent thalamic input specifically onto postsynaptic LA neurons recruited into the fear memory trace. Importantly, no changes in paired pulse ratio were observed while AMPA/NMDA ratios were significantly enhanced, indicating that the learning-induced synaptic potentiation was postsynaptically mediated. All of these physiologic changes were observed exclusively in *Arc*-dVenus⁺ cells in the LA of animals that underwent fear conditioning. Thus, our work, together with previous work in the field conclusively demonstrates that synaptic strengthening in LA memory trace neurons underlies the encoding of fear memories.

3. *Arc* as a marker for novel fear learning in the LA

Immediate early genes are induced within minutes in specific brain regions during neuronal activity associated with behavioral tasks, and are thus widely used to tag neurons specifically activated after a given experience¹²⁻¹⁶. The most common IEGs used to tag memory trace neurons after fear-conditioning are *c-Fos*, *Arc* and *Egr1* (*Zif268*)^{32,52}. Pharmacogenetic manipulation of these tagged neurons is sufficient to modulate subsequent memory expression^{32,53}. While the majority of molecular tagging studies have focused on *c-Fos* expressing engrams^{27,43,54-56}, there is relatively little known about the degree of overlap between neuronal ensembles expressing different IEGs. In Chapter 2, we convincingly show that *c-Fos* activation is highly co-localized with *Arc* expression 1 h post-training, indicating that fear memory traces in the LA express both IEGs during memory encoding. However, it is very interesting to note that while *c-Fos* faithfully labels neurons that have been activated by experience, the expression of *Arc* is more selective. In Chapter 3, we demonstrate this discrepancy in a series of behavioral tests. Re-training animals using the identical or similar conditioning protocols results in a robust expression of *c-Fos* in the LaVL, but no/very low expression of *Arc* indicating the novelty of the second experience attenuates the expression of *Arc*. Taken together, these experiments

indicate that *Arc* may be a specific tag for novel learning, when there is a prominent difference between expectation and actual experience. This feature of *Arc* regulation is further validated by the fact that it is not optimally expressed after the retrieval of memory, while *c-Fos* expression has been documented under similar conditions²⁸. *Arc* induction in neuronal ensembles is associated with metaplastic changes of network properties⁵⁷ and is important for both Hebbian and homeostatic plasticity^{58,59} along with modification of synaptic structure⁶⁰. Thus, given its critical role in the consolidation of synaptic plasticity and long-term memory, we speculate that *Arc* may be a more specific marker for new learning than other IEGs like *c-Fos*. Finally, we also hypothesize that methylation of the *Arc* promoter might be responsible for silencing the expression of this IEG once it has been expressed after conditioning. New learning would then recruit a new subset of neighboring cells, preventing the emergence of overlapping engrams and contributing to memory specificity. Future studies are required to examine this property of *Arc* in more detail.

4. Immediate shock, a model of associative learning

Animals do not form a fear memory to the contextually conditioned stimulus, as measured by their fear response to this CS, when the aversive unconditioned stimulus is presented immediately after an animal is placed in the conditioning chamber. This phenomenon is known as the immediate shock deficit (ISD)⁶¹, and it is widely used to control for non-specific molecular, cellular and behavioral effects of the US presentation^{42,43,62–65}. However, in our study shown in Chapter 3, we observed that although the animals did not freeze to the contextual CS after immediate shock training, the memory trace in the LaVL was robustly activated. This indicates that the animals may indeed form an aversive memory, albeit different from the CS-associated memory encoded after fear conditioning. In line with this, we demonstrate that fear conditioning after immediate shock training results in the formation of a new memory, as evidenced by the expression of *Arc* in the LaVL. Furthermore, rescuing the ISD by pre-exposure to the context results in a CS-US memory being formed and attenuates the expression of *Arc* after subsequent fear conditioning. Historically either a contextual- or an unconditioned stimulus – processing deficit^{66–69} has been theorized to underlie the ISD. It would be interesting to speculate that the immediate shock paradigm is not a deficit *per se*, but the formation

of a new aversive memory to other environmental stimuli present around the time of training. Indeed a previous study has shown that in the immediate shock paradigm, an association occurs between the US (foot-shock), and other environmental cues such as the experimenter, which are present around the time that the animals receive the US⁷⁰. Thus, immediate shock models require more detailed investigation since they are widely used as controls, even though it is very possible that fear-learning induced cellular alterations are also involved in these paradigms.

5. *CeL regulates associative motor learning*

A large body of evidence has established that motor associative learning and plasticity is mediated by the cerebellum, making a distinction between cerebellar-dependent responses and amygdala-dependent emotional learning^{8,71-73}. However, in recent years, a few studies have suggested that an adaptive interaction between these two structures exists^{74,75} indicating that the acquisition of amygdala-related CRs accelerates the acquisition of cerebellum-mediated eye-blink CRs, and that the central nucleus of the amygdala (CeA) is responsible for modulation of cerebellar learning⁷⁶. Given the fact that the CeA is sensitive to aversive and fear learning-induced challenges, and controls phasic and sustained fear related responses⁷⁷, recent findings indicate that eye-blink conditioning is not solely a motor associative learning but rather shares components of the fear associative learning responses. However, the extension and mechanisms by which the CeA cells regulates the eyelid CRs are not yet fully understood.

To address the above questions more selectively in the CeA, we adopted an optogenetic approach in which a direct link between SOM⁺ cells in the CeL of the CeA and fear conditioning responses was shown⁷⁸. In Chapter 4, we investigated the outcome of temporal SOM⁺ stimulation in the CeL both unilaterally and bilaterally on eye-blink learning which resulted in enhancements of both the SLR and CR. Therefore, the triggering effect of the CeL on the acquisition of eyelid conditioning responses observed in our study confirms that associative motor eye-blink responses exhibit fear learning-induced features, which are mediated by SOM⁺ interneurons in the CeL. Mechanistic pathways in which the CeA affects cerebellar learning have been previously investigated. It has been shown that CeA efferents terminate in the pontine nucleus⁷⁹, which in turn conveys auditory CS input to the cerebellum^{80,81,82},

indicating a sensory gating role for the CeA. However, indirect evidence provided in our study suggests that the CeA might have its effect by enhancing alertness through an attentional mechanism. This notion is supported by our finding of efferent projections from SOM⁺ cells of the CeL to brainstem nuclei including locus coeruleus, periaqueductal gray (PAG) and parabrachial nucleus. In contrast, we observed only very sparse projections from the CeL to the pontine nuclei, suggesting that the CeL does not exert its modulatory effect via the pontine nuclei but rather through neuromodulatory stations. Additional studies are required to precisely confirm and define the CeL projections, to selectively manipulate its pathways, to study its interaction with other brain subregions in the brainstem and cerebellum, and to investigate its feedback inhibitory and excitatory circuits in the acquisition and encoding of eye-blink conditioning.

Conclusions and future directions

In my thesis, I have tried to further our understanding of how the amygdala contributes to Pavlovian learning, using classical fear conditioning and eye-blink conditioning as behavioral models. In Chapters 2 and 3, we employed a sensitive system that utilized the IEG, *Arc*, to tag LA neurons that form a fear memory trace/engram. This technique enabled us to elegantly and precisely characterize the distribution and cellular characteristics of sparsely distributed trace neurons. We proposed a model of fear learning in which non-associative neuronal selection and Hebbian synaptic encoding of the learned association are distinct physiological processes: intrinsic excitability determines neuronal selection, whereas learning-related encoding is governed by synaptic plasticity. Furthermore, we showed that a discrete population of cells in the LaVL is activated after fear learning and that IEG expression after a behavioral experience may differ depending on the IEG studied, with *Arc* being a selective marker for novelty learning. Along with excitatory neurons, the amygdala also contains a vast inhibitory network, and in Chapter 4 we demonstrated that somatostatin⁺ interneurons in the CeL modulate conditioned responses in the eye-blink conditioning task, indicating that extra-cerebellar mechanisms function in the generation of eye-blink motor responses. Retrograde- and anterograde-tracing approaches undertaken in the future will help us to dissect the precise nature of this modulation by defining the projections between the CeL and downstream targets in

the brainstem and cerebellum.

The role of GABAergic inhibition in fear conditioning is less understood. Although disinhibition in the CeA is critical to associative learning⁸³, it would be very interesting to understand how inhibition also contributes to the size and stability of the memory engram at the network level. Furthermore, the advent of sensitive molecular techniques like single-cell transcriptomics and proteomics^{84,85} in combination with trace-tagging will enable us to understand how memory trace cells process, store and retrieve memory.

References

1. Eguchi, M. & Yamaguchi, S. In vivo and in vitro visualization of gene expression dynamics over extensive areas of the brain. *NeuroImage* **44**, 1274–83 (2009).
2. Rudinskiy, N. *et al.* Orchestrated experience-driven Arc responses are disrupted in a mouse model of Alzheimer’s disease. *Nat Neurosci* **15**, 1422–9 (2012).
3. Nonaka, A. *et al.* Synaptic Plasticity Associated with a Memory Engram in the Basolateral Amygdala. *Journal of Neuroscience* **34**, 9305–9309 (2014).
4. Sah, P., Faber, E. S. L., Lopez De Armentia, M. & Power, J. The amygdaloid complex: anatomy and physiology. *Physiological reviews* **83**, 803–34 (2003).
5. Sotres-Bayon, F. & Quirk, G. J. Prefrontal control of fear: more than just extinction. *Current opinion in neurobiology* **20**, 231–5 (2010).
6. Fanselow, M. S. & LeDoux, J. E. Why we think plasticity underlying Pavlovian fear conditioning occurs in the basolateral amygdala. *Neuron* **23**, 229–32 (1999).
7. Maren, S. & Quirk, G. J. Neuronal signalling of fear memory. *Nature Reviews Neuroscience* **5**, 844–852 (2004).
8. LeDoux, J. E. Emotion circuits in the brain. *Annual review of neuroscience* **23**, 155–84 (2000).
9. Kandel, E. R. *Cellular basis of behavior: an introduction to behavioral neurobiology*. (W.H. Freeman, 1976).
10. Bliss, T. V & Collingridge, G. L. A synaptic model of memory: long-term potentiation in the hippocampus. *Nature* **361**, 31–9 (1993).
11. K.S. Lashley. *Brain Mechanisms and Intelligence*. (University of Chicago Press, 1929).
12. Greenberg, M. E. & Ziff, E. B. Stimulation of 3T3 cells induces transcription of the c-fos proto-oncogene. *Nature* **311**, 433–8
13. Curran, T. & Morgan, J. I. Superinduction of c-fos by nerve growth factor in the presence of peripherally active benzodiazepines. *Science (New York, N.Y.)* **229**, 1265–8 (1985).
14. Morgan, J. I. & Curran, T. Stimulus-transcription coupling in neurons: role of cellular immediate-early genes. *Trends in neurosciences* **12**, 459–62 (1989).
15. Link, W. *et al.* Somatodendritic expression of an immediate early gene is regulated by synaptic activity. *Proceedings of the National Academy of Sciences of the United States of America* **92**, 5734–8 (1995).
16. Lyford, G. L. *et al.* Arc, a growth factor and activity-regulated gene, encodes a novel cytoskeleton-associated protein that is enriched in neuronal dendrites. *Neuron* **14**, 433–45 (1995).
17. Cajal, S. R. Y. The Croonian Lecture: La Fine Structure des Centres Nerveux. *Proceedings of the Royal Society of London* **55**, 444–468 (1894).

18. Rogan, M. T., Stäubli, U. V & LeDoux, J. E. Fear conditioning induces associative long-term potentiation in the amygdala. *Nature* **390**, 604–7 (1997).
19. Blair, H. T., Schafe, G. E., Bauer, E. P., Rodrigues, S. M. & LeDoux, J. E. Synaptic plasticity in the lateral amygdala: a cellular hypothesis of fear conditioning. *Learning & memory (Cold Spring Harbor, N.Y.)* **8**, 229–42
20. O’Keefe, J. Place units in the hippocampus of the freely moving rat. *Experimental neurology* **51**, 78–109 (1976).
21. Sutherland, G. R. & McNaughton, B. Memory trace reactivation in hippocampal and neocortical neuronal ensembles. *Current opinion in neurobiology* **10**, 180–6 (2000).
22. Thompson, R. F. In Search of Memory Traces. (2004). at <<http://www.annualreviews.org/doi/abs/10.1146/annurev.psych.56.091103.070239>>
23. Sigurdsson, T., Doyère, V., Cain, C. K. & LeDoux, J. E. Long-term potentiation in the amygdala: A cellular mechanism of fear learning and memory. *Neuropharmacology* **52**, 215–227 (2007).
24. Zhou, Y. *et al.* CREB regulates excitability and the allocation of memory to subsets of neurons in the amygdala. *Nat Neurosci* **12**, 1438–43 (2009).
25. Yiu, A. P. *et al.* Neurons Are Recruited to a Memory Trace Based on Relative Neuronal Excitability Immediately before Training. *Neuron* **83**, 722–735 (2014).
26. Sekeres, M. J. *et al.* Increasing CR1 Function in the Dentate Gyrus during Memory Formation or Reactivation Increases Memory Strength without Compromising Memory Quality. *Journal of Neuroscience* **32**, 17857–17868 (2012).
27. Radulovic, J., Kammermeier, J. & Spiess, J. Relationship between fos production and classical fear conditioning: effects of novelty, latent inhibition, and unconditioned stimulus preexposure. *The Journal of neuroscience : the official journal of the Society for Neuroscience* **18**, 7452–61 (1998).
28. Hall, J., Thomas, K. L. & Everitt, B. J. Cellular imaging of zif268 expression in the hippocampus and amygdala during contextual and cued fear memory retrieval: selective activation of hippocampal CA1 neurons during the recall of contextual memories. *The Journal of neuroscience : the official journal of the Society for Neuroscience* **21**, 2186–93 (2001).
29. Zhang, W.-P., Guzowski, J. F. & Thomas, S. A. Mapping neuronal activation and the influence of adrenergic signaling during contextual memory retrieval. *Learning & memory (Cold Spring Harbor, N.Y.)* **12**, 239–47
30. Guzowski, J. F. *et al.* Mapping behaviorally relevant neural circuits with immediate-early gene expression. *Current Opinion in Neurobiology* **15**, 599–606 (2005).
31. Han, J.-H. *et al.* Neuronal competition and selection during memory

- formation. *Science (New York, N.Y.)* **316**, 457–60 (2007).
32. Reijmers, L. G., Perkins, B. L., Matsuo, N. & Mayford, M. Localization of a stable neural correlate of associative memory. *Science (New York, N.Y.)* **317**, 1230–3 (2007).
 33. Repa, J. C. *et al.* Two different lateral amygdala cell populations contribute to the initiation and storage of memory. *Nature neuroscience* **4**, 724–31 (2001).
 34. Rumpel, S., LeDoux, J., Zador, A. & Malinow, R. Postsynaptic receptor trafficking underlying a form of associative learning. *Science (New York, N.Y.)* **308**, 83–8 (2005).
 35. An, B., Hong, I. & Choi, S. Long-term neural correlates of reversible fear learning in the lateral amygdala. *J Neurosci* **32**, 16845–56 (2012).
 36. Liu, X. *et al.* Optogenetic stimulation of a hippocampal engram activates fear memory recall. *Nature* **484**, 381–5 (2012).
 37. Clem, R. L. & Huganir, R. L. Calcium-permeable AMPA receptor dynamics mediate fear memory erasure. *Science* **330**, 1108–12 (2010).
 38. Josselyn, S. A. Continuing the search for the engram: examining the mechanism of fear memories. *Journal of psychiatry & neuroscience : JPN* **35**, 221–8 (2010).
 39. Josselyn, S. A. *et al.* Long-term memory is facilitated by cAMP response element-binding protein overexpression in the amygdala. *The Journal of neuroscience : the official journal of the Society for Neuroscience* **21**, 2404–12 (2001).
 40. Frankland, P. W. & Josselyn, S. A. Memory allocation. *Neuropsychopharmacology : official publication of the American College of Neuropsychopharmacology* **40**, 243 (2015).
 41. Sakaguchi, M. *et al.* Catching the engram: strategies to examine the memory trace. *Molecular Brain* **5**, 32 (2012).
 42. Wilson, Y. M. & Murphy, M. A discrete population of neurons in the lateral amygdala is specifically activated by contextual fear conditioning. *Learning & Memory* **16**, 357–361 (2009).
 43. Trogrlic, L., Wilson, Y. M., Newman, A. G. & Murphy, M. Context fear learning specifically activates distinct populations of neurons in amygdala and hypothalamus. *Learning & Memory* **18**, 678–687 (2011).
 44. Schafe, G. E. & LeDoux, J. E. Memory consolidation of auditory pavlovian fear conditioning requires protein synthesis and protein kinase A in the amygdala. *The Journal of neuroscience : the official journal of the Society for Neuroscience* **20**, RC96 (2000).
 45. Rashid, A. J. *et al.* Competition between engrams influences fear memory formation and recall. *Science (New York, N.Y.)* **353**, 383–7 (2016).
 46. Hebb, D. . *The Organization of Behavior*. (John Wiley and Sons, 1949).
 47. Pape, H.-C. & Pare, D. Plastic synaptic networks of the amygdala for the

- acquisition, expression, and extinction of conditioned fear. *Physiological reviews* **90**, 419–63 (2010).
48. McKernan, M. G. & Shinnick-Gallagher, P. Fear conditioning induces a lasting potentiation of synaptic currents in vitro. *Nature* **390**, 607–11 (1997).
 49. Schroeder, B. W. & Shinnick-Gallagher, P. Fear memories induce a switch in stimulus response and signaling mechanisms for long-term potentiation in the lateral amygdala. *European Journal of Neuroscience* **20**, 549–556 (2004).
 50. Paré, D. & Collins, D. R. Neuronal correlates of fear in the lateral amygdala: multiple extracellular recordings in conscious cats. *The Journal of neuroscience : the official journal of the Society for Neuroscience* **20**, 2701–10 (2000).
 51. Johansen, J. P. *et al.* Optical activation of lateral amygdala pyramidal cells instructs associative fear learning. *Proceedings of the National Academy of Sciences of the United States of America* **107**, 12692–7 (2010).
 52. Nakayama, D. *et al.* Late Arc/Arg3.1 expression in the basolateral amygdala is essential for persistence of newly-acquired and reactivated contextual fear memories. *Scientific Reports* **6**, 21007 (2016).
 53. Garner, A. R. *et al.* Generation of a synthetic memory trace. *Science* **335**, 1513–6 (2012).
 54. Strelakova, T. *et al.* Memory retrieval after contextual fear conditioning induces c-Fos and JunB expression in CA1 hippocampus. *Genes, brain, and behavior* **2**, 3–10 (2003).
 55. Do-Monte, F. H., Quiñones-Laracuente, K. & Quirk, G. J. A temporal shift in the circuits mediating retrieval of fear memory. *Nature* **519**, 460–463 (2015).
 56. Hall, J., Thomas, K. L. & Everitt, B. J. Fear memory retrieval induces CREB phosphorylation and Fos expression within the amygdala. *The European journal of neuroscience* **13**, 1453–8 (2001).
 57. Minatohara, K., Akiyoshi, M. & Okuno, H. Role of Immediate-Early Genes in Synaptic Plasticity and Neuronal Ensembles Underlying the Memory Trace. *Frontiers in molecular neuroscience* **8**, 78 (2015).
 58. Shepherd, J. D. *et al.* Arc/Arg3.1 mediates homeostatic synaptic scaling of AMPA receptors. *Neuron* **52**, 475–84 (2006).
 59. Korb, E., Wilkinson, C. L., Delgado, R. N., Lovero, K. L. & Finkbeiner, S. Arc in the nucleus regulates PML-dependent GluA1 transcription and homeostatic plasticity. *Nature neuroscience* **16**, 874–83 (2013).
 60. Peebles, C. L. *et al.* Arc regulates spine morphology and maintains network stability in vivo. *Proceedings of the National Academy of Sciences* **107**, 18173–18178 (2010).
 61. Landeira-Fernandez, J., DeCola, J. P., Kim, J. J. & Fanselow, M. S. Immediate shock deficit in fear conditioning: effects of shock manipulations. *Behavioral neuroscience* **120**, 873–9 (2006).

-
62. Zelikowsky, M., Hersman, S., Chawla, M. K., Barnes, C. A. & Fanselow, M. S. Neuronal ensembles in amygdala, hippocampus, and prefrontal cortex track differential components of contextual fear. *The Journal of neuroscience : the official journal of the Society for Neuroscience* **34**, 8462–6 (2014).
 63. Frankland, P. W. *et al.* Consolidation of CS and US Representations in Associative Fear Conditioning. doi:10.1002/hipo.10208
 64. Shukla, K., Kim, J., Blundell, J. & Powell, C. M. Learning-induced glutamate receptor phosphorylation resembles that induced by long term potentiation. *The Journal of biological chemistry* **282**, 18100–7 (2007).
 65. Ota, K. T., Monsey, M. S., Wu, M. S. & Schafe, G. E. Synaptic Plasticity and NO-cGMP-PKG Signaling Regulate Pre- and Postsynaptic Alterations at Rat Lateral Amygdala Synapses Following Fear Conditioning. *PLoS ONE* **5**, e11236 (2010).
 66. Fanselow, M. S. Conditioned fear-induced opiate analgesia: a competing motivational state theory of stress analgesia. *Annals of the New York Academy of Sciences* **467**, 40–54 (1986).
 67. Fanselow, M. S. Factors governing one-trial contextual conditioning. *Animal Learning & Behavior* **18**, 264–270 (1990).
 68. Rudy, J. W., Barrientos, R. M. & O'reilly, R. C. Hippocampal Formation Supports Conditioning to Memory of a Context. doi:10.1037//0735-7044.116.4.530
 69. Kiernan, M. J., Westbrook, R. F. & Cranney, J. Immediate shock, passive avoidance, and potentiated startle: Implications for the unconditioned response to shock. *Animal Learning & Behavior* **23**, 22–30 (1995).
 70. Bevins, R. A. & Ayres, J. J. B. One-trial context fear conditioning as a function of the interstimulus interval. *Animal Learning & Behavior* **23**, 400–410 (1995).
 71. Gallagher, M. & Chiba, A. A. The amygdala and emotion. *Current Opinion in Neurobiology* **6**, 221–227 (1996).
 72. Kim, J. *et al.* Cerebellar circuits and synaptic mechanisms involved in classical eyeblink conditioning. *Trends in Neurosciences* **20**, 177–181 (1997).
 73. Yeo, C. H. & Hesslow, G. Cerebellum and conditioned reflexes. *Trends in cognitive sciences* **2**, 322–30 (1998).
 74. Lennartz, R. C. & Weinberger, N. M. Analysis of response systems in Pavlovian conditioning reveals rapidly versus slowly acquired conditioned responses: Support for two factors, implications for behavior and neurobiology. *Psychobiology* **20**, 93–119 (1992).
 75. Boele, H.-J., Koekkoek, S. K. E. & De Zeeuw, C. I. Cerebellar and extracerebellar involvement in mouse eyeblink conditioning: the ACDC model. *Frontiers in cellular neuroscience* **3**, 19 (2010).
 76. Farley, S. J., Radley, J. J. & Freeman, J. H. Amygdala Modulation of

- Cerebellar Learning. *Journal of Neuroscience* **36**, 2190–2201 (2016).
77. Davis, M., Walker, D. L., Miles, L. & Grillon, C. Phasic vs Sustained Fear in Rats and Humans: Role of the Extended Amygdala in Fear vs Anxiety. *Neuropsychopharmacology* **35**, 105–135 (2010).
 78. Li, H. *et al.* Experience-dependent modification of a central amygdala fear circuit. *Nature neuroscience* **16**, 332–9 (2013).
 79. Siegel, J. J. *et al.* Trace Eyeblink Conditioning in Mice Is Dependent upon the Dorsal Medial Prefrontal Cortex, Cerebellum, and Amygdala: Behavioral Characterization and Functional Circuitry(1,2,3). *eNeuro* **2**, (2015).
 80. Steinmetz, J. E. *et al.* Initial localization of the acoustic conditioned stimulus projection system to the cerebellum essential for classical eyelid conditioning. *Proceedings of the National Academy of Sciences of the United States of America* **84**, 3531–5 (1987).
 81. Campolattaro, M. M. & Freeman, J. H. Eyeblink conditioning in 12-day-old rats using pontine stimulation as the conditioned stimulus. *Proceedings of the National Academy of Sciences of the United States of America* **105**, 8120–3 (2008).
 82. Halverson, H. E., Lee, I. & Freeman, J. H. Associative plasticity in the medial auditory thalamus and cerebellar interpositus nucleus during eyeblink conditioning. *The Journal of neuroscience : the official journal of the Society for Neuroscience* **30**, 8787–96 (2010).
 83. Letzkus, J. J. *et al.* Disinhibition, a Circuit Mechanism for Associative Learning and Memory. *Neuron* **88**, 264–276 (2015).
 84. Neuner, S. M. *et al.* TRPC3 channels critically regulate hippocampal excitability and contextual fear memory. *Behavioural Brain Research* **281**, 69–77 (2015).
 85. Tang, F., Lao, K. & Surani, M. A. Development and applications of single-cell transcriptome analysis. *Nature methods* **8**, S6–11 (2011)

Appendices

SUMMARY

The amygdala, a structure deep in the temporal lobe of the brain, is an essential region for emotional and fearful processing. Neuronal coding in the lateral nucleus of the amygdala (LA) endows the brain with the ability to acquire enduring aversive associations, physically represented by experience-dependent synaptic modifications within a small population of neurons selectively recruited during learning. Understanding the precise mechanisms underlying neuronal selection and plasticity during memory formation has been among the most fundamental questions in neuroscience for the past century. Defining the distribution of neuronal activity would further elucidate the conditions by which memories are expressed and how neurons are differentially recruited into distinct memory engrams. The aim of this thesis was to utilize reliable methods to capture, visualize, monitor and modulate defined neuronal populations to expand our knowledge regarding the above questions.

Chapter 1 of this thesis is an overview of the history of progress in understanding fear and eye-blink conditioning. It describes the core principles and particularly highlights recent findings that have been elucidated in the process by which fear memory and motor learning are acquired and encoded.

Chapter 2 describes a novel method to study fear memory traces. *Arc::dVenus* transgenic mice were used to visualize neurons that underwent cellular modifications during fear learning in the lateral amygdala (LA). Our findings demonstrate that intrinsic neuronal excitability is a major driving force for the fear memory neuronal selection. This chapter also demonstrates that the potentiation of glutamatergic synaptic transmission from the thalamic input pathway to the LA is learning-specific, and highly localized to *Arc* expressing neurons.

Chapter 3 reports the distinct pattern of *Arc* expression following learning in the art of the LA. We find that this subregion demonstrates a chronically enduring plasticity by which neurons in this subregion are uniquely active only upon the acquisition of novel aversive associations.

Chapter 4 focuses on the role of somatostatin+ (SOM⁺) interneurons in the lateral division of central nucleus of the amygdala (CeL) in eye-blink conditioning. We find that the CeL has a regulatory effect on associative eyelid responses, indicating that eye-blink conditioning shares key mechanistic components of fear associative learning responses.

Chapter 5 is a general discussion about the outcomes and major conclusions of our studies. In addition, it proposes future approaches that could advance some important unanswered questions in the field.

SAMENVATTING

De amygdala, een hersenstructuur diep gelegen in onze temporaalkwab, is een essentiële regio voor emotionele- en angstregulatie. Neuronale codering in de laterale nucleus van de amygdala (LA) geeft de hersenen de mogelijkheid om langdurige negatieve associaties te vormen. Deze negatieve associaties zijn fysiek gelegen in ervarings-afhankelijke synaptische modificaties binnen een kleine populatie van neuronen die worden gerekruteerd tijdens het leerproces. Het begrijpen van de precieze mechanismen die ten grondslag liggen aan de neuronale selectie en plasticiteit tijdens het vormen van een herinnering behoort tot de meest fundamentele vraagstellingen in de neurowetenschappen van de afgelopen eeuw. Het in kaart brengen van de verdeling van de neuronale activiteit zou aanvullende verduidelijking brengen over de omstandigheden waarin herinneringen tot expressie komen en hoe neuronen op verschillende wijzen worden opgenomen in afzonderlijke herinnering “engrams”. Het doel van de huidige thesis was om via betrouwbare methoden afzonderlijke neuronale cel groepen te visualiseren, bestuderen en moduleren om zo onze kennis over bovenstaande vraagstellingen te verbreden.

Hoofdstuk 1 van deze thesis is een overzicht van de geschiedenis van de vooruitgang in het begrijpen van angst en ooglid conditioneren. Het beschrijft de kernprincipes en in het bijzonder recente vindingen in het proces waarbij angstherinneringen en motorisch leren worden verworven en gecodeerd.

Hoofdstuk 2 beschrijft een nieuwe methode om angstherinneringen te bestuderen. *Arc::dVenus* transgene muizen worden gebruikt om neuronen te visualiseren waar cellulaire veranderingen zijn ondergaan tijdens het aanleren van angstherinneringen in de laterale amygdala (LA). Onze bevindingen laten zien dat intrinsieke excitabiliteit een bepalende factor is voor de selectie van neuronen in een angstherinnering. Dit hoofdstuk laat ook zien dat versterking van glutamaterge synaptische transmissie van de input route van de thalamus naar de LA leer-specifiek is, en zeer specifiek is voor neuronen die *Arc* tot expressie brengen.

Hoofdstuk 3 beschrijft een kenmerkend patroon van *Arc* expressie in de ventrolaterale regio van de LA als gevolg van leren. We vinden dat deze sub regio een

chronische plasticiteit laat zien waarbij neuronen in deze regio op een unieke manier alleen actief zijn wanneer er vorming plaatsvindt van nieuwe aversieve associaties.

Hoofdstuk 4 focust op de rol van somatostatine⁺ interneuronen in de laterale regio van de centrale nucleus van de amygdala (CeL) in ooglid conditioneren. We vinden dat de CeL een regulatorisch effect heeft op associatieve ooglid responsen, wat aangeeft dat ooglid conditioneren kernmechanismen deelt met associatieve processen in het aanleren van angstherinneringen.

Hoofdstuk 5 is een algemene discussie over de uitkomsten en voornaamste conclusies van onze studies. Hierin worden de toekomstige aanpakken beschreven die belangrijke huidig onbeantwoorde vragen in het veld zou kunnen doen beantwoorden.

PhD PORTFOLIO

Name: Behdokht Hosseini
PhD period: September 2010- September 2016
Department: Psychiatry
Promoter: Prof.dr. Steven A. Kushner
Co-promoter: Dr. Priyanka Rao-Ruiz
Research school: Graduate School Neuroscience Amsterdam Rotterdam
(ONWAR)

PhD training

Stereology course at VUmc, Amsterdam, 2012

Conferences

(ONWAR) PhD annual meeting (Attended with oral presentation), 2015
EBBS-EBPS meeting. Verona/Italy, 2015

Coaching

Introduction to Confocal microscopy for Neuroscience MSc students 2013-2016
Supervising review paper assignment for second year medical students 2015/2016

LIST OF PUBLICATIONS

Arc expression identifies the lateral amygdala fear memory trace

Gouty-Colomer LA*, **Hosseini B***, Marcelo IM, Schreiber J, Slump DE, Yamaguchi S, Houweling AR, Jaarsma D, Elgersma Y, Kushner SA

Molecular Psychiatry **21**, 364-375 (2016)

Human gaze following response is affected by visual acuity

Spoor M, **Hosseini B**, van Alphen B, Frens MA, van der Geest JN

Journal of Ophthalmology, Article ID 543478 (2014)

*: *Shared first authorship*

CURRICULUM VITAE

Behdokht Hosseini was born on the 10th of January 1978 in Firoozkooh-Tehran, Iran. She started her undergraduate study in Chemistry at Faculty of Science, University of Tehran in 1998 and received her BSc degree in 2003. In 2006, she moved to Tripoli, Libya. A year later, she started her MSc in Biochemistry at University of Manchester in the UK via the distance-learning program of that University while in Tripoli. In 2008, she left Libya to the Netherlands where she commenced a research master at the Department of Neuroscience, Erasmus University Medical Centre in Rotterdam. For her research, she worked on human gaze following responses affected by visual acuity, under supervision of Prof. dr. Maarten Frens. In 2010, she started her PhD research project at the Department of Neurobiological Psychiatry at the Erasmus University Medical Centre in Rotterdam where she worked under supervision of Prof. dr. Steven Kushner. Her main research focus was on the neurobiology of fear memory engrams.

ACKNOWLEDGMENT

This work was to display my attempt in scientific observation and approach, my trial in learning how to study scientific events, exploring and enjoying their revelations, in the hope of better perception of myself and the world around me through the process. These steps have given me the courage to hope for more, so that I could aim to think, learn and understand more. Here, I offer my thanks and respect to those who made this attempt possible and unforgettable.

Dear Prof. dr. Steven Kushner, dear Steven, doing science with you was a dream-come-true. I cannot thank you enough for this great opportunity. Thank you for being a living example of scientific passion, a role model in hard work and a kind and considerate mentor at the same time. Thank you for your great lessons, motivating trust and encouragement. I will always cherish all these memorable years.

Dear Dr. Priyanka Rao-Ruiz, dear Priyanka, thank you for all the great help and advice that you gave me through the process of preparing this thesis. It was truly a fine learning experience on how to think critically and write beautifully.

Many thanks to Prof. dr, Ype Elgersma, Dr. Tom Ruigrok and Dr. Harm Krugers for your time as members of the reading committee. Thank you for your insightful comments. To Prof. dr. Chris De Zeeuw, Prof. dr. Maarten Frens and Dr. Dick Jaarsma, many thanks for your help as committee members. It has been a great honor to have your support.

To Dr. Joke Tulen, dear Joke, many thanks for all your great support during the past 6 years.

Dear Dick, I am very thankful of you for giving me the opportunity to learn what scientific design, perfection, precision and efficiency truly mean.

Dear Henk-Jan, doing optogenetic study with you was filled with great deal of new learning for me and proved to me how perseverance pays. Thank you for teaching me the magic of reaching the living brain. You have my greatest gratitude for your tremendous contribution to this book.

Dear Mariëlle, leaving your room always meant an answered question or a solved problem. Thank you for your never-ending support.

Many thanks to my lab-mates from the past and now; Ane, Bas, Cato, Christian, Demi, Denise, Femke, Guy, Ineke, Ivo, Jaime, Jay, Jeffery, Katie, Laurie- Anne, Lucia, Mark, Mariëlle, Maarouf, Nilhan, Priyanka, Roberto, Sander, Shashini, Sid, Stefano, Yagmur and Wouter.

Laurie- Anne, thank you for the years of working closely together. Without your magical recording, the fear memory trace project could not evolve into this beautiful story. Ivo, I truly enjoyed your knowledge and great sense of humor, thank you. Katie, thanks for all your guidance when I joined the lab. Lucia, thanks for the serious effort to shed light on the spot mystery. Jeffrey, your science-is-fun motto and your enthusiasm for research will not be so easy to forget. Thank you for all the scientific, fun and “meaningful” talks. I really enjoyed your friendship. Femke, thanks for being an inspiration for me. Christian, heel bedankt for all the cultural and social exchanges. Nilhan, dear Nilosh, wonder why we never tried to develop our own secret language using a lot of words shared in both Turkish and Persian(!) ;-). Thank you for your very positive energy, teşekkür. Shashini, Shini jan, I certainly enjoyed our time and talks on yoga, dance, career and life. Mark, thank you for all your help and the good conversations. Bas, thank you for your clever and witty comments Mr. Hunter. Demi, our shared time was limited, but was certainly of high quality. Thank you for that. I will stay tuned to hear more of your success. Enjoy the confocal and surgery rooms, both can be very fulfilling. Maarouf, it was great to know you on your scientific way of thinking and views, thank you. Sander, I can hardly imagine saying goodbye to you. Perhaps because we will meet again to unlock the green cells distribution mystery (?) ;-). I always think of you as a super intelligent hard-working person with little need to sleep! Cato and Yagmur, it was great knowing you both. Thank you for the sweet memories.

To Denise and Guy, thank you for accepting to be my paranymphs. Denise, thank you for putting up with teaching me how to hold and work with a pipette! Thank you for being supportive during happy or sad times, and while working in the lab or riding your horse. Guy, every single conversation with you has been a reminder that there is hope for humanity. Thank you for being such a good friend through all these years.

Dear Maarten, thank you for being very welcoming and encouraging when I was new to the Netherlands as well as Neuroscience. Dear Jos, it was great to have your support and positive energy while doing my MSc, thank you. Dear Arthur, thank you for all the scientific discussions. Dear Wai, thank you for your kind assistance through all these years. Dear Gert, thanks for introducing me to the world of confocal microscopy. Dear Jaga, Geeske, Rüdiger, Mehrnoosh, Martijn, Diana, Minetta, Edwin, Martina, Azar, Loes, Aaron and Erika, thank you for your help and support. Dear Elize, thanks for being helpful and resourceful and for all the tremendous work that you do in the hisology lab. Dear Masha and Ben, thank you for your amazing non-stop help and support while I was working with the Stereo Investigator software. Dear Ilja, thank you for all your technical support in the eye-blink conditioning lab. Dear Hans, Gerard, Freek and Bas, it was a pleasure knowing you all, thank you for your lessons and advice.

To the Iranian fellows that I met at the Erasmus MC, Negah, Azadeh, Mehrnoosh, Mehrnaz, Mana, Siawosh, Melika, Farnaz, Farshid and Parham, thank you all for your warmth. Negah, thank you for all the laughter, our silly and serious talks. Azadeh,

being with you means comfort and home, thank you.

To my parents, maman, your daily self-sacrifices, never-ending compassion and hard-work seemed just another regular day with you. Now I know it was not. You were/are extraordinary. Baba, you are the true example of good heart, passion, modesty and tirelessness. Thank you for teaching me the essence of willing to go high and showing me how one can live a passionate life.

To my lovely family in Iran, Switzerland, UK and Canada; Banafsheh, Alireza, Golpar, Zahra, Maryam, Morteza, Parham, maman and baba Bashokooh, Behzad, Zohreh, Mehran, Maryam, Behnam, Hiva, Nima, Kiarash and Soren, thank you for being inspiring on so many levels. I am proud of your success and everlasting achievements. Banafsheh, your pure ambitions and generous nature have kept me warm all my life, thank you. Morteza, my example of free spirit, vigor and honesty, and Mehran, my role model of many many years and great source of joy and laughter, thank you big brothers! Cheers to all of you.

To my best friend of 16 years, I am finishing now believing that without your unconditional care, beautiful mind and amazing upbeat being, none of these would have ever been possible. I need another book to thank you properly. Love you, Behrooz.

Behdokht Hosseini

November 2016

